Coordination chemistry with fluorinated chelators and *m*-terphenyl isocyanides

Inaugural-Dissertation
to obtain the academic degree
Doctor rerum naturalium (Dr. rer. nat.)

submitted to the Department of Biology, Chemistry, Pharmacy
of Freie Universität Berlin

by
Federico Salsi

2020

The work for the present dissertation has been conducted between May 2016 and June 2020 under the guidance of Prof. Dr. Ulrich Abram at the Institute of Chemistry and Biochemistry (Department of Biology, Chemistry and Pharmacy) of the Freie Universität Berlin.

First Reviewer:	Prof. Dr. Ulrich Abram
Second Reviewer:	Prof. Dr. Dieter Lentz
Day of the disputation:	21.09.2020

Acknowledgments

First of all, I would like to thank my doctoral supervisor, Prof. Dr. Ulrich Abram, for giving me the possibility of working in his group, for his competent scientific guidance, for supporting me with enthusiasm in these four years, for trusting me and believing in my ideas.

I also want to thank Prof. Dr. Dieter Lentz for accepting the position of second reviewer, for reading and evaluating my work.

Many thanks to Adelheid Hagenbach for her help and indications in the experimental practice in the radioactive lab, for correcting my manuscripts and for the fundamental help with the crystallographic analyses.

A special thank also goes to Jacqueline Grewe for her efficient and constant technical support, for being always there when something was missing or not working properly and for helping with the preparation of the rhenium starting materials.

My sincere thanks go to Prof. Dr. Joshua Figueroa, for giving me the chance to work in his lab at UC San Diego, for his scientific advice and for being a wonderful and helpful host. I also thank his amazing research group for the warm welcome and the useful practical tipps and tricks, which they taught me in the lab; I am especially grateful to Alejandra Arroyave, Myles Drance, Haeun Chang and Michael Neville.

I would like to express my gratitude to Prof. Dr. Pedro Ivo da Silva Maia and Prof. Dr. Sérgio de Albuquerque for allowing and supporting my research trip to Riberão Preto, for the amazing and productive time there and for their warm hospitality. I also sincerely thank Dr. Gisele Bulhões Portapilla for her amazing work in the evaluation of the bioactivity of my compounds and for the nice time together.

I also would like to thank Detlef Wille and Falk Wenzlaff for the efficient service in the radioactive lab; Kersten Leo for her competence and helpfulness at the material store; Simon Steinhauer for the technical support with NMR spectroscopy.

I also thank all my talented and diligent students, in particular Saskia Simon, Maximilian Roca Jungfer and Konstantin Schutjajew for their amazing work. The whole Abram group shall be thanked as well for the cooperative atmosphere, the nice time together and the productive discussions.

I thank the coordinator Dr. Carsten Müller and all members and speakers of the research training network GRK 1582 “Fluor als Schlüsselelement” for the insights into fluorine chemistry, the interesting seminars and the fun time at the workshops. I am also thankful for the financial support and the opportunities to travel.

To conclude I would like to thank all my lovely friends and my wonderful partner for the beautiful time I had during my PhD in Berlin and for the substantial support they always gave me.

Contents

1 Introduction

1.1 The role of fluorine in chemistry and technology

Modern chemistry has deepened the understanding of how the special position of fluorine in the periodic table of elements affects the structure, reactivity, and function of fluorine-containing molecules.[1] As a result, a large variety of fluorine-containing materials, catalysts and agrochemicals or pharmaceutical drugs have been developed.[2] The field extends far beyond these advances, since the unique reactivity of fluorine can also be used to access fluorine-free molecules.[3]

Fluorine chemistry has played a central role in many significant and highly diverse technological developments over the recent 80 years. Because of the special synthetic challenges that it presents and because of the unique structure/reactivity relationships observed for fluorine-containing compounds, fluorine chemistry is also a field of great fundamental interest.

The uniqueness of compounds containing fluorine can be attributed, among others, to the fact that:

1. Fluorine is the most electronegative element on the Periodic Table of Elements (3.98 on the Pauling electronegativity scale, compared to 2.20 for H, 3.44 for O, and 2.55 for C).
2. Fluorine is a small atom with a van der Waals radius of 1.47 Å, close to the value of 1.20 Å for hydrogen.[4]

In addition, the high sensitivity of ^{19}F in nuclear magnetic resonance (NMR) experiments makes this nucleus ideal for biological and chemical studies.[5]

1.2 Fluorine in medicinal chemistry

The highest impact of fluorine in the biochemical sciences is undoubtedly associated with the development of agrochemicals and, most importantly, in medicinal chemistry. In 1955, the U.S. Food and Drug Administration (FDA) approved the first fluorine-containing drug, the steroid fludrocortisone.[6] Since then, more than 150 fluorinated molecules have been managed to reach the market (Fig. 1). In 2010, it was calculated that about 20% of the administered drugs contained fluorine atoms or fluoroalkyl groups.[7] However, the current trend is increasing from 20% to about 30% for all new approved drugs (excluding biopharmaceutical products) in the most recent years. These fluorinated drugs cover all possible therapeutic areas and, according to a recent survey, several of them are among the most-prescribed and/or profitable in the U.S. pharmaceutical market.[8]

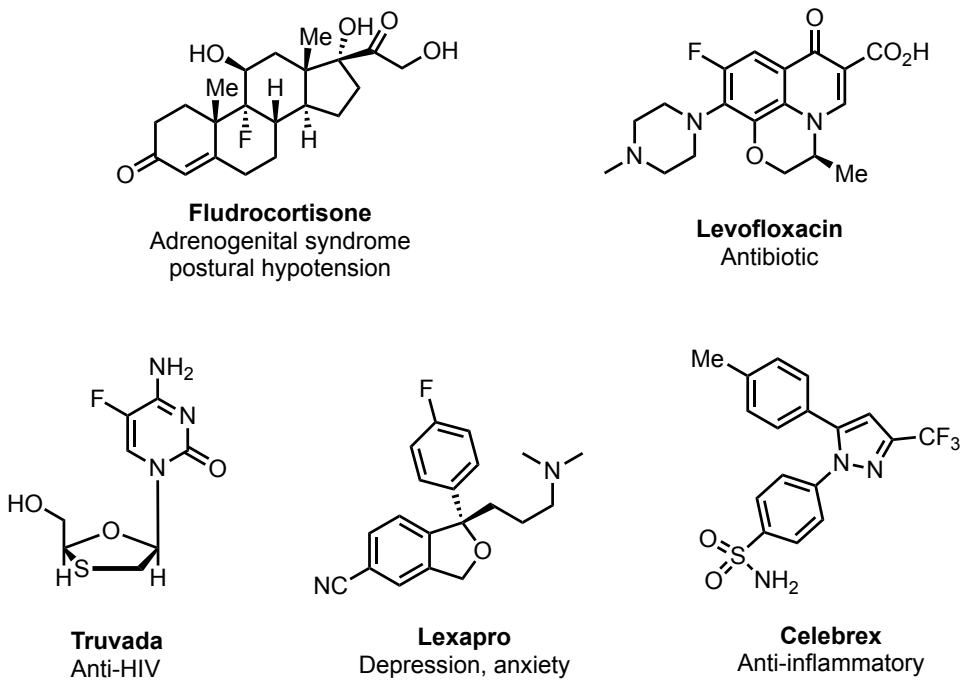

Figure 1. Common organic pharmaceuticals containing fluorine.

In addition, ^{18}F has been established as a useful positron-emitting isotope for *in vivo* imaging technology that potentially has large application in drug discovery and development, often limited only by convenient synthetic accessibility to appropriate labeled compounds.[9] The wide ranging applications of fluorine in drug design provide a strong stimulus for the development of new synthetic methodologies that allow more facile access to a wide range of fluorinated compounds.

The introduction of fluorine into bioactive molecules is a well-established strategy in the designing of new drugs to increase pharmaceutical effectiveness, biological half-life, and bio-absorption. The advantage of introducing fluorine atoms or fluoroalkyl groups into organic compounds is a consequence of the alteration of their physicochemical properties, which in some cases are substantially modified in comparison to their non-fluorinated counterparts. For instance, the modulation of the acidity and lipophilicity,[10] as well as the control of conformation, can be achieved by judicious substitution of hydrogen atoms or functional groups by fluorine; ultimately this may result in an improvement of the biological and/or pharmacological properties. Another useful application is the blocking of potential oxidation sites in order to prevent undesired metabolic pathways, for instance the replacement of a methyl-arene substituent by trifluoromethyl.[11] Even if there is a certain degree of predictability when designing bioactive fluoroorganic compounds, medicinal chemists still need to synthesize very large libraries of derivatives through a systematic trial and error process until the desired molecule is finally obtained. In addition, in some cases, a desired fluorine-containing molecule might not be accessible because of unsurmountable synthetic difficulties.

1.3 Coordination compounds in nuclear medicine

The development of metal-based radiopharmaceuticals represents a dynamic and rapidly growing research area that requires a deep knowledge of metal coordination chemistry and ligand design.[12]

For *in vivo* applications, kinetic inertness and/or thermodynamic stability of metal complexes is required.[13] In general, acyclic chelator complexes are kinetically less inert than macrocyclic complexes of comparable stability.[14] On the other hand, acyclic chelators typically have faster metal-binding kinetics compared with their macrocyclic analogues, which can be a significant advantage for shorter-lived radiometals.[15]

Diagnostic nuclear medicine relies outstandingly on the use ^{99m}Tc because of its nuclear properties ($t_{1/2}$ = 6.02 h, E_γ = 140 KeV), its availability from a ^{99}Mo/^{99m}Tc generator and its relatively low costs. The main γ emission (140 KeV, 89%) can be efficiently detected by gamma detectors used for imaging. ^{99m}Tc has no beta emission and emits only low-energy Auger electrons. Its half-life is long enough to carry out the synthesis of various radiopharmaceuticals, and yet it is short enough to minimize the radiation dose to the patient. In fact, ^{99m}Tc is used for roughly 80% of the diagnostic scans performed in nuclear medicine departments worldwide.[16]

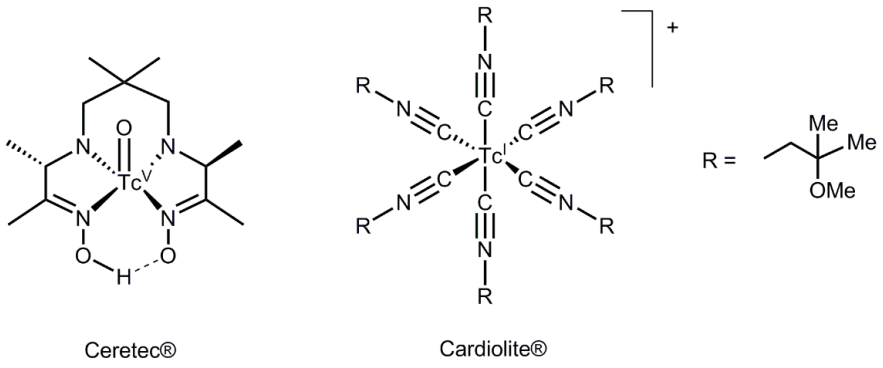

Figure 2. Examples of ^{99m}Tc radiopharmaceuticals, in which technetium presents different oxidation states.

The screening of the thyroid is often conducted directly with a diluted solution of $^{99m}TcO_4^-$,[16] yet in most applications metal complexes in which Tc is in a lower oxidation state are used. Tc(V) oxo complexes, Tc(IV) and organometallic compounds of Tc are common in radiopharmaceutical chemistry. Ceretec® (Fig. 2) is a neutral complex with high lipophilicity that is efficiently accumulated in the brain and it can be prepared from a commercial Kit. The most successful imaging agent is Cardiolite® (Fig. 2), a cationic isocyanide complex of Tc(I), which accumulates in the heart.[17]

^{99m}Tc has a short half-life and is used in nanomolar concentrations, while the long-lived isotope ^{99}Tc (2.1×10^5 y, E_{max} = 0.292 MeV) is applied to investigate the chemistry of technetium. The element technetium does not possess any stable isotope, but its heavier homologue, rhenium, is a good model for the non-radioactive study of its chemistry.

Moreover, rhenium itself presents two β-emitting radionuclides with convenient properties for the application in therapeutic nuclear medicine: ^{186}Re ($t_{1/2}$ = 89.2 h, E_{max} = 1.1 MeV) und ^{188}Re ($t_{1/2}$ = 16.9 h, E_{max} = 2.1 MeV).[18] Its potential applicability is demonstrated in a number of clinical studies and

Rhenium-188-HEDP (HEDP = hydroxyethyldiphosphonate) is used in hospitals for the treatment of bone cancer.[19]

Another widely studied and used radionuclide is ^{111}In ($t_{1/2}$ = 2.8 d; $E_{\gamma1}$ = 171 keV; $E_{\gamma2}$ = 245 keV). It is produced commercially by irradiating a natural cadmium target with high-energy protons according to the reactions: ^{111}Cd(p,n)^{111}In or ^{112}Cd(p,2n)^{111}In.[20]

^{111}In radiopharmaceuticals are the main medical applications of indium(III) complexes.[21] Cell labelling with ^{111}In, developed to allow clinical imaging of infection and inflammation sites, entered general clinical use in the 1980s.[22] In addition, ^{111}In may be employed in cancer therapy through the emission of Auger electrons, offering a method to achieve DNA damage and eventual cell death.[23]

1.4 Au(III) complexes in medicinal chemistry

The small energetic separation of the d and s valence shells of gold, in comparison to its lighter homologue silver, is responsible for the efficient formation of linear, dicoordinate gold(I) complexes. At the same time, the destabilization of the 5d orbitals leads to the occurrence of the oxidation state +3, which is almost absent for silver. Au(III) complexes are diamagnetic and normally have a square-planar geometry. Great progresses have been made in the last 20 years in the investigation of the chemistry of Au(III), drawing the attention to possible applications in medicinal chemistry.[24] Au(III) is isoelectronic with Pt(II) and many of their complexes are isosteric with square-planar geometry. This may indicate a similar anti-tumor activity as observed for Pt(II) compounds, such as Cisplatin (Fig. 3). Investigations of the anti-proliferative activity of gold(III) complexes revealed that their mechanism of action is DNA

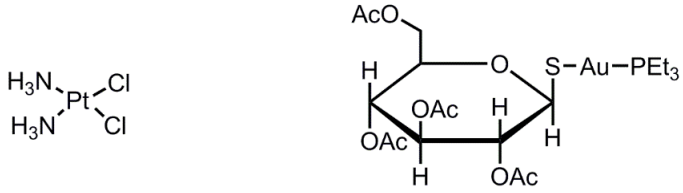

Cisplatin Auranofin

Figure 3. Coordination compounds featuring Au and Pt applied as anti-cancer (Cisplatin) and anti-rheumatic agents (Auranofin).

independent (differently from Cisplatin) and might offer an alternative against Cisplatin-resistant tumors. Gold(III) complexes should be easily reduced by naturally occurring reductants, such as thiols or disulphides, but with an appropriate choice of the ligand system it is possible to increase the reduction potential and avoid unwanted decomposition.[25]

The clinical use of gold(I) compounds has been established with Auranofin (Fig. 3), a drug for the treatment of rheumatoid arthritis.[26] During the recent years, a number of potential applications in therapeutic medicine have been identified for gold(III) compounds as well as such for cancer treatment[27] and such with antibacterial activity.[28]

1.5 Thiosemicarbazone ligands and their pharmaceutical properties

Thiosemicarbazones and similar compounds are of considerable interest with respect to their biological and pharmaceutical properties. A thiosemicarbazone is the sulfur equivalent of semicarbazone, in which a thiocarbonyl group substitutes the carbonyl group, and is obtained by condensation of a ketone with a thiosemicarbazide (Fig. 4).

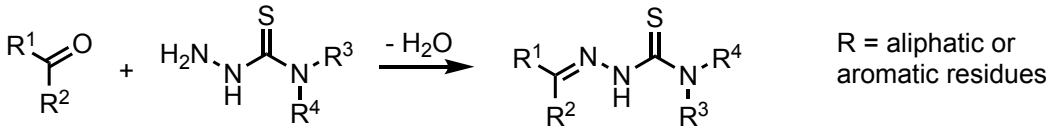

Figure 4. Formation of a thiosemicarbazone by condensation of a ketone and a thiosemicarbazide under elimination of water.

Thiosemicarbazones usually react with metal cations giving complexes, in which they behave as chelating ligands.[29] The easy functionalization of thiosemicarbazones makes it possible to increase the denticity of the ligands by the addition of further donating atoms. Research on the coordination chemistry,[30] analytical applications[31] and biological activities[32] of such complexes has increased steadily for many years: a search of the Cambridge Structural Database found more than a 500 crystal structures of thiosemicarbazone complexes with a large variety of main group and transition metals.

Many of these compounds and their metal complexes possess remarkable activities against a number of diseases such as cancer,[33] HIV,[34] tuberculosis,[35] and also against parasitic diseases.[36]

For example, 2-acetyl pyridine-derived thiosemicarbazones and their metal complexes have been extensively investigated for their cytotoxic effects against human solid tumor and leukemia cell lines, as well as for their antifungal activity.[37]

2-Acetylpyridine 4N-(2-acetoxyethoxymethyl)thiosemicarbazone was shown to have, among a fairly large number of thiosemicarbazones, the highest inhibitory activity against the growth of the following microorganisms: *Staphylococcus aureus, Escherichia coli, Pseudomonas aeruginosa, Candida albicans and Aspergillus niger*. It also has activity against resistant strains of *W-2 Indochina Plasmodium falciparum* and *D-6 African Plasmodium falciparum*.[38]

The indirect condensation of the carbonyl group of a benzoylthiourea with a nucleophile was first described by Weber et al. The formation of a bis-chelate with Ni(II) and its reaction with $SOCl_2$ gives a benzimidoyl chloride (**3**) (Fig. 5),[39] which can be efficiently reacted with a number of nucleophiles.[40]

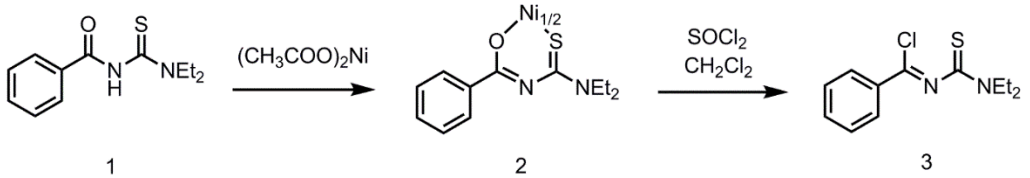

Figure 5. Synthesis of the benzimidoyl chloride according to the method of Weber.[39]

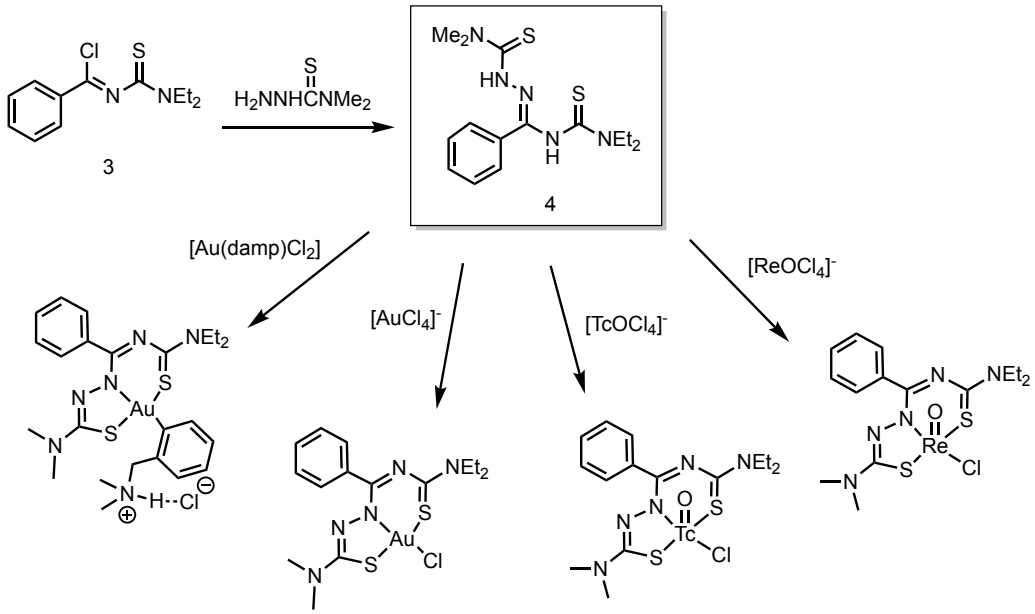

Figure 6. Transition metal complexes with *S,N,S*-tridentate thiosemicarbazones.[1c, 41-42]

H. H. Nguyen exploited this reaction for the creation of a novel tridentate thiosemicarbazone-type ligand class with an *S,N,S* donor set (**4**), which resulted from the condensation of the benzimidoyl chloride with a thiosemicarbazide. As depicted in Figure 6, the obtained ligand readily reacts with $(NBu_4)[TcOCl_4]$ in methanol under the formation of red oxotechnetium(V) complexes of the composition [TcOCl(L)]. The monomeric, five-coordinate compounds are air-stable. The same reaction with $(NBu_4)[ReOCl_4]$ leads to the formation of the isostructural [ReOCl(L)] compounds. Ligands that stabilize the $(M^{V}{=}O)^{3+}$ cores (M = Re, Tc) are of particular interest, since the reduction of $[MO_4]^-$ ions from commercial generator systems with common reducing agents allows the facile production of oxidometallates(V).[1c]

$Na[AuCl_4]{\cdot}2H_2O$ reacts with tridentate thiosemicarbazone ligands, under formation of air-stable, green Au(III) complexes of the composition [Au(L)Cl]. The organic ligands coordinate in a planar *S,N,S* coordination mode (Fig. 6).[41] Stable organogold(III) compounds of the composition $[Au^{III}(Hdamp)(L)]Cl$ are formed from reactions of $[AuCl_2(damp)]$ with H_2L ($damp^-$ = dimethylaminomethylphenyl).[42b] The *in vitro* anti-parasitic activity was evaluated against the intracellular form of *Trypanosoma cruzi*, a hemoflagellate protozoan, responsible for the American Trypanosomiasis or "Chagas disease".[42a] This disease is endemic in Latin America and affects 18 million people causing 50,000 deaths per year.[43] The current treatment based on Nifurtimox and Benznidazole is unsatisfactory due to poor efficacy and serious side effects of the used medications. The choice of gold compounds for the treatment of Chagas' disease is not arbitrary; its etiological agent, *T. cruzi*, is rich of thiol containing proteins, which are fundamental for its life cycles.[44] The most abundant cysteine protease for *T. cruzi* is the protein Cruzain, which is essential for parasite development and survival within host cells. This protein has been identified as a drug target.[36a, 45] In this context, the high affinity of gold compounds for thiol and selenol donor atoms contained in the proteins of the

trypanosomes makes them promising agents for the treatment of Chagas' disease and other tropical diseases.[44]

The organometallic complexes [Au^{III}(Hdamp)(L)]Cl (Fig. 6) display a remarkable activity, which is dependent on the alkyl substituents of the thiosemicarbazone building blocks of the ligands. One representative of the cationic complexes, where H_2L contains a dimethylthiosemicarbazide building block, shows a trypanocidal activity against the intracellular amastigote form in the same order of magnitude as that of the standard drug Benznidazole. Furthermore, no appreciable toxicity to mice spleen cells was observed for this compound.[42a]

1.6 *meta*-Terphenyl isocyanide ligands for the stabilization of low-valent and highly reduced metal complexes.

Isocyanides have been widely recognized as effective and versatile ligands for transition metals. Their isolobal relation to CO impart them similar coordination properties, for instance their ability to stabilize low oxidation states through strong π-acceptor properties (Fig. 7). The fundamental advantage of the isocyanides over CO is the presence of an organic residue and, thus, the possibility of tuning their electronic and steric properties by change of the substitution pattern.[46]

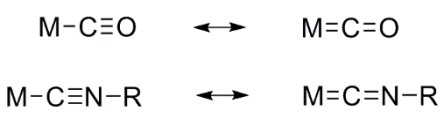

Figure 7. Schematic representation of the π-acceptor properties of carbonyl and isocyanide ligands.

Isocyanides differ from CO being in general stronger σ-donors and weaker π-acceptors. Nevertheless, perfluorination of the organic residue strongly enhances the π-acceptor properties of isocyanides by lowering the energy of the π* orbital. The synthesis of the first trifluoromethyl isocyanide complexes [$(CF_3NC)Cr(CO)_5$] and [$CF_3NC)W(CO)_5$] indicated that the trifluoromethyl isocyanide ligand has a very similar, maybe even superior, ratio of π-acceptor and σ-donor strengths than CO.[47]

J. S. Figueroa et al. demonstrated that sterically encumbered isocyanides, in particular *meta*-terphenyl isocyanides are able to enforce low metal coordination numbers, fostering exotic structural motifs and coordinatively unsaturated metal centers. Combination of cuprous chloride and the isocyanide ligand $CNAr^{Mes2}$ (Mes = 2,4,6-$Me_3C_6H_2$) in a 1:2 molar ratio in CH_2Cl_2 solution allows for the isolation of the three-coordinate bis-isocyanide complex [$ClCu(CNAr^{Mes2})_2$], which represents a very rare example of a structurally authenticated monomeric bis-isocyanide Cu(I) halide complex (Fig. 8). Indeed, most related Cu bis-isocyanide examples contain a (μ-halide)$_2$ functionality in the solid state.[48] The Figueroa group also compared the ligation properties of two isocyanides $CNAr^{Dipp2}$ (Dipp = 2,6-diisopropylphenyl) and $CNAr^{Mes2}$, having different steric requirements, with Cu(I) and Ag(I). It was found that only two units of the sterically more protective $CNAr^{Dipp2}$ ligand are accommodated by monovalent Cu and Ag centers, whereas three $CNAr^{Mes2}$ units can readily bind (Fig. 8).[49] Therefore, using metal centers that lack of

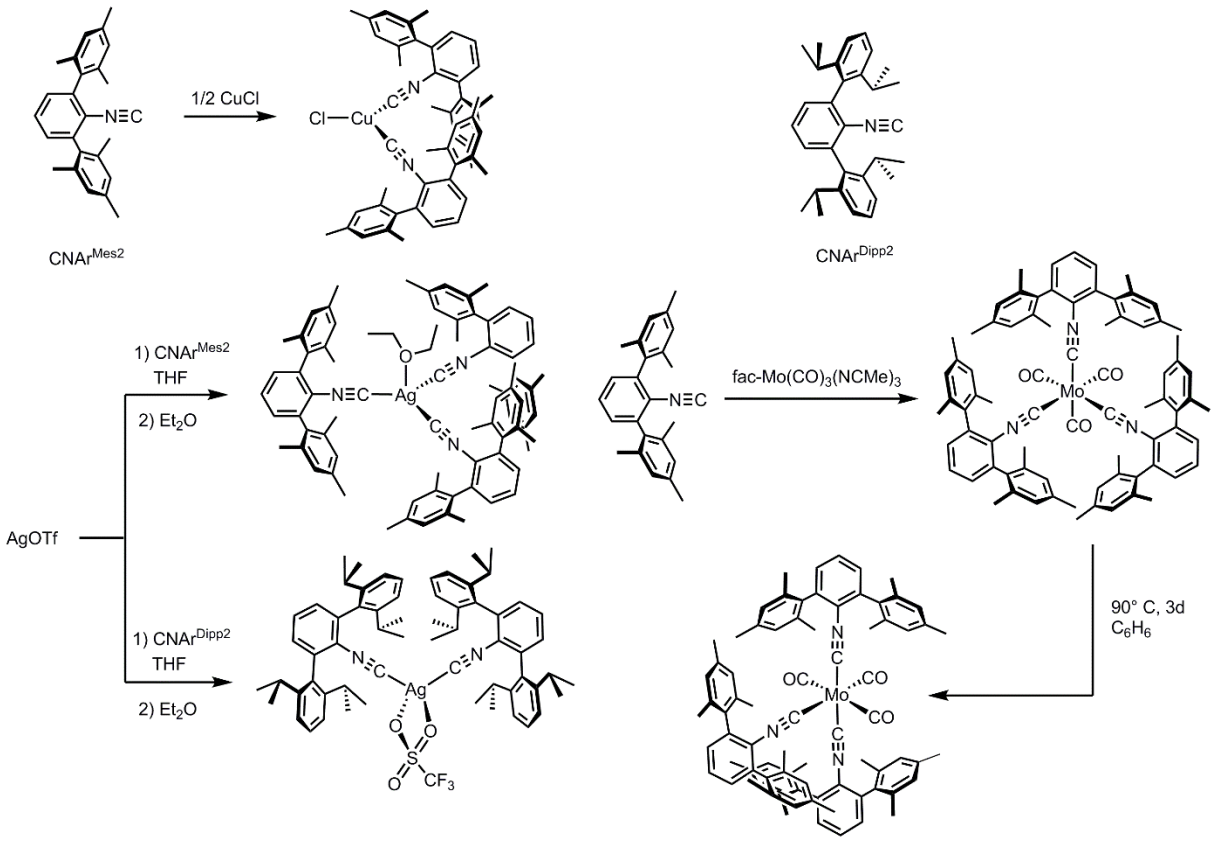

Figure 8. Complexes of meta-terphenyl isocyanides in presence of weak (Ag^I, Cu^I) and strong (Mo^0) backdonation.

significant π-basicity, they established that steric hindrance can be exploited to stabilize low coordinated metal centers.

Also in the case of π-basic metal centers, such as Mo(0), sterical effects play an important role. Three $CNAr^{Mes2}$ ligands react with *fac*-$[Mo(CO)_3(NCMe)_3]$ to afford the octahedral complex *fac*-$[Mo(CO)_3(CNAr^{Mes2})_3]$, which can be converted irreversibly to the *mer* isomer upon heating in solution without decomposition, thus indicating that the *mer* isomer is robust and thermodynamically favoured over the *fac* isomer. This is due to the relive of the significant steric pressure present in the *fac* isomer, generated by the encumbering terphenyl groups. The preference of $[Mo(CO)_3(CNAr^{Mes2})_3]$ to adopt its meridional isomeric form is particularly noteworthy since the facial disposition of isocyanide ligands is the preferred coordination geometry in the overwhelming majority of Group VI $[M(CO)_3(CNR)_3]$ complexes. In the absence of significant steric hindrance, the preference for *fac* over *mer* configurations in Group VI $[M(CO)_3(CNR)_3]$ complexes may be attributed to electronic factors: (i) the preference for each CNR ligand to be *trans* to the relatively weaker σ-donating CO ligands and (ii) the maximization of π-acceptor ability of the CO units in the *fac*-geometry.[49] The only exceptions are the fluorinated *trans*-$[Cr(CNCH_3)(CNC_6F_5)(CO)_4]$ and *trans*-$[Cr(CNCH_3)(CNCF_3)(CO)_4]$ complexes prepared by Lentz et al.[50] In these cases, the strong π-accepting properties of perfluorinated isocyanides are responsible for the preference for the meridional disposition of the CO ligands.

Addition of $CNAr^{Dipp2}$ to *fac*-$[Mo(CO)_3(NCMe)_3]$ results in a mixture of both the tetracarbonyl and the tricarbonyl complexes *trans*-$[Mo(CO)_4(CNAr^{Dipp2})_2]$ and *trans*-$[Mo(NCMe)(CO)_3(CNAr^{Dipp2})_2]$, respectively, in which the encumbering $CNAr^{Dipp2}$ ligands are in a *trans*-disposition.

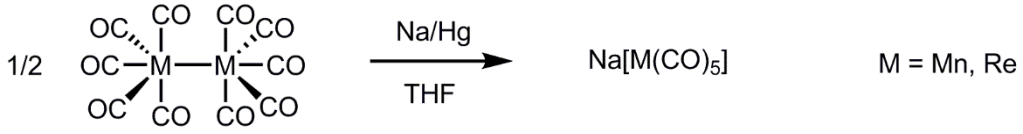

Figure 9. Formation of the pentacarbonyl metallates of group VII metals.

With exception of the well-studied carbonylmetalate $[Re(CO)_5]^-$, organometallic monoanions of rhenium and technetium have received limited attention.[51] Thus, except for CO, little information is available concerning the influence of ligand modifications on the stability or reactivity properties of monoanionic Mn, Tc and Re centers. Moreover, $[Tc(CO)_5]^-$, which should be easily prepared by reduction of $[Tc_2(CO)_{10}]$ with Na/Hg (Fig. 9), is in practice hardly accessible, because of the absence of a synthetic procedure for the decacarbonyl $[Tc_2(CO)_{10}]$ that is conform with the actual radiation protection regulations. A high-yield synthesis from pertechnetate requires, indeed, high pressure (100 atm of CO), high temperature (120° C) and long reaction time (three days).[52] The possibility of using isocyanides as CO analogues is, in this case, particularly profitable.

Figueroa *et al*. described that the encumbering *m*-terphenyl isocyanide ligands, $CNAr^{Mes2}$ and $CNAr^{Dipp2}$ (Fig. 8), readily furnish mixed carbonyl/isocyanide manganese(I) complexes, which can be reduced to the corresponding monoanions.[53] Subsequent treatment of $[BrMn(CO)_2(CNAr^{Mes2})_3]$ with potassium anthracenide ($K[C_{14}H_{10}]$) and 18-crown-6 in THF solution resulted in the formation of [K(18-crown-6)]$[Mn(CO)_2(CNAr^{Mes2})_3]$ in low yields (20%). X-ray structural determination on crystals grown from 1,2-dimethoxyethane (DME) solution revealed the salt, [K(DME)(18-crown-6)]$[Mn(CO)_2(CNAr^{Mes2})_3]$, in which the five-coordinate manganese monoanion features a trigonal bipyramidal (tbp) coordination geometry with apical CO ligands. Once crystallized at –35° C, [K(DME)(18-crown-6)]$[Mn(CO)_2(CNAr^{Mes2})_3]$ can be readily manipulated in the solid state. However, it decomposes over the course of 4 h at room temperature in C_6D_6 solution.

This observation arises the question whether the higher steric protection ensured by $CNAr^{Dipp2}$ might further stabilize the metallate. In contrast to $[BrMn(CO)_2(CNAr^{Mes2})_3]$, Na/Hg reduction of *mer,trans*-$[BrMn(CO)_3(CNAr^{Dipp2})_2]$ generates the bright red salt $Na[Mn(CO)_3(CNAr^{Dipp2})_2]$ in 47% isolated yield. This compound is significantly more stable and retains its integrity in C_6D_6 solution for several days. Moreover, $Na[Mn(CO)_3(CNAr^{Dipp2})_2]$ shows a well-defined reactivity with a range of electrophiles. For example, the reaction of the nucleophilic metal center with HCl generates the corresponding hydride, *mer,trans*-$[HMn(CO)_3(CNAr^{Dipp2})_2]$, and treatment with methyl iodide (MeI) readily generates the corresponding methyl complex, *mer,trans*-$[MeMn(CO)_3(CNAr^{Dipp2})_2]$. Heavier main-group electrophiles also react cleanly with $Na[Mn(CO)_3(CNAr^{Dipp2})_2]$. Accordingly, treatment of

$Na[Mn(CO)_3(CNAr^{Dipp2})_2]$ with trichloromethylsilane ($MeSiCl_3$) smoothly provides *mer,trans*-$[Cl_2(Me)SiMn(CO)_3(CNAr^{Dipp2})_2]$ and treatment of a Et_2O solution of $Na[Mn(CO)_3(CNAr^{Dipp2})_2]$ with $SnCl_2$ generates the metallostannylene complex, *mer,trans*-$[ClSnMn(CO)_3(CNAr^{Dipp2})_2]$ as a thermally stable solid.[53]

As observed by Lentz, incorporation of fluorine on the organic residue of the isocyanide can increase its π-acceptor properties.[50] This is true in general for electron-withdrawing substituents on aryl isocyanides, in particular in the *para*-position of the aromatic ring.[54] Fluorinated substituents are able to diminish the σ-donor/π-acid ratio, offering a strategy to mimic the electronic properties of CO. The Figueroa group developed the synthesis of the fluorinated *meta*-terphenyl isocyanide $CNAr^{DArF2}$, by palladium-catalyzed cross-coupling of 2,6-dibromoaniline with 3,5-$(CF_3)_2C_6H_3B(OH)_2$ and subsequently formylation/dehydration steps (Fig. 10).[55]

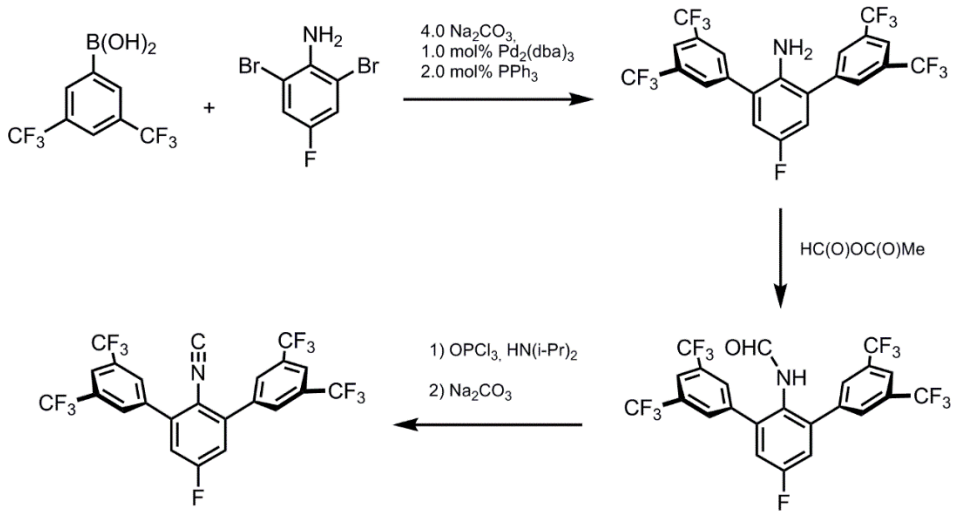

Figure 10. Synthesis of $CNAr^{DArF2}$ by palladium cross-coupling. [55]

They also reported that in the zerovalent *mer*-$[Mo(CO)_3(CNAr)_3]$ complexes, $CNAr^{DArF2}$ gives rise to significantly blue-shifted ν_{CO} bands relative to $CNAr^{Mes2}$, which features electron-releasing alkyl-substituted flanking rings. Furthermore, the presence of flanking 3,5-$(CF_3)_2C_6H_3$ rings on the *m*-terphenyl framework qualitatively presents the greatest steric encumbrance on the vicinity of the metal center, among the investigated *meta*-terphenyl isocyanides. This encumbrance results in significant steric pressure that affects the preference of $[Mo(CO)_3(CNAr^{DArF2})_3]$ complexes for the meridional isomer, which could not in any way be converted (thermally or photochemically) to the facial form.[55] Also the $[W(CO)_3(CNCF_3)_3]$ and $[W(CO)_3(CNC_6F_5)_3]$ prepared by Lentz exhibited a strong preference for the *mer*-isomers. [47a]

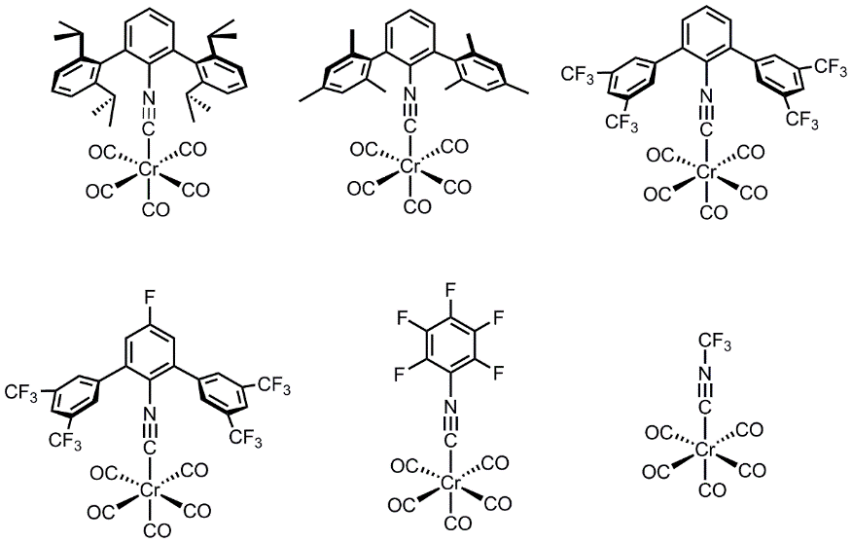

Figure 11. $[Cr(CO)_5(CNR)]$ complexes in comparison. Force constants of the CO bonds for the axial (k_1) and equatorial (k_2) carbonyl ligands. Force constants are an empirical measure of the σ-donating/π-acceptor properties of the isocyanides: (k_1, k_2): $[Cr(CO)_5(CNAr^{Dipp2})]$, (15.60, 15.92); $[Cr(CO)_5(CNAr^{Mes2})]$, (15.64, 15.95); $[Cr(CO)_5(CNAr^{DArF2})]$, (15.69, 15.96); $[Cr(CO)_5(CN\textit{p}\text{-}FAr^{DArF2})]$, (15.72, 15.98); $[(C_6F_5NC)Cr(CO)_5]$, (15.75, 16.00), $[(CF_3NC)Cr(CO)_5]$, (16.36, 16.779).

In order to enhance the electronic effects of *meta*-terphenyl isocyanide ligands, the Figueroa group synthetized the para-fluorinated terphenyl isocyanide $CN\textit{p}\text{-}FAr^{DArF2}$ and systematically compared it with a number of terphenyl isocyanides bearing different electron-withdrawing and donating substituents in their π-acidity relative to $[Cr(CNAr)(CO)_5]$ complexes (Fig. 11). This analysis suggested that σ-donor/π-acid ratios matching or exceeding that of CO may only be achieved by perfluorinated alkyl isocyanides, which are very difficult to handle due to their high instability, which severely limits their applicability. However, distant polyfluorination, as in the case of $CN\textit{p}\text{-}FAr^{DArF2}$, can effectively lower the σ-donor/π-acid ratio of the isocyano group, in a synthetically and operationally convenient manner. In conclusion, $CN\textit{p}\text{-}FAr^{DArF2}$ offers a large degree of steric encumbrance, combined with enhanced π-acceptor properties, which are very promising for the generation of low-coordinate isocyanide complexes.[56]

1.7 References

[1] a) W. R. Dolbier, *J. Fluorine Chem.* **2005**, *126*, 157-163; b) H. H. Nguyen, P. I. d. S. Maia, V. M. Deflon, U. Abram, *Inorg. Chem.* **2009**, *48*, 25-27.

[2] S. Purser, P. R. Moore, S. Swallow, V. Gouverneur, *Chem. Soc. Rev.* **2008**, *37*, 320-330.

[3] a) B. M. Kraft, R. J. Lachicotte, W. D. Jones, *J. Am. Chem. Soc.* **2001**, *123*, 10973-10979; b) J. L. Kiplinger, T. G. Richmond, C. E. Osterberg, *Chem. Rev.* **1994**, *94*, 373-431.

[4] A. Bondi, *The Journal of Physical Chemistry* **1964**, *68*, 441-451.

[5] a) C. Dalvit, *Prog. Nucl. Magn. Reson. Spectrosc.* **2007**, *51*, 243-271; b) M. A. Danielson, J. J. Falke, *Annu. Rev. Biophys. Biomol. Struct.* **1996**, *25*, 163-195.

[6] J. Fried, E. F. Sabo, *J. Am. Chem. Soc.* **1954**, *76*, 1455-1456.

[7] D. O'Hagan, *J. Fluorine Chem.* **2010**, *131*, 1071-1081.

[8] N. A. McGrath, M. Brichacek, J. T. Njardarson, *J. Chem. Educ.* **2010**, *87*, 1348-1349.

[9] a) P. W. Miller, N. J. Long, R. Vilar, A. D. Gee, **2008**, *47*, 8998-9033; b) L. Cai, S. Lu, V. W. Pike, **2008**, *2008*, 2853-2873; c) A. F. Brooks, J. J. Topczewski, N. Ichiishi, M. S. Sanford, P. J. H. Scott, *Chemical Science* **2014**, *5*, 4545-4553.

[10] M. Schlosser, **1998**, *37*, 1496-1513.

[11] E. P. Gillis, K. J. Eastman, M. D. Hill, D. J. Donnelly, N. A. Meanwell, *J. Med. Chem.* **2015**, *58*, 8315-8359.

[12] E. W. Price, C. Orvig, *Chem. Soc. Rev.* **2014**, *43*, 260-290.

[13] a) C. J. Anderson, M. J. Welch, *Chem. Rev.* **1999**, *99*, 2219-2234; b) L. A. Bass, M. Wang, M. J. Welch, C. J. Anderson, *Bioconjug. Chem.* **2000**, *11*, 527-532.

[14] a) J. B. Stimmel, M. E. Stockstill, F. C. Kull, *Bioconjug. Chem.* **2002**, *6*, 219-225; b) J. B. Stimmel, F. C. Kull, *Nucl. Med. Biol.* **1998**, *25*, 117-125.

[15] a) Y. H. Jang, M. Blanco, S. Dasgupta, D. A. Keire, J. E. Shively, W. A. Goddard, *J. Am. Chem. Soc.* **1999**, *121*, 6142-6151; b) S. Liu, D. S. Edwards, *Bioconjug. Chem.* **2001**, *12*, 7-34.

[16] World Nuclear association, Radioisotopes in Medicine, https://www.world-nuclear.org/information-library/non-power-nuclear-applications/radioisotopes-research/radioisotopes-in-medicine.aspx (updated December 2019).

[17] Z. A. S. M. Rathmann, S. Slikboer, H. A. Bilton, D. P. Snider, J. F. Valliant *The Radiopharmaceutical Chemistry of Technetium-99m*, Springer, Cham ed., **2019**.

[18] P. J. Blower, J. R. Dilworth, R. I. Maurer, G. D. Mullen, C. A. Reynolds, Y. Zheng, *J. Inorg. Biochem.* **2001**, *85*, 15-22.

[19] a) J. M. O'Sullivan, V. R. McCready, G. Flux, A. R. Norman, F. M. Buffa, S. Chittenden, M. Guy, K. Pomeroy, G. Cook, J. Gadd, J. Treleaven, A. Al-Deen, A. Horwich, R. A. Huddart, D.

P. Dearnaley, *Br. J. Cancer* **2002**, *86*, 1715-1720; b) S. Li, J. Liu, H. Zhang, M. Tian, J. Wang, X. Zheng, *Clin. Nucl. Med.* **2001**, *26*, 919-922.

[20] F. M. Nortier, S. J. Mills, G. F. Steyn, *Appl. Radiat. Isot.* **1990**, *41*, 1201-1208.

[21] M. L. T. R. E. Weiner, *Handbook of radiopharmaceuticals – radiochemistry and applications, Vol. 11*, John Wiley & Sons, Inc., Chichester ed., **2005**.

[22] P. J. Blower, *Dalton Trans.* **2015**, *44*, 4819-4844.

[23] S. I. P. J. R. Dilworth, *The Chemistry of Molecular Imaging, Vol. 7*, John Wiley & Sons, Inc., New Jersey ed., **2009**.

[24] a) M. L. P. Schwerdtfeger, in *Gold Chemistry, Applications and Future Directions in the Life Sciences*, Wiley-VCH, Weinheim, Germany ed., **2009**, pp. 183-248; b) A. L. M. C. Gimeno, in *Comprehensive Coordination Chemistry II, Vol. 9*, Elsevier Ltd, London UK ed., **2003**, pp. 883-911.

[25] P. I. Maia, V. M. Deflon, U. Abram, *Future Med Chem* **2014**, *6*, 1515-1536.

[26] A. E. Finkelstein, D. T. Walz, V. Batista, M. Mizraji, F. Roisman, A. Misher, *Ann. Rheum. Dis.* **1976**, *35*, 251-257.

[27] a) C. Gabbiani, A. Casini, L. J. G. B. Messori, **2007**, *40*, 73-81; b) A. Casini, C. Hartinger, C. Gabbiani, E. Mini, P. J. Dyson, B. K. Keppler, L. Messori, *J. Inorg. Biochem.* **2008**, *102*, 564-575.

[28] B. Đ. Glišić, M. I. Djuran, *Dalton Trans.* **2014**, *43*, 5950-5969.

[29] J. S. Casas, M. S. García-Tasende, J. Sordo, *Coord. Chem. Rev.* **2000**, *209*, 197-261.

[30] D. X. West, M. M. Salberg, G. A. Bain, A. E. J. T. M. C. Liberta, **1997**, *22*, 180-184.

[31] R. B. Singh, H. Ishii, *Crit. Rev. Anal. Chem.* **1991**, *22*, 381-409.

[32] a) A. A. Oliveira, G. M. Perdigao, L. E. Rodrigues, J. G. da Silva, E. M. Souza-Fagundes, J. A. Takahashi, W. R. Rocha, H. Beraldo, *Dalton Trans.* **2017**, *46*, 918-932; b) A. R. Aguirre, G. L. Parrilha, R. Diniz, B. C. Ribeiro, R. G. D. Santos, H. Beraldo, *Polyhedron* **2019**, *164*, 219-227.

[33] K. S. O. Ferraz, J. G. Da Silva, F. M. Costa, B. M. Mendes, B. L. Rodrigues, R. G. dos Santos, H. J. B. Beraldo, **2013**, *26*, 677-691.

[34] P. N. Fonteh, F. K. Keter, D. Meyer, *J. Inorg. Biochem.* **2011**, *105*, 1173-1180.

[35] S. D. Khanye, B. Wan, S. G. Franzblau, J. Gut, P. J. Rosenthal, G. S. Smith, K. Chibale, *J. Organomet. Chem.* **2011**, *696*, 3392-3396.

[36] a) N. Fujii, J. P. Mallari, E. J. Hansell, Z. Mackey, P. Doyle, Y. M. Zhou, J. Gut, P. J. Rosenthal, J. H. McKerrow, R. K. Guy, *Bioorg. Med. Chem. Lett.* **2005**, *15*, 121-123; b) S. D. Khanye, G. S. Smith, C. Lategan, P. J. Smith, J. Gut, P. J. Rosenthal, K. Chibale, *J. Inorg. Biochem.* **2010**, *104*, 1079-1083; c) R. Arancibia, A. H. Klahn, M. Lapier, J. D. Maya, A. Ibañez, M. T. Garland, S. Carrère-Kremer, L. Kremer, C. Biot, *J. Organomet. Chem.* **2014**, *755*, 1-6; d) A. R. Rettondin, Z. A. Carneiro, A. C. Goncalves, V. F. Ferreira, C. G. Oliveira,

A. N. Lima, R. J. Oliveira, S. de Albuquerque, V. M. Deflon, P. I. Maia, *Eur. J. Med. Chem.* **2016**, *120*, 217-226.

[37] A. E. Liberta, D. X. West, *Biometals* **1992**, *5*, 121-126.

[38] D. X. West, A. E. Liberta, S. B. Padhye, R. C. Chikate, P. B. Sonawane, A. S. Kumbhar, R. G. Yerande, *Coord. Chem. Rev.* **1993**, *123*, 49-71.

[39] G. Weber, J. Hartung, L. Beyer, *Tetrahedron Lett.* **1988**, *29*, 3475-3476.

[40] L. Beyer, J. Hartung, R. Widera, *Tetrahedron* **1984**, *40*, 405-412.

[41] P. I. da S. Maia, H. H. Nguyen, D. Ponader, A. Hagenbach, S. Bergemann, R. Gust, V. M. Deflon, U. Abram, *Inorg. Chem.* **2012**, *51*, 1604-1613.

[42] a) P. I. Maia, Z. A. Carneiro, C. D. Lopes, C. G. Oliveira, J. S. Silva, S. de Albuquerque, A. Hagenbach, R. Gust, V. M. Deflon, U. Abram, *Dalton Trans.* **2017**, *46*, 2559-2571; b) P. I. Maia, H. H. Nguyen, A. Hagenbach, S. Bergemann, R. Gust, V. M. Deflon, U. Abram, *Dalton Trans.* **2013**, *42*, 5111-5121.

[43] a) E. Chatelain, *J. Biomol. Screen.* **2015**, *20*, 22-35; b) J. Bermudez, C. Davies, A. Simonazzi, J. P. Real, S. Palma, *Acta Trop.* **2016**, *156*, 1-16.

[44] S. P. Fricker, R. M. Mosi, B. R. Cameron, I. Baird, Y. Zhu, V. Anastassov, J. Cox, P. S. Doyle, E. Hansell, G. Lau, J. Langille, M. Olsen, L. Qin, R. Skerlj, R. S. Wong, Z. Santucci, J. H. McKerrow, *J. Inorg. Biochem.* **2008**, *102*, 1839-1845.

[45] D. Vital, M. Arribas, G. Trossini, *Letters in Drug Design & Discovery* **2014**, *11*, 249-255.

[46] a) L. Malatesta, F. Bonati, *Isocyanide complexes of metals*, Wiley-Interscience, **1969**; b) H. E. O. Eric Singleton, in *Adv. Organomet. Chem., Vol. 22* (Ed.: R. W. F.G.A. Stone), **1983**, pp. 209-310; c) Y. Yamamoto, *Coord. Chem. Rev.* **1980**, *32*, 193-233; d) P. M. Treichel, in *Adv. Organomet. Chem., Vol. 11*, Academic Press ed. (Ed.: R. W. F.G.A. Stone), **1973**, pp. 21-86.

[47] a) D. Lentz, *J. Organomet. Chem.* **1990**, *381*, 205-212; b) D. Lentz, M. Anibarro, D. Preugschat, G. Bertrand, *J. Fluorine Chem.* **1998**, *89*, 73-81; c) D. Lentz, **1994**, *33*, 1315-1331.

[48] B. J. Fox, Q. Y. Sun, A. G. DiPasquale, A. R. Fox, A. L. Rheingold, J. S. Figueroa, *Inorg. Chem.* **2008**, *47*, 9010-9020.

[49] T. B. Ditri, B. J. Fox, C. E. Moore, A. L. Rheingold, J. S. Figueroa, *Inorg. Chem.* **2009**, *48*, 8362-8375.

[50] D. Lentz, B. Pötter, R. Marschall, I. Brüdgam, J. Fuchs, *Chem. Ber.* **1990**, *123*, 257-260.

[51] G. P. T. J. C. M. Lukehart, V. Zeile K. P. Darst, L. T. Warfield, B. Duane Dombek Robert, J. Angelici, J. A. Gladysz, J. C. Selover in *Inorg. Synth.* (Ed.: R. J. Angelici), **1990**, pp. 199-202.

[52] H. H. Knight Castro, A. Meetsma, J. H. Teuben, W. Vaalburg, K. Panek, G. Ensing, *J. Organomet. Chem.* **1991**, *410*, 63-71.

[53] M. A. Stewart, C. E. Moore, T. B. Ditri, L. A. Labios, A. L. Rheingold, J. S. Figueroa, *Chem Commun (Camb)* **2011**, *47*, 406-408.

[54] a) R. F. Johnston, J. C. Cooper, *Journal of Molecular Structure: THEOCHEM* **1991**, *236*, 297-307; b) G. J. Essenmacher, P. M. Treichel, *Inorg. Chem.* **2002**, *16*, 800-806.

[55] T. B. Ditri, A. E. Carpenter, D. S. Ripatti, C. E. Moore, A. L. Rheingold, J. S. Figueroa, *Inorg. Chem.* **2013**, *52*, 13216-13229.

[56] A. E. Carpenter, C. C. Mokhtarzadeh, D. S. Ripatti, I. Havrylyuk, R. Kamezawa, C. E. Moore, A. L. Rheingold, J. S. Figueroa, *Inorg. Chem.* **2015**, *54*, 2936-2944.

2 Abstract

In this thesis, a series of novel fluorinated ligands and corresponding metal complexes is presented. All compounds were spectroscopically and/or crystallographically characterized.

The synthesis of a series of differently halogenated *S,N,S*-tridentate thiosemicarbazone ligands and their Re(V), Tc(V), Au(III) and In(III) complexes is described. The fluorination reduces the stability of the free ligands against hydrolysis but does not influence significantly the structure and stability of the Re, Tc and Au complexes. On the contrary, the structures and properties of the In(III) complexes are affected by fluorination. Some of the compounds were investigated regarding to their biological activity against *Trypanosoma cruzi*, a parasite responsible for a tropical disease, known as *Chagas disease*.

Subsequently, the synthesis of Re(I) and Tc(I) complexes with fluorinated and non-fluorinated *meta*-terphenyl isocyanides is described. Reactions of $[Re(CO)_5Br]$ and $(NBu_4)[Tc_2(CO)_6(\mu\text{-}Cl)_3]$ with the encumbering isocyanides give stable complexes with a high degree of steric protection, which are suitable starting materials for the formation of highly-reduced and low-coordinated metal species. The reaction of the Re(I) and Tc(I) isocyanide complexes with different reducing agents is reported, leading to defined products containing persistent monomeric Re(0) complexes or rhenium in a negative formal oxidation state. Moreover, the first known complex with Tc in the formal –1 oxidation state was characterized with NMR spectroscopy.

3 Zusammenfassung

Eine Reihe neuer halogenierter Liganden und entsprechender Metallkomplexe wurde hergestellt. Alle Verbindungen wurden spektroskopisch und/oder kristallographisch charakterisiert.

Die Synthese einer Serie halogensubstituierter *S,N,S*-dreizähniger Thiosemicarbazonliganden und ihrer Re(V)-, Tc(V)-, Au(III)- und In(III)-Komplexe ist beschrieben. Die Fluorierung erhöht die Hydrolyse-empfindlichkeit der freien Liganden, aber es wurden keine Auswirkungen auf die Stabilität der Komplexe beobachtet. Dagegen werden die Strukturen der erhaltenen In(III)-Komplexe stark von der Fluorierung beeinflusst. Die biologische Aktivität der fluorierten Thiosemicarbazone sowie ihrer Metallkomplexe gegen *Trypanosoma cruzi*, einen Parasit, der die sogenannte Chagas Krankheit verursacht, wurde untersucht und für einige Vertreter wurde eine bemerkenswerte Wirksamkeit festgestellt.

Im zweiten Teil der vorliegenden Arbeit wird die Synthese von Re(I) und Tc(I) Komplexen mit fluorierten und nicht fluorierten *meta*-Terphenyl-isocyaniden beschrieben. Die Umsetzung von $[Re(CO)_5Br]$ and $(NBu_4)[Tc_2(CO)_6(\mu\text{-}Cl)_3]$ mit den sterisch anspruchvollen Isocyaniden ergibt stabile Komplexe, in denen die Metallzentren effizient von den Terphenyl-Gruppen abgeschirmt werden. Sie sind geeignete Ausgangsverbindungen für die Synthese hoch-reduzierter und koordinativ ungesättigter Metallkomplexe.

Die Umsetzung der Re(I)- und Tc(I)-Isocyanidkomplexe mit verschiedenen Reduktionsmitteln wurde untersucht. Auf diese Weise konnten stabile monomere Rhenium(0)-Komplexe isoliert werden sowie Verbindungen, in denen das Metallatom eine negative formale Oxidationsstufe aufweist. Außerdem wurde der erste Technetiumkomplex in der formalen Oxidationsstufe ‚-1' durch ^{99}Tc-NMR-Spektroskopie charakterisiert.

4 Publications

4.1 List of the publications

I. Thiosemicarbazones and Thiadiazines Derived from Fluorinated Benzoylthioureas: Synthesis, Crystal Structure and Anti-*Trypanosoma cruzi* Activity.

Federico Salsi, Gisele Bulhões Portapilla, Konstantin Schutjajew, Zumira Aparecida Carneiro, Adelheid Hagenbach, Sérgio de Albuquerque, Pedro Ivo da Silva Maia, Ulrich Abram.

Journal of Fluorine Chemistry **2018**, *215*, 52–61.

II. Organometallic Gold(III) Complexes with Tridentate Halogen-Substituted Thiosemicarbazones: Effect of Halogenation on Cytotoxicity and Anti-Parasitic Activity.

Federico Salsi, Gisele Bulhões Portapilla, Konstantin Schutjajew, Maximilian Roca Jungfer, Amanda Goulart, Adelheid Hagenbach, Sérgio de Albuquerque, Ulrich Abram.

European Journal of Inorganic Chemistry **2019**, *41*, 4455–4462.

III. Effect of Fluorination on the Structure and Anti-*Trypanosoma cruzi* Activity of Oxorhenium(V) Complexes with *S,N,S*-Tridentate Thiosemicarbazones and Benzoylthioureas. Synthesis and Structures of Technetium(V) Analogues.

Federico Salsi, Gisele Bulhões Portapilla, Saskia Simon, Maximilian Roca Jungfer, Adelheid Hagenbach, Sérgio de Albuquerque, Ulrich Abram.

Inorganic Chemistry **2019**, *58*, 10129-10138.

IV. Trigonal-bipyramidal vs. Octahedral Coordination in In(III) Complexes with Potentially *S,N,S*-Tridentate Thiosemicarbazones.

Federico Salsi, Maximilian Roca Jungfer, Adelheid Hagenbach, Ulrich Abram.

European Journal of Inorganic Chemistry **2020**, *13*, 1222–1229.

V. Structural and Redox Variations in Technetium Complexes Supported by m-Terphenyl Isocyanides.

Guilhem Claude, Federico Salsi, Adelheid Hagenbach, Milan Gembicky, Michael Neville, Chinglin Chan, Joshua S. Figueroa, Ulrich Abram.

Organometallics **2020**, *39*, 2287−2294, https://doi.org/10.1021/acs.organomet.0c00238.

VI. A Closed-shell Monomeric Rhenium(1-) Anion Provided by m-Terphenyl Isocyanide Ligation.

Federico Salsi, Michael Neville, Myles Drance, Adelheid Hagenbach, Chinglin Chan, Joshua S. Figueroa, Ulrich Abram

Chemical Communications **2020**, https://doi.org/10.1039/d0cc03043k.

VII. $[M^{I}(CO)X(CNAr^{DArF2})_4]$ (DArF = 3,5-$(CF_3)_2C_6H_3$; M = Re, Tc; X = Br, Cl) complexes: convenient platforms for the synthesis of low-valent rhenium and technetium compounds.

Federico Salsi, Michael Neville, Myles Drance, Adelheid Hagenbach, Joshua S. Figueroa, Ulrich Abram.

Manuscript to be submitted to *Organometallics.*

4.2 Thiosemicarbazones and Thiadiazines Derived from Fluorinated Benzoylthioureas: Synthesis, Crystal Structure and Anti-*Trypanosoma cruzi* Activity

Authors	Federico Salsi, Gisele Bulhões Portapilla, Konstantin Schutjajew, Zumira Aparecida Carneiro, Adelheid Hagenbach, Sérgio de Albuquerque, Pedro Ivo da Silva Maia, Ulrich Abram
Journal	Journal of Fluorine Chemistry **2018**, *215*, 52–61
DOI	10.1016/j.jfluchem.2018.08.004
Links	https://www.sciencedirect.com/science/article/abs/pii/S002211391830277X
Detailed scientific contribution	Federico Salsi and Ulrich Abram designed the project. Federico Salsi performed the synthesis and characterization of the compounds and wrote the manuscript. Gisele Bulhões Portapilla designed and performed the biological tests and took part to the preparation of the manuscript. Zumira Aparecida Carneiro, Pedro Ivo da Silva Maia and Sérgio de Albuquerque supervised the biological experiments. Konstantin Schutjajew did some of the chemical experiments during his research internship, which was supervised by Federico Salsi. Adelheid Hagenbach performed the diffractometric measurements and the refinement of the crystal structures. Ulrich Abram supervised the project, provided scientific guidance and suggestions and corrected the manuscript.
Estimated own contribution	80%

4.3 Organometallic Gold(III) Complexes with Tridentate Halogen-Substituted Thiosemicarbazones: Effet of Halogenation on Cytotoxicity and Anti-Parasitic Activity

Authors	Federico Salsi, Gisele Bulhões Portapilla, Konstantin Schutjajew, Maximilian Roca Jungfer, Amanda Goulart, Adelheid Hagenbach, Sérgio de Albuquerque, Ulrich Abram
Journal	European Journal of Inorganic Chemistry **2019***, 41,* 4455–4462
DOI	10.1002/ejic.201900904
Links	https://chemistry-europe.onlinelibrary.wiley.com/doi/full/10.1002/ejic.201900904

Detailed scientific contribution

Federico Salsi and Ulrich Abram designed the project. Federico Salsi performed the synthesis and characterization of the compounds and wrote the manuscript.

Gisele Bulhões Portapilla designed and performed the biological tests and took part to the preparation of the manuscript. Amanda Goulart did some of the biological tests during her research internship, which was supervised by Gisele Bulhões Portapilla. Sérgio de Albuquerque supervised the biological experiments. Konstantin Schutjajew and Maximilian Roca Jungfer did some of the chemical experiments during his research internship, which was supervised by Federico Salsi. Adelheid Hagenbach performed the diffractometric measurements and helped with the refinement of the crystal structures.

Ulrich Abram supervised the project, provided scientific guidance and suggestions and corrected the manuscript.

Estimated own contribution	70%

4.4 Effect of Fluorination on the Structure and Anti-*Trypanosoma cruzi* Activity of Oxorhenium(V) Complexes with *S,N,S*-Tridentate Thiosemicarbazones and Benzoylthioureas. Synthesis and Structures of Technetium(V) Analogues

Authors	Federico Salsi, Gisele Bulhões Portapilla, Saskia Simon, Maximilian Roca Jungfer, Adelheid Hagenbach, Sérgio de Albuquerque, Ulrich Abram
Journal	Inorganic Chemistry **2019**, *58*, 10129-10138
DOI	10.1021/acs.inorgchem.9b01260
Links	https://pubs.acs.org/doi/full/10.1021/acs.inorgchem.9b01260
Detailed scientific contribution	Federico Salsi and Ulrich Abram designed the project. Federico Salsi performed the synthesis and characterization of the compounds and wrote the manuscript. Gisele Bulhões Portapilla designed and performed the biological tests and took part to the preparation of the manuscript. Sérgio de Albuquerque supervised the biological experiments. Saskia Simon and Maximilian Roca Jungfer did some of the chemical experiments during their research internships, which were supervised by Federico Salsi. Adelheid Hagenbach performed the diffractometric measurements and helped with the refinement of the crystal structures. Ulrich Abram supervised the project, provided scientific guidance and suggestions and corrected the manuscript
Estimated own contribution	70%

4.5 Trigonal-bipyramidal vs. Octahedral Coordination in In(III) Complexes with Potentially *S,N,S*-Tridentate Thiosemicarbazones

Authors	Federico Salsi, Maximilian Roca Jungfer, Adelheid Hagenbach, Ulrich Abram
Journal	European Journal of Inorganic Chemistry **2020**, *13*, 1222–1229
DOI	10.1002/ejic.201901356
Links	https://chemistry-europe.onlinelibrary.wiley.com/doi/full/10.1002/ejic.201901356
Detailed scientific contribution	Federico Salsi and Ulrich Abram designed the project. Federico Salsi performed the synthesis and characterization of the compounds and wrote the manuscript. Maximilian Roca Jungfer did some of the chemical experiments during his research internship, which was supervised by Federico Salsi, performed the theoretical calculations and took part to the preparation of the manuscript. Adelheid Hagenbach performed the diffractometric measurements and helped with the refinement of the crystal structures. Ulrich Abram supervised the project, provided scientific guidance and suggestions and corrected the manuscript.
Estimated own contribution	80%

4.6 Structural and Redox Variations in Technetium Complexes Supported by m-Terphenyl Isocyanides

Authors	Guilhem Claude, Federico Salsi, Adelheid Hagenbach, Milan Gembicky, Michael Neville, Chinglin Chan, Joshua S. Figueroa, Ulrich Abram
Journal	Organometallics **2020**, *39*, 2287−2294
DOI	10.1021/acs.organomet.0c00238
Links	https://pubs.acs.org/doi/10.1021/acs.organomet.0c00238
Detailed scientific contribution	Federico Salsi performed the synthesis, analysis and structural characterization of the first known *meta*-terphenyl complex of technetium: $[Tc(CNAr^{Dipp2})_2(CO)_3Cl]$ and took part to the preparation of the manuscript. Guilhem Claude, Ulrich Abram and Joshua Figueroa designed the project. Chinglin Chan synthetized the ligands. Guilhem Claude and Ulrich Abram performed the remaining syntheses and characterizations of the compounds and wrote the manuscript. Adelheid Hagenbach and Milan Gembicky performed the diffractometric measurements and helped with the refinement of the crystal structures. Ulrich Abram and Joshua S. Figueroa supervised the project, provided scientific guidance and suggestions and corrected the manuscript.
Estimated own contribution	30%

4.7 A Closed-shell Monomeric Rhenium(1-) Anion Provided by m-Terphenyl Isocyanide Ligation

Authors	Federico Salsi, Michael Neville, Myles Drance, Adelheid Hagenbach, Chinglin Chan, Joshua S. Figueroa, Ulrich Abram
Journal	Chemical Communications **2020**
DOI	10.1039/d0cc03043k
Links	https://pubs.rsc.org/en/content/articlelanding/2020/cc/d0cc03043k#!divAbstract
Detailed scientific contribution	Federico Salsi, Ulrich Abram and Joshua Figueroa designed the project. Federico Salsi performed the synthesis and characterization of the compounds and wrote the manuscript. Michael Neville and Myles Drance performed some diffractometric measurements and provided scientific advice; Michael Neville also performed the theoretical calculations and took part in the preparation of the manuscript. Chinglin Chan synthetized the ligand. Adelheid Hagenbach performed one diffractometric measurement and helped with the refinement of the crystal structures. Joshua S. Figueroa and Ulrich Abram supervised the project, provided scientific guidance and suggestions, and corrected the manuscript.
Estimated own contribution	80%

4.8 $[M^{I}(CO)X(CNAr^{DArF2})_4]$ (DArF = 3,5-$(CF_3)_2C_6H_3$; M = Re, Tc; X = Br, Cl) complexes: convenient platforms for the synthesis of low-valent rhenium and technetium compounds

Authors	Federico Salsi, Michael Neville, Myles Drance, Adelheid Hagenbach, Joshua S. Figueroa, Ulrich Abram
Journal	
DOI	–
Links	–
Detailed scientific contribution	Federico Salsi, Ulrich Abram and prof. Joshua Figueroa designed the project. Federico Salsi performed the synthesis and characterization of the compounds and wrote the manuscript. Michael Neville and Myles Drance performed diffractometric measurements and provided scientific advice. Adelheid Hagenbach performed diffractometric measurements and helped with the refinement of the crystal structures. Joshua S. Figueroa and Ulrich Abram supervised the project, provided scientific guidance and suggestions, and corrected the manuscript.
Estimated own contribution	80%

$[M^{I}(CO)X(CNAr^{DArF2})_4]$ (DArF = 3,5-$(CF_3)_2C_6H_3$; M = Re, Tc; X = Br, Cl) complexes: convenient platforms for the synthesis of low-valent rhenium and technetium compounds

Federico Salsi,[†] Michael Neville,[‡] Myles Drance,[‡] Adelheid Hagenbach,[†] Joshua S. Figueroa,[‡*] and Ulrich Abram[†*]

[†] Freie Universität Berlin, Institute of Chemistry and Biochemistry, Fabeckstr. 34/36, D-14195 Berlin, Germany

[‡] Department of Chemistry and Biochemistry, University of California, San Diego, 9500 Gilman Drive, Mail Code 0358, La Jolla, CA 92093, USA

Supporting Information Placeholder

ABSTRACT: $[Re(CO)Br(CNAr^{DArF2})_4]$ and $[Tc(CO)Cl(CNAr^{DArF2})_4]$ (Ar^{DArF} = 2,6-(3,5-$(CF_3)_2C_6H_3)_2$-4-F-C_6H_2) were prepared by reactions of $[Re(CO)Br_5]$ or $(NBu_4)[Tc_2(CO)_6(\mu\text{-}Cl)_3]$ with the sterically encumbered isocyanide $CNAr^{DArF2}$. These two compounds proved to be excellent starting materials for the synthesis of unprecedented low-valent rhenium and technetium complexes. The reduction of $[Re(CO)Br(CNAr^{DArF2})_4]$ with Na/Hg produces an equimolar mixture of $[Re(CO)(CNAr^{DArF2})_4]$ and $[Na(THF)_6][Re(CO)(CNAr^{DArF2})_4]$ containing the transition metal in the oxidation states "0" and "-1", respectively. The reduction of $[Tc(CO)Cl(CNAr^{DArF2})_4]$ with Na/Hg produces $Na[Tc(CO)(CNAr^{DArF2})_4]$, which was characterized by ^{19}F and ^{99}Tc NMR spectroscopy. The reactivities of the M(-1) compounds (M = Re, Tc) resemble that of $[Re(CO)_5]^-$, which was proven by reactions with a number of electrophiles such as MeI, HCl or $F_6C_5C(O)Cl$.

INTRODUCTION

Sterically encumbered isocyanides, in particular *meta*-terphenyl isocyanides, are able to form stable complexes with a wide variety of transition metals, which efficiently mimic low-valent and highly reactive carbonyl species, which otherwise would be inaccessible for preparative chemistry.[1-4] Very recently, we described the isolation and structural characterization of the rhenium monoanion $[Re(CO)_3(CNAr^{Dipp2})_2]^-$ (Dipp2 = 2,6-diisopropylphenyl, see Chart 1), which is an analog of the well-known $[Re(CO)_5]^-$ anion, as a contact ion pair with a K^+ counterion.[5] Moreover, the extensive π-delocalization and the efficient steric protection of the *meta*-terphenyl groups enabled us to isolate a rare example of a monomeric rhenium(0) complex, $[Re(CO)_3(CNAr^{Dipp2})_2]$, which was characterized through EPR and IR spectroscopy.

These promising results and previous studies on manganese[1,6] encouraged us to consider that a similar chemistry might also be extended to the homologous element technetium. Technetium is the lightest element of the periodic table that only possesses radioactive isotopes. The short-lived γ-emitting nuclear isomer ^{99m}Tc is used in nuclear medicine as imaging agent for a wide variety of diagnostic tests.[7] The ground state of this nuclide, ^{99}Tc, is a low-energy β^--emitter (E_{max} = 0.292 MeV). Its long half-life (2.1 × 10^5 years) and availability in macroscopic amounts make it the ideal candidate for chemical studies.[8]

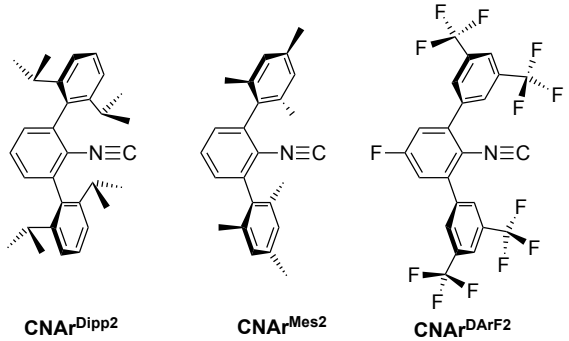

Chart 1. Sterically encumbering isocyanides used or discussed in this paper.

In contrast to its rhenium analog, the pentacarbonyltechnetate $[Tc(CO)_5]^-$, is in practice hardly accessible, because of the absence of a facile synthetic procedure, which is conform with the actual radiation protection regulations.[9] For this reason, a possible use of isocyanides as CO surrogates would be of particular value, since it opens the door to a completely unexplored field of technetium chemistry.

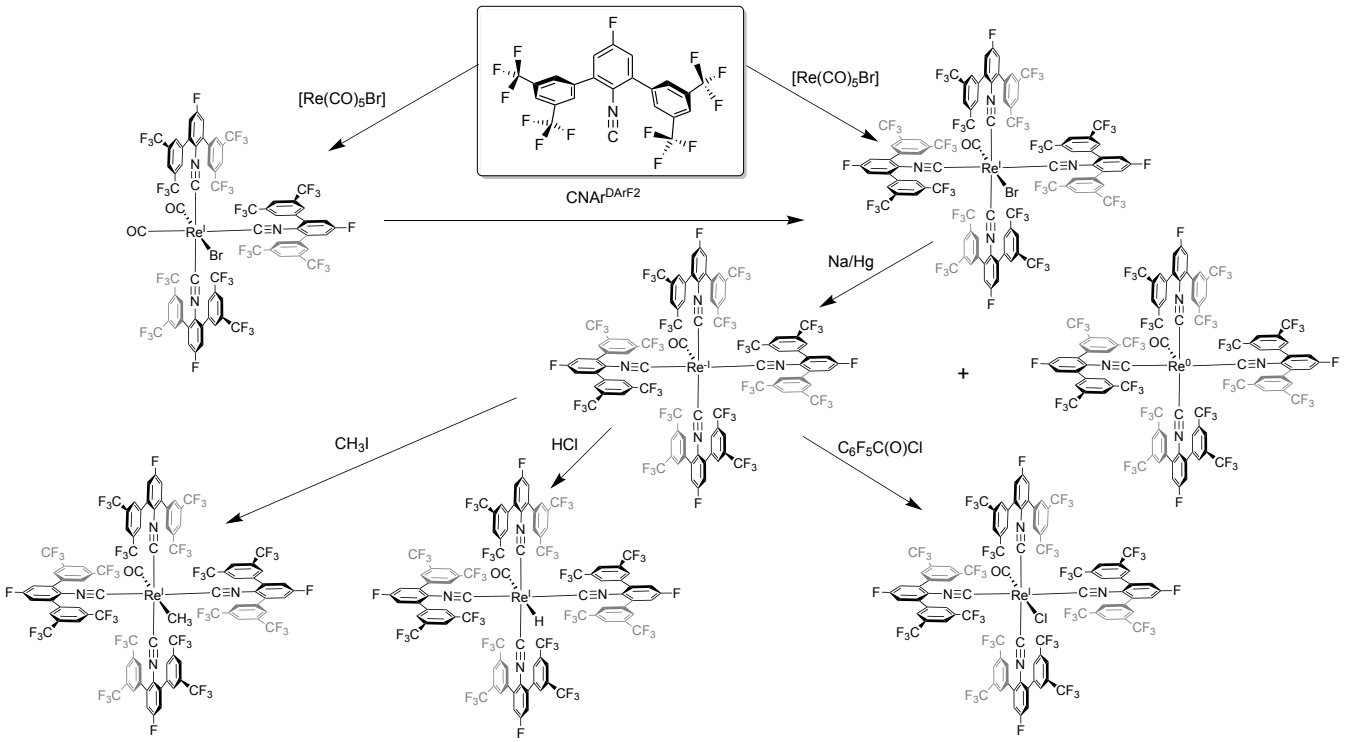

Scheme 1. Rhenium complexes with $CNAr^{DArF2}$.

As reported by Lentz, perfluorination of the organic residue of an isocyanide can increase its π-acceptor properties, offering a strategy to more finely mimicking the electronic properties of CO.[10] This is true, in general, for electron-withdrawing substituents on aryl isocyanides, and particularly for such in the *para*-position of the aromatic ring.[11]

Recently, the fluorinated *meta*-terphenyl isocyanide $CNAr^{DArF2}$ (Ar^{DArF} = 2,6-(3,5-$(CF_3)_2C_6H_3)_2$-4-F-C_6H_2, see Chart 1) has been introduced. It can be synthesized by palladium-catalyzed cross-coupling of 2,6-dibromoaniline with 3,5-$(CF_3)_2$-4-F-$C_6H_2B(OH)_2$ and subsequent formylation/dehydration steps.[12] Although σ-donor/π-acid ratios matching or exceeding that of CO may only be achieved by perfluorinated alkyl isocyanides, which are unstable and very difficult to handle, $CNAr^{DArF2}$ might be a suitable candidate to mimic the bonding situation of CO ligands. Distant polyfluorination can effectively lower the σ-donor/π-acid ratio of the isocyano group, in a synthetically and operationally convenient manner.[13] At the same time, $CNAr^{DArF2}$ offers a large degree of steric encumbrance, which, combined with enhanced π-acceptor properties, makes it very promising for the generation of low-coordinate isocyanide complexes.

In the present paper, we report an initial survey of the coordination capabilities of $CNAr^{DArF2}$ to low-valent rhenium and technetium species. These studies are intended (i) to serve as the framework for uncovering the hitherto less explored (Re) or unknown (Tc) chemistry of these two elements in the formal oxidation states "0" and "-1" and (ii) to develop a new generation of organometallic Tc(I) cores with the required stability for nuclear-medical labelling experiments.

RESULTS AND DISCUSSION

The interesting results of a previous report, which describes the formation of the tris-isocyanide complex $[Mn(CO)_2Br(CNAr^{Mes2})_3]$ by a facile reaction of $[Mn(CO)_5Br]$ and three equivalents of the sterically encumbered isocyanide $CNAr^{Mes2}$ (Mes = 2,4,6-$Me_3C_6H_2$, see Chart 1) in THF,[6] encouraged us to undertake similar reactions with corresponding technetium and rhenium starting materials. A summary of the performed reactions between $CNAr^{DArF2}$ and [Re(CO)Br] and subsequent reactions of the formed products is given in Scheme 1. Scheme 2 shows similar reactions done with technetium compounds. Unexpectedly, the reaction of $[Re(CO)_5Br]$ with three equivalents of $CNAr^{DArF2}$ in boiling THF led only to an

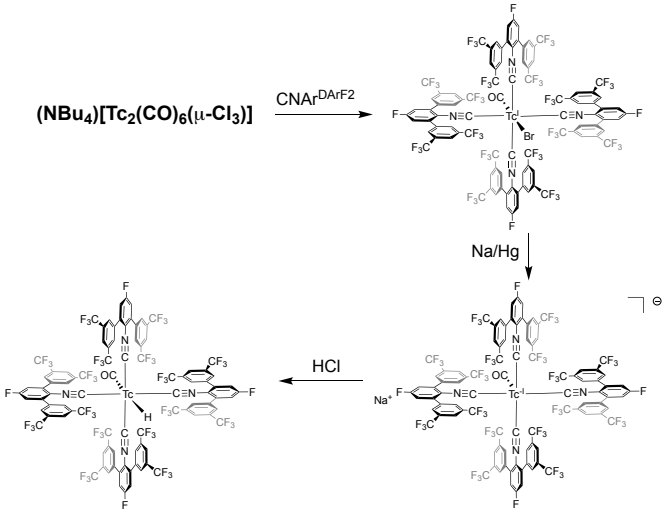

Scheme 2. Technetium complexes with $CNAr^{DArF2}$.

intractable mixture from which no crystalline compounds could be isolated. Defined products, however, were obtained at higher temperature. Prolonged heating of such a reaction mixture in toluene afforded the complete consumption of the reactants and an orange-red solid was isolated. The ^{19}F NMR spectrum of the raw product surprisingly shows three triplets around –109 ppm (each one belonging to the *para*-fluoride substituent of the aryl group of a $CNAr^{DArF2}$ molecule). They can be assigned to two different species: (i) two of the signals exhibit an approximate 1:2 integral ratio, which is consistent with a tris-ligated *mer*-$[Re(CO)_2Br(CNAr^{DArF2})_3]$ complex and (ii) one additional triplet suggests the formation of a complex with magnetically identical ligands. The presence of two new species is also confirmed by the IR spectrum of the product mixture, which shows two different carbonyl patterns. Interestingly, also some unreacted starting material $[Re(CO)_5Br]$ seems to be left, while the bulky isocyanide was completely consumed. These findings suggest the formation of at least one complex with four $CNAr^{DArF2}$ ligands, which was confirmed by X-ray structural analyses.

A few orange-red single crystals were hand-picked and identified as *cis,mer*-$[Re(CO)_2Br(CNAr^{DArF2})_3]$. The molecular structure of the compound is shown in Fig. 1. Three isocyanide ligands are coordinated in a *meridional* arrangement by the rhenium atom, the coordination sphere of which is completed by two *cis*-coordinated carbonyls and a Br^- ligand.

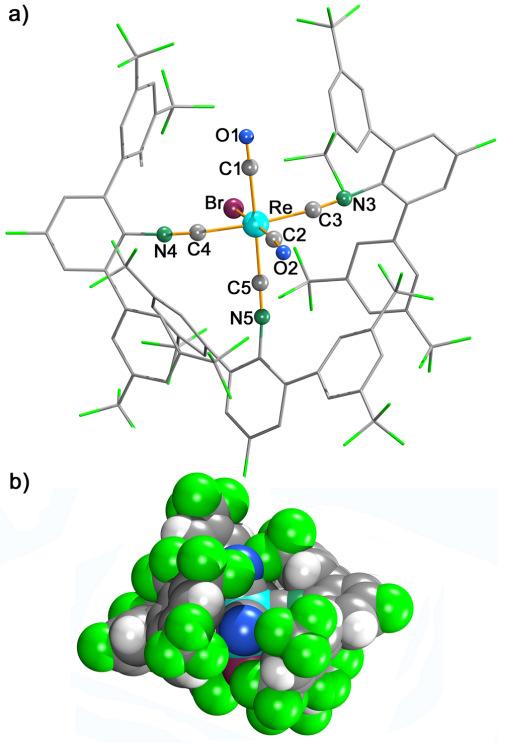

Figure 1. a) Molecular structure of *cis,mer*-$[Re(CO)_2Br(CNAr^{DArF2})_3]$ and b) space-filling model of the molecule.

The third ^{19}F NMR signal observed in the raw product mixture can be assigned to a complex with higher symmetry. It represents the "thermodynamic product" of the performed reaction, $[Re(CO)Br(CNAr^{DArF2})_4]$, and can be isolated in high yields and pure form, when at least four equivalents of $CNAr^{DArF2}$ are used and the reaction is performed in boiling toluene.

The ^{19}F NMR of $[Re(CO)Br(CNAr^{DArF2})_4]$ reveals a perfect axial symmetry in solution through the magnetic equivalence of the four isocyanide ligands, which produces only one triplet for the para fluorine atoms at –109 ppm and one singlet for the CF_3 groups at –63 ppm. The solid-state IR spectrum displays a broad band at 2051 cm^{-1} for the isocyanides and a splitted band at 1920 cm^{-1} for the CO ligand. The significant red-shift of the cyano stretch in comparison to the non-coordinated isocyanide (ν_{CN} = 2118 cm^{-1}) denotates an efficient π-back donation, which was not observed in rhenium and technetium complexes with the non-fluorinated *m*-terphenyl isocyanides $CNAr^{Dipp2}$ or $CNAr^{Mes2}$.[5,14,15]

Single crystal X-ray diffraction confirms the equivalence of the four $CNAr^{DArF2}$ ligands, which are coordinated in one plane (Fig. 2). Selected bond lengths and angles as well as an ellipsoid representation of $[Re(CO)_2Br(CNAr^{DArF2})_3]$ and $[Re(CO)Br(CNAr^{DArF2})_4]$ are given in the Supplementary Information.

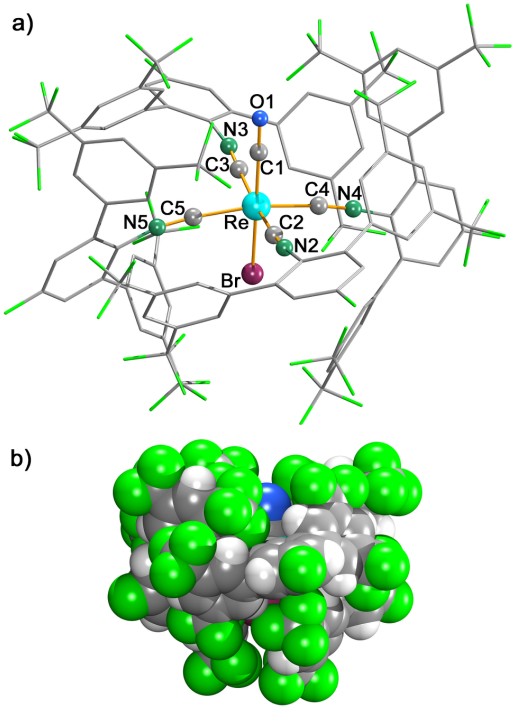

Figure 2. a) Molecular structure of $[Re(CO)Br(CNAr^{DArF2})_4]$ and b) space-filling model of the molecule.

The space-filling model of $[Re(CO)Br(CNAr^{DArF2})_4]$ (Fig. 2b) illustrates that the rhenium atom is perfectly shielded in this compound by the interdigitation observed for the fluorinated flanking rings. This creates a qualitatively high degree of shielding for the central transition metal ion, which is clearly higher than that in the dicarbonyl compound $[Re(CO)_2Br(CNAr^{DArF2})_3]$ (Fig. 1b).

The efficient steric protection of the metal atom in $[Re(CO)Br(CNAr^{DArF2})_4]$ provided by four encumbering *meta*-terphenyl isocyanides and the enhanced π-back donation through fluorination makes this compound a convenient candidate for the preparation of highly reduced rhenium complexes. Indeed, treatment of [Re(CO)Br-

$(CNAr^{DArF2})_4$] with 0.1% sodium amalgam in THF led to a very dark solution, from which black crystals precipitated at –35° C after the addition of pentane. The crystals rapidly decompose at room temperature by the loss of solvent THF. Solid state IR analysis of the product confirms the complete consumption of the reactants and the formation of (a) new compound(s) with broad CN absorption(s) around 1906 cm^{-1}. Such a drastic red-shift of almost 150 cm^{-1} is indicative for the formation of a highly reduced rhenium compound as has been reported recently for similar $CNAr^{Dipp2}$ complexes.[5] ^1H and ^{19}F NMR spectra confirm that the coordinated isocyanide ligands maintain their magnetic equivalence: only one singlet at –62 ppm is found for the CF_3 substituents of the four ligands and only one triplet at –116 ppm for the *para*-fluorine atoms. The NMR signals are slightly shifted in comparison to the starting material (-63 and -109 ppm).

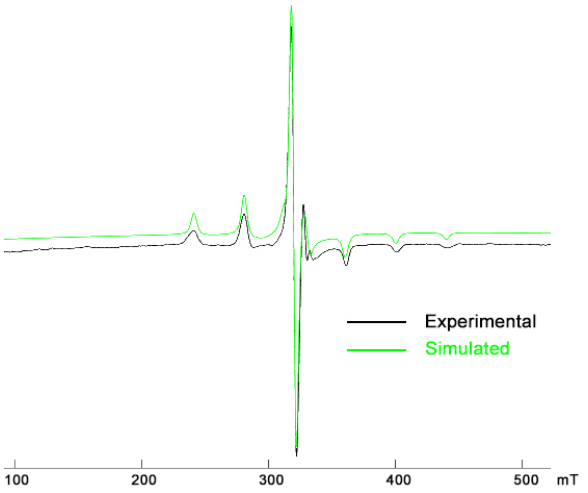

Figure 3. Frozen-solution X-band EPR spectrum of $[Re(CO)(CNAr^{DArF2})_4]$ in benzene/THF (g_x = 2.864, g_y = 2.068, g_z = 1.978, $A_x^{Re} = 22 \cdot 10^{-4}$ cm^{-1}, $A_y^{Re} = 35 \cdot 10^{-4}$ cm^{-1}, $A_z^{Re} = 368 \cdot 10^{-4}$ cm^{-1}).

Remarkably, a benzene/THF solution of the same black crystals also give an intense EPR spectrum (Fig. 3). It shows well resolved $^{185,187}Re$ hyperfine couplings, which clearly prove the presence of a paramagnetic rhenium complex with the unpaired electron being mainly located at the transition metal. With respect to the experimental conditions (the treatment of a rhenium(I) compound with a strong reductant), it can be assigned to a monomeric rhenium(0) compound, most probably $[Re(CO)(CNAr^{DArF2})_4]$. Persistent monomeric complexes of rhenium(0) are rare and only two of them were stable enough to allow structural and/or spectroscopic studies: $[Re(CO)_3$(tricyclohexylphosphine)$_2]$ and the recently published isocyanide complex $[Re(CO)_3(CNAr^{Dipp2})_2]$.[5,16,17] The EPR spectrum of $[Re(CO)(CNAr^{DArF2})_4]$ is essentially axially symmetric with an only marginal rhombic component. Interactions of the unpaired electron with the nuclear spin of I =5/2 of $^{185,187}Re$ result in the observed six-line pattern with a hyperfine coupling of $368 \cdot 10^{-4}$ cm^{-1} in the parallel part of the spectrum, while that in the parallel part is significantly smaller. Generally, the spectrum is very similar to that of $[Re^0(CO)_3(CNAr^{Dipp2})_2]$ with a less pronounced rhombic component, which is in agreement with the proposed higher symmetry of the axial coordination sphere of rhenium.

Surprisingly, $[Re(CO)(CNAr^{DArF2})_4]$ is relatively robust and does not suffer from degradation after standing at room temperature for at least one day. Even the addition of an equimolar quantity of water does not induce decomposition as long as the access of atmospheric oxygen is precluded.

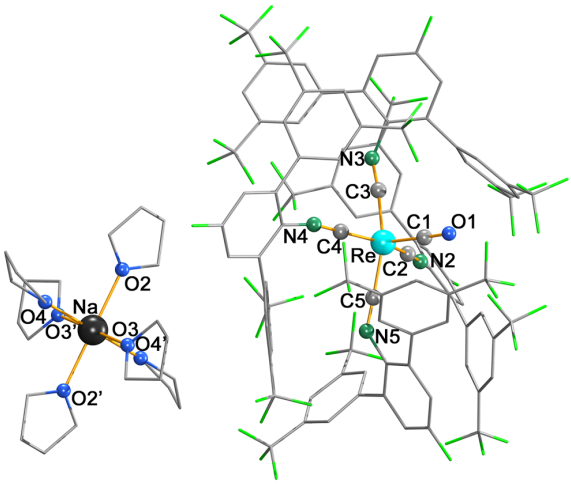

Figure 4. Molecular structures of the co-crystallized compounds $[Na(THF)_6][Re^{-1}(CO)(CNAr^{DArF2})_4]$ and $[Re^0(CO)(CNAr^{DArF2})_4]$ (symmetry operation: (') -x, 2-y, 2-z). Note that the $[Na(THF)_6]^+$ cation has only 50 per cent occupancy.

The results of an X-ray structure determination explain the unusual spectroscopic behavior of the dark solid, which gives high-quality NMR and EPR spectra at the same time: The black crystals represent a co-crystallization of two species: $[Na(THF)_6][Re^{-1}(CO)(CNAr^{DArF2})_4]$ and $[Re^0(CO)(CNAr^{DArF2})_4]$. Figure 4 shows the crystallographic results. The structure has been solved and refined in the triclinic space group $P\bar{1}$. The rhenium part of the structure has an occupancy of 1, while that of the $[Na(THF)_6]^+$ is 0.5. This is in agreement with the above-mentioned co-crystallization of two species. Such an interpretation is only sound, when an almost uniform structure of the Re^0 and the Re^{-1} complex species is assumed. And indeed, there is no crystallographic evidence for significant differences between these two species. Both contain rhenium in a square-pyramidal coordination sphere with the carbonyl ligand in apical position. The structural similarity between both compounds also includes the fact that each two of the isocyanide ligands are coordinated 'regularly' with Re-C-N angles of 172° and 167°, while the other two show a clearly bent arrangement with Re-C-N angles of 130° and 134°. Such a bent coordination of isocyanides to rhenium has recently also been found for the rhenium(-1) complex $K[Re(CO)_3(CNAr^{Dipp2})_2]$.[5] For a more detailed discussion of the bonding situation, however, structural data of the pure Re(0) and Re(-1) species would be highly appreciated. We are currently working on the isolation of suitable single crystals of the two compounds.

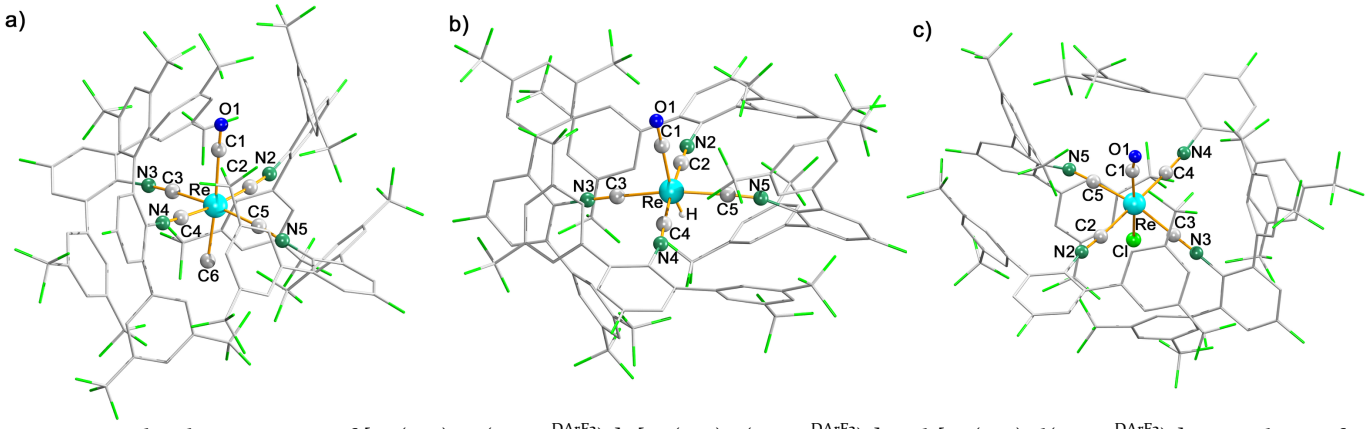

Figure 5. Molecular structures of $[Re(CO)Me(CNAr^{DArF2})_4]$, $[Re(CO)H(CNAr^{DArF2})_4]$ and $[Re(CO)Cl(CNAr^{DArF2})_4]$ as products of reactions of $[Na(THF)_6][Re^{-I}(CO)(CNAr^{DArF2})_4]/[Re^{0}(CO)(CNAr^{DArF2})_4]$ with MeI, HCl and $C_6F_5C(O)Cl$, respectively.

The highly reduced rhenium species should show pronounced reactivity against electrophilic agents as has been demonstrated before for similar manganese or molybdenum species.[4,6] Thus, we tested their reactivity with electrophiles such as MeI, HCl or $C_6F_5C(O)Cl$. Addition of methyl iodide to a solution of the black crystals consisting of the equimolar $[Na(THF)_6][Re^{-I}(CO)(CNAr^{DArF2})_4]/[Re^{0}(CO)(CNAr^{DArF2})_4]$ mixture in THF afforded the formation of $[Re(CO)Me(CNAr^{DArF2})_4]$, as is indicated by the detection of a CH_3 signal at –1.8 ppm in the ^{1}H NMR spectrum of the compound and a single crystal structure determination (see Fig. 5a).

Treatment of $[Na(THF)_6][Re^{-I}(CO)(CNAr^{DArF2})_4]/[Re^{0}(CO)(CNAr^{DArF2})_4]$ with HCl led to the formation of the hydrido complex $[Re(CO)H(CNAr^{DArF2})_4]$, which could be isolated in form of yellow crystals and characterized by X-ray diffraction (Fig. 5b). The ^{1}H NMR spectrum of the compound displays a characteristic hydride signal at –5 ppm. The IR spectrum of $[Re(CO)H(CNAr^{DArF2})_4]$ shows bands at 2021, 1979 and 1938 cm^{-1}, which can be assigned to the $\nu_{C\equiv N}$, ν_{Re-H} and $\nu_{C\equiv O}$ vibrations. As a side product in the synthesis of the hydrido compound, some amount of $[Re(CO)Cl(CNAr^{DArF2})_4]$ was formed. The yellow, crystalline material could be separated manually and characterized by NMR spectroscopy and X-ray diffraction. The compound is isostructural to the corresponding bromide complex. It's molecular structure is shown in Fig. 5c. $[Re(CO)Cl(CNAr^{DArF2})_4]$ is also the main product of a reaction of $[Na(THF)_6][Re^{-I}(CO)(CNAr^{DArF2})_4]/[Re^{0}(CO)(CNAr^{DArF2})_4]$ with $C_6F_5C(O)Cl$, which was performed for an attempted synthesis of a complex with a perfluorinated aryl ligand.

The obtained results demonstrate that the $\{Re(CO)(CNAr^{DArF2})_4\}^+$ core is well suitable for the stabilization of species with highly reduced metal centers, in which the metal ion has a pronounced nucleophilic character and its reactivity resembles in some cases that of $[Re(CO)_5]^-$.

The possibility of extending this results to technetium is particularly intriguing, since it would provide a synthetically accessible analogue of the practically unknown species $[Tc(CO)_5]^-$. Reactions of $(NBu_4)[Tc_2(\mu\text{-}Cl)_3(CO)_6]$ with 3 equivalents of $CNAr^{DArF2}$ in boiling toluene gave an intractable oil, but the use of 4 equivalents of the ligand and prolonged heating in boiling toluene gave pure orange-red crystals of $[Tc(CO)Cl(CNAr^{DArF2})_4]$ in good yield. X-ray structural determination demonstrates that the complex is isostructural to the rhenium analog with four axially arranged $CNAr^{DArF2}$ ligands and the CO and Cl$^-$ ligands in *trans* position to each other (Fig. 6). Two well-separated bands for the $\nu_{C\equiv N}$ stretch at 2064 cm^{-1} and for the $\nu_{C\equiv O}$ stretch at 1935 cm^{-1} are resolved in the IR spectrum of the compound. The red-shift of the isocyanide band is less pronounced than in the isostructural rhenium complex. ^{99}Tc NMR spectroscopy exhibits a broad signal at –1542 ppm, which is in the typical range of Tc(I) tricarbonyl complexes. The ^{19}F NMR spectrum of $[Tc(CO)Cl(CNAr^{DArF2})_4]$ shows the signal of the magnetically equivalent CF3 groups as a singlet at –66 ppm, while a triplet at –124 ppm can be assigned to the fluorine atom of the aromatic rings. These signals are slightly shifted with respect to the corresponding values for $[Re(CO)Br(CNAr^{DArF2})4]$ (-63 and -109 ppm).

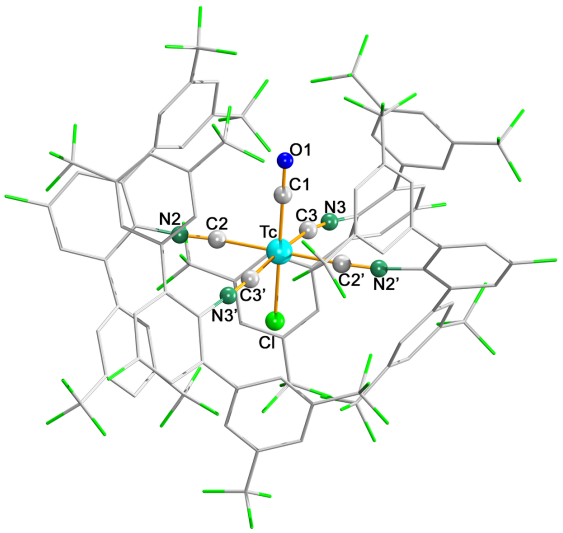

Figure 6. Molecular structure of $[Tc(CO)Cl(CNAr^{DArF2})_4]$ (symmetry operation: (') 1-x, y, 1.5-z).

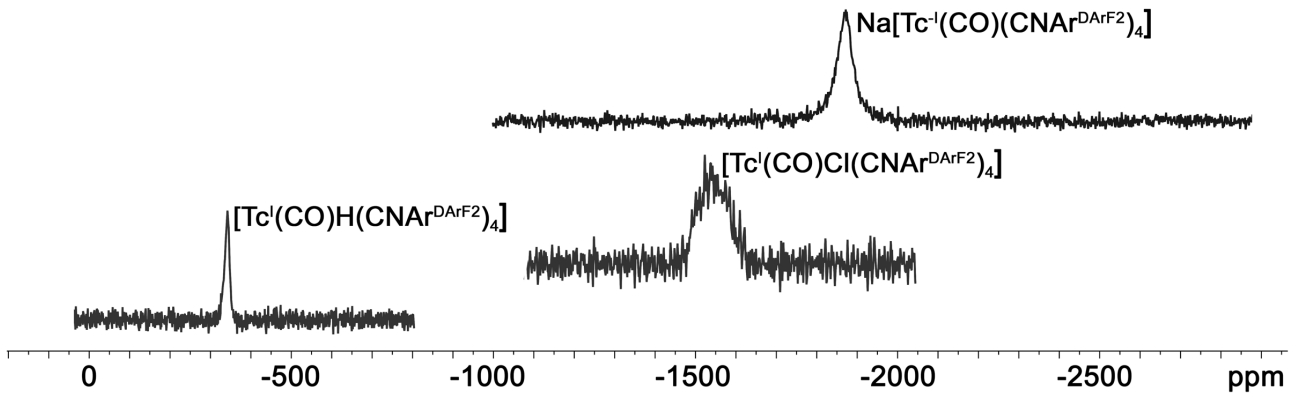

Figure 7. ^{99}Tc NMR spectra of [Tc(CO)H(CNAr^{DArF2})$_4$], Na[Tc(CO)(CNAr^{DArF2})$_4$] and [Tc(CO)Cl(CNAr^{DArF2})$_4$] (chemicals shifts relative to TcO_4^-).

The reduction of [Tc(CO)Cl(CNAr^{DArF2})$_4$] with 0.1% Na/Hg in THF led to a unique red diamagnetic compound of the composition Na[Tc(CO)(CNAr^{DArF2})$_4$], as can be concluded from its NMR spectra, which are very close to the values obtained for the analogous rhenium complex. The ^{19}F NMR spectrum confirms the purity of the obtained product by showing only one singlet at –65 ppm and one triplet at –112 ppm. The ^{99}Tc NMR spectrum of Na[Tc(CO)(CNAr^{DArF2})$_4$] shows the complete consumption of [Tc(CO)Cl(CNAr^{DArF2})$_4$] and the formation of a new signal at –1865 ppm, which is the first detection of a technetium complex with the formal oxidation state "-1" by ^{99}Tc NMR spectroscopy (Fig. 7).

Similarly to [Na(THF)$_6$][Re(CO)(CNAr^{DArF2})$_4$], the highly reduced technetium complex reacts with nucleophiles such as $(CF_3CO)_2O$, $SnCl_2$, P_4 or HCl. Unfortunately, up to now no crystalline products could be isolated from such reactions. But there is clear evidence by ^{99}Tc NMR spectroscopy that the Tc(-1) compound is consumed and Tc(I) products are formed. One example, in which only one product was formed is the reaction with HCl. The ^{99}Tc NMR spectrum of the formed product [Tc(CO)H(CNAr^{DArF2})$_4$] shows only one signal at -355 ppm. It is compared to the spectra of the other diamagnetic technetium complexes mentioned in this study in Fig. 7.

CONCLUSIONS

Compounds with a central {M^{I}(CO)(CNAr^{DArF2})$_4$}$^+$ unit (M = Re, Tc) contain highly shielded metal ions. The four encumbering isocyanide ligands provide adequate steric protection in the proximity of the metal center, avoiding dimerization reactions and other degradation pathways. In addition, the fluorination in the periphery of the ligands increases the π-accepting properties of the isocyanides, which is fundamental for the stabilization of very low oxidation states. The reduction of the [M(CO)X(CNAr^{DArF2})$_4$] species (M = Re, X = Br; M = Tc, X = Cl) with Na/Hg produces low-valent complexes such as [Re^{0}(CO)(CNAr^{DArF2})$_4$], [Na(THF)$_6$][Re^{-I}(CO)(CNAr^{DArF2})$_4$] or Na[Tc^{-I}(CO)(CNAr^{DArF2})$_4$]. The encumbering fluorinated substituents donate a surprisingly high robustness to the reduced compounds, which readily undergo reactions with electrophiles. Further work is required to investigate the structure and chemical properties of these intriguing compounds.

EXPERIMENTAL SECTION

General Considerations. All manipulations were carried out under an argon atmosphere using standard Schlenk and glovebox techniques. Unless otherwise stated, reagent-grade starting materials were purchased from commercial sources and either used as received or purified by standard procedures. Solvents were dried and deoxygenated according to standard procedures. Benzene-d_6 was distilled from NaK alloy and stored under Ar prior to use. Celite 405 (Fisher Scientific) was dried at a temperature above 250°C and stored in the glovebox prior to use. CNAr^{DArF2} and $(NBu_4)[Tc_2(CO)_6(\mu\text{-}Cl)_3]$ were prepared as previously described.[13,18]

Physical Measurements: NMR spectra were recorded at 20°C with a JEOL 400 MHz multinuclear spectrometer. Positive- and negative-mode ESI mass spectra were measured for the rhenium compounds with an Agilent 6210 ESI-TOF (Agilent Technology) mass spectrometer. EPR spectra were recorded in the X-band at 78 K in THF with a Magnetech Miniscope spectrometer. Simulations were done with Easyspin.[19] Elemental analysis of carbon, hydrogen and nitrogen were performed using a Heraeus elemental analyzer. For the IR spectra, a Nicolet iS10 FT-IR or a Shimadzu FTIR Affinity-1 spectrometer were used. The following abbreviations were used for the intensities and characteristics of IR absorption bands: vs = very strong, s = strong, m = medium, w = weak, sh = shoulder.

The technetium contents of the samples were measured by a HIDEX 300 SL liquid scintillation counter. An aliquot of three probes per sample with different concentrations was added to 10 mL of a scintillation cocktail (Rotiszint ecoplus, Carl Roth), and the net count rates were measured over 1024 channels with a counting time of 60 s. An average value was calculated for each sample.

Radiation Precautions. ^{99}Tc is a long-lived weak β^- emitter (E_{max} = 0.292 MeV). Normal glassware provides adequate protection against the weak beta radiation when milligram amounts are used. Secondary X-rays (Bremsstrahlung) play a significant role only when larger amounts of ^{99}Tc are handled. All manipulations were done in a laboratory approved for the handling of radioactive materials.

X-Ray Crystallography. The intensities for the X–ray determinations were collected on a Bruker D8 Venture instrument with Mo Kα radiation. The space groups were determined by the detection of systematical absences. Absorption corrections were carried out by SADABS.[20] Structure solution and refinement were performed with the SHELX program package.[21,22] Hydrogen atoms were placed at calculated positions and treated with the 'riding

model' option of SHELXL. The representation of molecular structures was done using the program DIAMOND 4.2.2.[23]

Additional information on the structure determinations is contained in the Supporting Information and has been deposited with the Cambridge Crystallographic Data Centre.

Synthesis of the Complexes.

[Re(CO)Br(CNAr^{DArF2})$_4$]. To a suspension of [Re(CO)$_5$Br] (266 mg, 0.655 mmol, 100 mL) in toluene, CNAr^{DArF2} (1.5 g, 2.75 mmol, 4.2 equiv) was added. The mixture was heated under reflux with stirring under argon for 24 h. The resulting yellow solution was concentrated to a volume of 8 mL and hexane (20 mL) was added. Storage at 4 °C for 12 h resulted in the precipitation of orange-red crystals of [Re(CO)Br(CNAr^{DArF2})$_4$], which were collected and dried *in vacuo*. Crystals suitable for X-ray structure determination were obtained from CH$_3$CN/Et$_2$O. Yield: 1.284 g, 0.533 mmol, 82%. FTIR (in KBr, cm^{-1}): 2051s (CN, broad), 1926m (CO), 1916m (CO), also, 3054w, 2915w, 1622w, 1595w, 1479m, 1461m, 1433m, 1398m, 1362s, 1312w, 1276vs, 1220w, 1170s, 1127vs, 1105vs, 1056vs, 1000m, 971w, 952w, 912m, 902s, 879m, 861w, 847m, 798w, 750s, 735w. ^{1}H-NMR (THF, ppm): δ 7.58 (two overlapped s, 24H, Ph), 7.08 (d, *J* = 8 Hz, 8H, *Ar*-F). ^{19}F-NMR (THF, ppm): δ –62.8 (s, 48F, Ph-*CF$_3$*), –108.8 (t, *J* = 8 Hz, 4F, Ar-*F*). HRMS ESI+ (*m*/*z*): [M + Na]$^+$ 2497.1320, Calcd for C$_{93}$H$_{32}$BrF$_{52}$N$_4$NaORe: 2497.0384.

[Re(CO)$_2$Br(CNAr^{DArF2})$_3$]. To a suspension of [Re(CO)$_5$Br] (122 mg, 0.3 mmol, 30 mL) in toluene, CNAr^{DArF2} (491 mg, 0.9 mmol, 3.0 equiv) was added. The mixture was heated under reflux with stirring under argon for 24 h. The resulting yellow solution was concentrated to a volume of 2 mL and hexane (15 mL) was added. Storage at 4 °C for 12 h resulted in the formation of an orange-red solid consisting of a mixture of [Re(CO)$_2$BrCNAr^{DArF2})$_3$] and [Re(CO)Br(CNAr^{DArF2})$_4$]. The product was dried in vacuo and a few single crystals of pure [Re(CO)$_2$BrCNAr^{DArF2})$_3$] could be separated by slow evaporation of a Et$_2$O/hexane solution of the mixture. ^{19}F-NMR (THF, ppm): δ –64.7 (s, Ph-*CF$_3$*), –108.3 (t, *J* = 8 Hz, Ar-*F*), –109.5 (t, *J* = 8 Hz, Ar-*F*), –110.1 (t, *J* = 8 Hz, Ar-*F*).

[Na(THF)$_6$][Re(CO)(CNAr^{DArF2})$_4$]/[Re(CO)(CNAr^{DArF2})$_4$]. [Re(CO)Br(CNAr^{DArF2})$_4$] (60 mg, 0.024 mmol) was dissolved in THF (3 mL) and 0.1% Na/Hg (Na: 0.003 g; Hg: 3 g; 5 equiv Na/Re) was added. The mixture was vigorously stirred for 3 h giving a very dark solution, which was concentrated under reduced pressure. Addition of pentane and storage at -35° C for 12 h yielded black crystals, which were collected and dried *in vacuo*. Yield: 60%. FTIR-ATR (cm^{-1}): 2010w (CN), 1906s (CN, broad), 1789s (CO, broad), 1619w, 1461m, 1409m, 1362s, 1306w, 1276vs, 1168s, 1130vs, 1094w, 967w, 910w, 875w, 846w, 705m, 682m, 636w, 546w. ^{1}H-NMR (C$_6$D$_6$, ppm): δ 7.60 (s, 16H, Ph), 7.53 (s, 8H, Ph), 6.52 (d, *J* = 8 Hz, 8H, *Ar*-F). ^{19}F-NMR (C$_6$D$_6$, ppm): δ –62.5 (s, 48F, Ph-*CF$_3$*), –115.7 (broad t, 4F, Ar-*F*). EPR (THF/benzene, 78 K): (g_x = 2.8638, g_y = 2.0676, g_z = 1.9783, A_x^{Re} = 22 · 10^{-4} cm^{-1}, A_y^{Re} = 35 · 10^{-4} cm^{-1}, A_z^{Re} = 368 · 10^{-4} cm^{-1}).

[Re(CO)Me(CNAr^{DArF2})$_4$]. [Re(CO)Br(CNAr^{DArF2})$_4$] (60 mg, 0.024 mmol) was dissolved in THF (3 mL) and 0.1% Na/Hg (Na: 0.003 g; Hg: 3 g; 5 equiv Na/Re) was added. The mixture was vigorously stirred for 3 h and filtered over celite. The resulting solution was cooled to –95° C and 350 µL of MeI solution (0.08 M in THF) was slowly added to the reaction mixture, whereupon its color turned yellow. Yellow crystals suitable for X-ray diffraction were obtained from THF/toluene/benzene. FTIR-ATR (cm^{-1}): 2015s (CN/CO, broad), 1917m (CO), 1622w, 1596w, 1461w, 1422w, 1398w, 1362s, 1311w, 1274vs, 1171s, 1126vs, 971w, 900s, 879m, 847m, 778s, 751w, 735w, 705w, 681s, 637s ,620w, 550m, 498w, 471s, 431w, 420w. ^{1}H-NMR (C$_6$D$_6$, ppm): δ 7.68 (s, 8H, Ph), 7.56 (s, 16H, Ph), 6.41 (d, *J* = 8 Hz, 8H, *Ar*-F), –1.85 (s, 1H, Re-*Me*). ^{19}F-NMR (C$_6$D$_6$, ppm): δ –62.6 (s, 48F, Ph-*CF$_3$*), –109.7 (broad t, 4F, Ar-*F*).

[Re(CO)H(CNAr^{DArF2})$_4$]. [Re(CO)Br(CNAr^{DArF2})$_4$] (60 mg, 0.024 mmol) was dissolved in THF (3 mL) and 0.1% Na/Hg (Na: 0.003 g; Hg: 3 g; 5 equiv Na/Re) was added. The mixture was vigorously stirred for 3 h and filtered over celite. The resulting solution was cooled to –95° C and 350 µL of a HCl solution (0.08 M in THF) was slowly added to the reaction mixture, whereupon its color turned yellow. Crystals suitable for X-ray structure determination were obtained from benzene. FTIR-ATR (cm^{-1}): 2021s (CN), 1979s (CO, broad), 1938s (CO), also, 2963w, 1597w, 1462w, 1420w, 1399w, 1363s, 1312w, 1276s, 1260s, 1171s, 1126vs, 1098vs, 1015vs, 913m, 901s, 877s, 847s, 796vs, 752w, 734w, 705m, 694m, 666s, 637s, 620w, 569w, 564w, 434w. ^{1}H-NMR (C$_6$D$_6$, ppm): δ 7.76 (s, 16H, Ph), 7.72 (s, 8H, Ph), 7.42 (d, *J* = 8 Hz, 8H, *Ar*-F), –4.96 (s, 1H, Re-*H*).

[Re(CO)Cl(CNAr^{DArF2})$_4$]. [Re(CO)Br(CNAr^{DArF2})$_4$] (60 mg, 0.024 mmol) was dissolved in THF (3 mL) and 0.1% Na/Hg (Na: 0.003 g; Hg: 3 g; 5 equiv Na/Re) was added. The mixture was vigorously stirred for 3 h and filtered over celite. The resulting solution was cooled to –95° C and 350 µL of a C$_6$F$_5$C(O)Cl solution (0.08M in THF) was slowly added to the reaction mixture, whereupon its color turned yellow. Crystals suitable for an X-ray structure determination were obtained from Et$_2$O/hexane. FTIR-ATR (cm^{-1}): 2101sh (CN), 2052s (CN), 2033s (CN), 2026sh (CN), 1923w (CO), 1913w (CO), also, 2963w, 1739br, 1652w, 1596w, 1524w, 1499m, 1475w, 1462w, 1422w, 1399m, 1363s, 1328w, 1314w, 1276vs, 1261s, 1222w, 1172s, 1127vs, 1099vs, 1006vs, 913w, 901s, 878m, 847m, 751vs, 735w, 705s, 694w, 681vs, 638m, 621w, 589w, 547w. ^{19}F-NMR (THF, ppm): δ –64.6 (s, 48F, Ph-*CF$_3$*), –111.9 (t, *J* = 8 Hz, 4F, Ar-*F*).

[Tc(CO)Cl(CNAr^{DArF2})$_4$]. CNAr^{DArF2} (439 mg, 0.80 mmol, 4.5 equiv) was added to a suspension of (NBu$_4$)[Tc$_2$(µ-Cl)$_3$(CO)$_6$] (60 mg, 0.0876 mmol) in 9 mL toluene. The resulting mixture was stirred for 20 h in boiling toluene. The resulting orange-red solution was concentrated to a minimum volume and hexane was added. Storage at 4 °C for 12 h resulted in the formation of orange-red crystals of [Tc(CO)Cl(CNAr^{DArF2})$_4$], which were collected and dried *in vacuo*. Crystals suitable for X-ray structure determination were obtained from THF/toluene. Yield: 0.304 g, 0.130 mmol, 74%. FTIR (in KBr, cm^{-1}): 2064s (CN), 1982w (CN), 1935s (CO), also, 3095w, 2961w, 2936w, 2874w, 1597m, 1460m, 1421w, 1398m, 1364s, 1312w, 1279s, 1175s, 1134s, 1109m, 972w, 903m, 879m, 847m, 752w, 735w, 706s, 683s, 638w, 594w, 523w, 463w. Elemental analysis: Tc, 4.6; calc. for C$_{93}$H$_{32}$ClF$_{52}$N$_4$OTc, 4.2 %. ^{1}H-NMR (THF, ppm): δ 7.74 (s, 16H, Ph), 7.73 (s, 8H, Ph), 7.42 (d, *J* = 8 Hz, 8H, *Ar*-F). ^{19}F-NMR (THF, ppm): δ –65.6 (s, 48F, Ph-*CF$_3$*), –123.9 (broad t, 4F, Ar-*F*). ^{99}Tc-NMR (THF, ppm): δ –1542.

Na[Tc(CO)(CNAr^{DArF2})$_4$]. [Tc(CO)Cl(CNAr^{DArF2})$_4$] (40 mg, 0.017 mmol) was dissolved in THF (3 mL) and 0.1% Na/Hg (Na: 0.003 g; Hg: 3 g; 8 equiv Na/Tc) was added. The mixture was vigorously stirred for 3 h giving a deep red solution. ^{19}F-NMR (THF, ppm): δ –65.1 (s, 48F, Ph-*CF$_3$*), –112.2 (t, *J* = 8 Hz, 4F, Ar-*F*). ^{99}Tc-NMR (THF, ppm): δ –1865.

[Tc(CO)H(CNAr^{DArF2})$_4$]. [Tc(CO)Cl(CNAr^{DArF2})$_4$] (40 mg, 0.017 mmol) was dissolved in THF (3 mL) and 0.1% Na/Hg (Na: 0.003 g; Hg: 3 g; 8 equiv Na/Tc) was added. The mixture was a vigorously stirred for 3 h. The resulting solution was cooled to –95° C and 200 µL of a HCl solution (0.2 M in THF) was slowly added to the reaction mixture, whereupon its color turned yellow. ^{1}H-NMR (C$_6$D$_6$, ppm): δ 7.62 (s, 8H, Ph), 7.59 (s, 16H, Ph), 6.38 (d, *J* = 8 Hz, 8H, *Ar*-F) ^{19}F-NMR (THF, ppm): δ –69.5 (s, 48F, Ph-*CF$_3$*), –112.5 (t, *J* = 8 Hz, 4F, Ar-*F*). ^{99}Tc-NMR (THF, ppm): δ –343.

ASSOCIATED CONTENT

Supporting Information

The Supporting Information is available free of charge on the ACS Publications website. Crystallographic Tables, bond lengths, angles and ellipsoid plots. Spectroscopic data (PDF).

AUTHOR INFORMATION

Corresponding Author

*Joshua S. Figueroa. E-mail jsfig@ucsd.edu
*Prof. Ulrich Abram. e-mail ulrich.abram@fu-berlin.de

ORCID

Ulrich Abram: 0000-0002-1747-7927
Joshua S. Figueroa: 0000-0003-2099-5984

Notes

The authors declare no competing financial interest.

ACKNOWLEDGMENT

We gratefully acknowledge financial support from the DFG (Deutsche Forschungsgemeinschaft: Graduated School "Fluorine as a key element"), the DAAD (German Academic Exchange Service), the U.S. National Science Foundation (International Supplement to CHE-1802646) and the Alexander von Humboldt Foundation (Fellowship to JSF). We acknowledge the assistance of the Core Facility BioSupraMol supported by the DFG.

REFERENCES

(1) Agnew, D. W.; Moore, C. E.; Rheingold, A. L.; Figueroa, J. S. Kinetic Destabilization of Metal-Metal Single Bonds: Isolation of a Pentacoordinate Manganese(0) Monoradical. *Angew. Chemie Int. Ed.* **2015**, *54*, 12673–12677.

(2) Margulieux, G. W.; Weidemann, N.; Lacy, D. C.; Moore, C. E.; Rheingold, A. L.; Figueroa, J. S. Isocyano Analogues of $[Co(CO)_4]_n$: A Tetraisocyanide of Cobalt Isolated in Three States of Charge. *J. Am. Chem. Soc.* **2010**, *132*, 5033–5035.

(3) Labios, L. A.; Millard, M. D.; Rheingold, A. L.; Figueroa, J. S. Bond Activation, Substrate Addition and Catalysis by an Isolable Two-Coordinate Pd(0) Bis-Isocyanide Monomer. *J. Am. Chem. Soc.* **2009**, *131*, 11318–11319.

(4) Ditri, T. B.; Moore, C. E.; Rheingold, A. L.; Figueroa, J. S. Oxidative Decarbonylation of M-Terphenyl Isocyanide Complexes of Molybdenum and Tungsten: Precursors to Low-Coordinate Isocyanide Complexes. *Inorg. Chem.* **2011**, *50*, 10448–10459.

(5) Salsi, F.; Neville, M.; Drance, M.; Hagenbach, A.; Figueroa, J. S.; Abram, U. Mixed M-Terphenyl Isocyanide/Carbonyl Complexes of Rhenium: Cis/Trans Isomerization and Reduction. *Chem. Commun.* **2020**, in press, DOI: 10.1039/docc03043k.

(6) Stewart, M. A.; Moore, C. E.; Ditri, T. B.; Labios, L. A.; Rheingold, A. L.; Figueroa, J. S. Electrophilic Functionalization of Well-Behaved Manganese Monoanions Supported by m-Terphenyl Isocyanides. *Chem. Commun.* **2011**, *47*, 406–408.

(7) Jurisson, S. S.; Lydon, J. D. Potential Technetium Small Molecule Radiopharmaceuticals. *Chem. Rev.* **1999**, *99*, 2205–2218.

(8) Schwochau, K. Technetium: Chemistry and Radiopharmaceutical Applications, Wiley,VCH **2000**.

(9) Alberto, R. High- and low-valency organometallic compounds of technetium and rhenium, in Yoshihara, K., Omori, T. Technetium and Rhenium Their Chemistry and Its Applications. Springer, **1996**; pp 149–187.

(10) Lentz, D.; Pötter, B.; Marschall, R.; Brüdgam, I.; Fuchs, J. $Cr(CO)_4(CNCF_3)(CNCH_3)$ Und $Cr(CO)_4(CNCF_3)$ (CNC_6H_5), Isocyanid-Komplexe mit +I- und -I-substituierten Isocyaniden. *Chem. Ber.* **1990**, *123*, 257–260.

(11) Johnston, R. F.; Cooper, J. C. Substituent Effects on the Frontier Molecular Orbitals of Aryl Isonitriles. *J. Mol. Struct. THEOCHEM* **1991**, *236*, 297–307.

(12) Ditri, T. B.; Carpenter, A. E.; Ripatti, D. S.; Moore, C. E.; Rheingold, A. L.; Figueroa, J. S. Chloro- and Trifluoromethyl-Substituted Flanking-Ring m-Terphenyl Isocyanides: H6-Arene Binding to Zero-Valent Molybdenum Centers and Comparison to Alkyl-Substituted Derivatives. *Inorg. Chem.* **2013**, *52*, 13216–13229.

(13) Carpenter, A. E.; Mokhtarzadeh, C. C.; Ripatti, D. S.; Havrylyuk, I.; Kamezawa, R.; Moore, C. E.; Rheingold, A. L.; Figueroa, J. S. Comparative Measure of the Electronic Influence of Highly Substituted Aryl Isocyanides. *Inorg. Chem.* **2015**, *54* , 2936–2944.

(14) Figueroa, J. S.; Abram, U. Oxidorhenium(V) and Rhenium(III) Complexes with m-Terphenyl Isocyanides. *Z. Anorg. Allg. Chem.*, **2020**, in press, DOI: 10.1002/zaac.202000147.

(15) Claude, G.; Salsi, F.; Hagenbach, A.; Gembicky, M.; Neville, M.; Chan, C.; Figueroa, J. S.; Abram, U. Structural and Redox Variations in Technetium Complexes Supported by m-Terphenyl Isocyanides. *Organometallics*, **2020**, in press, DOI: 10.1021/acs.organomet.0c00238.

(16) Walker, H. W.; Rattinger, G. B.; Belford, R. L.; Brown, T. L. Formation and characterization of the persistent rhenium radical bis(tricyclohexylphosphine)tricarbonylrhenium(0). *Organometallics*, **1983**, *2*, 775–776.

[17] Crocker, L. S.; Heinekey, D. M.; Schulte, G. K. Thermal synthesis and structural characterization of $Re(CO)_3(PCy_3)_2$, a rhenium(0) radical. *J. Am. Chem. Soc.* **1989**, *111*, 405–406.

[18] Hildebrandt, S. $(NBu_4)[Tc_2(\mu\text{-}Cl)_3(CO)_6]$ als Startverbindung für Technetiumtricarbonylkomplexe. PhD Thesis, FU Berlin, **2018**.

[19] Stoll, S.; Schweiger, A. EasySpin, a Comprehensive Software Package for Spectral Simulation and Analysis in EPR. *J. Magn. Reson.*, **2006**, *178*, 42–55.

[20] Sheldrick, G. M.; SADABS, Universität of Göttingen, Germany, **2014**.

[21] Sheldrick, G. M., A short history of SHELX, *Acta Crystallogr. Sect. A*, **2008**, *64*, 112-122.

[22] Sheldrick, G. M., Crystal structure refinement with SHELXL, *Acta Crystallogr. Sect. C*, **2015**, *71*, 3-8.

[23] Brandenburg, K., Diamond- Crystal and Molecular Structure Visualization, Crystal impact GbR, vers. 4.5.1, **2018**, Bonn (Germany).

Table of Contents

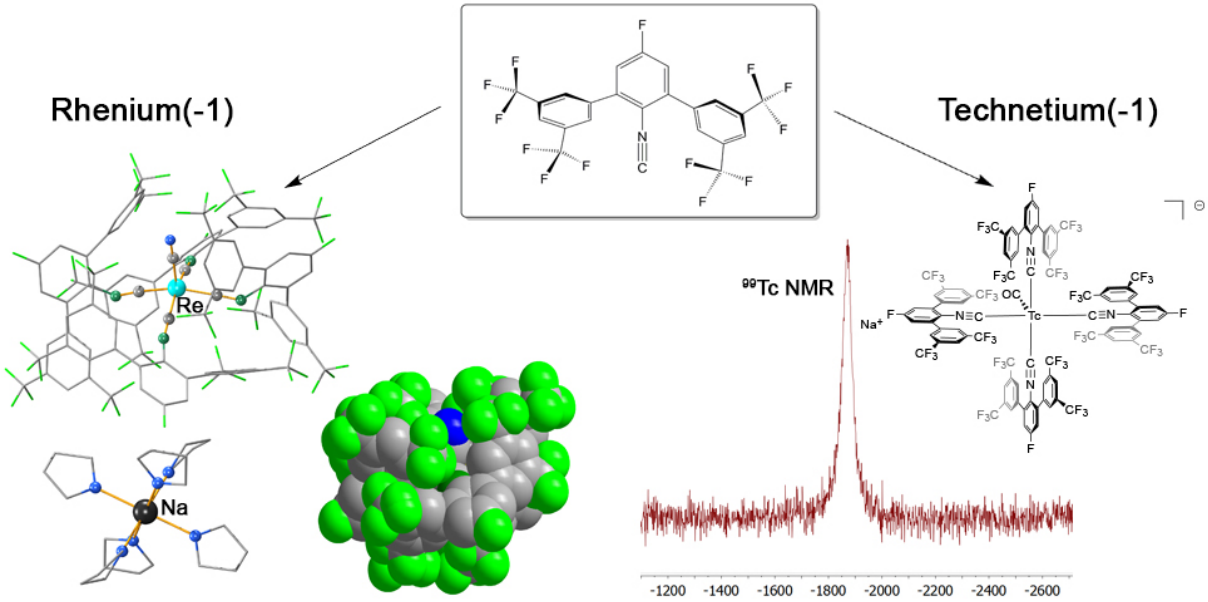

Supporting information for the paper entitled:

$[M^{I}(CO)X(CNAr^{DArF2})_4]$ (DArF = 3,5-$(CF_3)_2C_6H_3$; M = Re, Tc; X = Br, Cl) complexes: convenient platforms for the synthesis of low-valent rhenium and technetium compounds

Federico Salsi,[a] Michael Neville,[b] Myles Drance,[b] Adelheid Hagenbach,[a] Joshua S. Figueroa,[b*] and Ulrich Abram[a*]

[a]*Freie Universität Berlin, Institute of Chemistry and Biochemistry, Fabeckstr. 34–36, 14195 Berlin, Germany*

[b]*Department of Chemistry and Biochemistry, University of California, San Diego, 9500 Gilman Drive Mail Code 0358, La Jolla CA, 92093-0358.*

E-mail: ulrich.abram@fu-berlin.de

Contents

S1. Crystallographic structure determination.

S1.1 General. The intensities for the X–ray determinations were collected on a Bruker D8 Venture or on a Bruker APEX II Ultra instrument with Mo Kα radiation. Structure solution and refinement were performed with the SHELX program packages.[1,2] Hydrogen atoms were placed at calculated positions and treated with the 'riding model' option of SHELXL, except in the cases of $[Re(CO)H(CNAr^{DArF2})_4]$, where the position of the hydrido hydrogen atom was taken from the Fourier map. The representation of molecular structures was done using the program DIAMOND (vers. 4.5.1).[3] Additional information on the structure determinations has been deposited with the Cambridge Crystallographic Data Centre (see Table S1.1).

S1.2. Disorder and Refinement Specifics. The solid-state structures of the complexes $[XM(CO)_m(CNAr^{DArF2})_n]$ (with X = Br, Cl, Me; M = Tc, Re; m = 1, 2; n = 4, 3) suffered from positional disorder between the X ligand and one carbonyl ligand. The disorder did not affect the stereochemistry of the complexes and was adequately modeled and refined with an occupational ratio of ca. 0.5 in all cases. The completion of the crystal structure determination of $[Re(CO)Br(CNAr^{DArF2})_4]$ and $[Na(THF)_6]$-$[Re(CO)(CNAr^{DArF2})_4]$/$[Re(CO)(CNAr^{DArF2})_4]$ was hampered by the presence of seriously disordered solvent molecules. The *Platon Squeeze* tool was employed to remove the corresponding electron density. For $[Re(CO)Br(CNAr^{DArF2})_4]$, the electron density belonging to one molecule of solvent acetonitrile and one molecule of solvent diethylether (ca. 70 electrons/cell) was subtracted. For $[Na(THF)_6]$-$[Re(CO)(CNAr^{DArF2})_4]$/$[Re(CO)(CNAr^{DArF2})_4]$, the electron density corresponding to four molecules of solvent THF (400 electrons/cell) was subtracted.

Table S1.1. Crystal data and structure determination parameters.

	[Re(CO)Br(CNAr^{DArF2})] · CH_3CN	[Re(CO)$_2$Br(CNAr^{DArF2})$_3$]	[Na(THF)$_6$] [Re(CO)(CNAr^{DArF2})$_4$]/ [Re(CO)(CNAr^{DArF2})$_4$]
Formula	$C_{95}H_{35}BrF_{52}N_5OReCl$	$C_{71}H_{24}BrF_{39}N_3O_2Re$	$C_{210}H_{112}F_{104}N_8NaO_8Re_2$
Mw	2516.39	1958.04	5246.46
Crystal system	triclinic	triclinic	triclinic
a/Å	15.3241(7)	14.4956(9)	14.963(8)
b/Å	15.3479(7)	14.982(1)	16.997(15)
c/Å	23.2572(11)	17.564(1)	28.20(3)
α/°	88.417(2)	77.816(5)	87.44(5)
β/°	72.437(2)	71.084(5)	74.96(4)
γ/°	66.359(2)	82.385(4)	73.51(3)
V/Å^3	4749.9(4)	3518.7(5)	6638(9)
Space group	$P\bar{1}$	$P\bar{1}$	$P\bar{1}$
Z	2	2	1
D_{calc} g/cm^{-3}	1.759	1.848	1.312
No. reflect.	92645	15273	153422
No. indep.	21120	10883	29362
R_{int}	0.0573	0.0553	0.3057
R_1/wR_2 [$I>2\sigma(I)$]	0.0424/0.0824	0.0678/0.1376	0.1164/0.2495
GOF	1.031	0.977	1.029

Table S1.1. Crystal data and structure determination parameters (Continued).

	[Re(CO)H(CNAr^{DArF2})$_4$]	[Re(CO)Me(CNAr^{DArF2})$_4$] ·0.75(C_6H_6)·0.5($C_6H_5CH_3$)	[Re(CO)Cl(CNAr^{DArF2})$_4$] ·2(Et_2O)
Formula	$C_{93}H_{33}F_{52}N_4ORe$	$C_{102}H_{43.5}F_{52}N_4ORe$	$C_{101}H_{52}ClF_{52}N_4O_3Re$
Mw	2396.43	2515.11	2579.11
Crystal system	triclinic	triclinic	triclinic
a/Å	14.35(1)	15.1977(6)	14.3046(5)
b/Å	15.22(1)	16.6193(6)	15.9071(5)
c/Å	21.41(2)	23.670(1)	24.2007(7)
α/°	84.61(5)	86.296(3)	77.920(1)
β/°	86.75(7)	71.454(2)	78.021(1)
γ/°	74.07(6)	67.513(2)	68.619(1)
V/Å^3	4476(8)	5226.0(4)	4961.8(3)
Space group	$P\bar{1}$	$P\bar{1}$	$P\bar{1}$
Z	2	2	2
D_{calc} g/cm^{-3}	1.778	1.598	1.726
No. reflect.	142813	128820	103649
No. indep.	14837	18208	21910
R_{int}	0.1099	0.1011	0.0469
R_1/wR_2 [$I>2\sigma(I)$]	0.0642/0.1519	0.0786/0.2028	0.0354/ 0.0827
GOF	1.113	1.024	1.059

Table S1.1. Crystal data and structure determination parameters (Continued).

	$[Tc(CO)Cl(CNAr^{DArF2})_4]$ $\cdot C_6H_5CH_3$
Formula	$C_{107}H_{48}ClF_{52}N_4OTc$
Mw	2526.94
Crystal system	triclinic
a/Å	20.823(4)
b/Å	21.975(4)
c/Å	22.576(5)
α/°	90
β/°	98.33(1)
γ/°	90
V/Å^3	10221(4)
Space group	C2/c
Z	4
D_{calc} g/cm^{-3}	1.642
No. reflect.	54026
No. indep.	11342
R_{int}	0.0377
R_1/wR_2 [$I>2\sigma(I)$]	0.0438/0.0967
GOF	1.039

Figure S1.1. Ellipsoid representation (50% probability) of [Re(CO)Br(CNAr^{DArF2})$_4$]·CH$_3$CN. Hydrogen atoms are omitted for clarity.

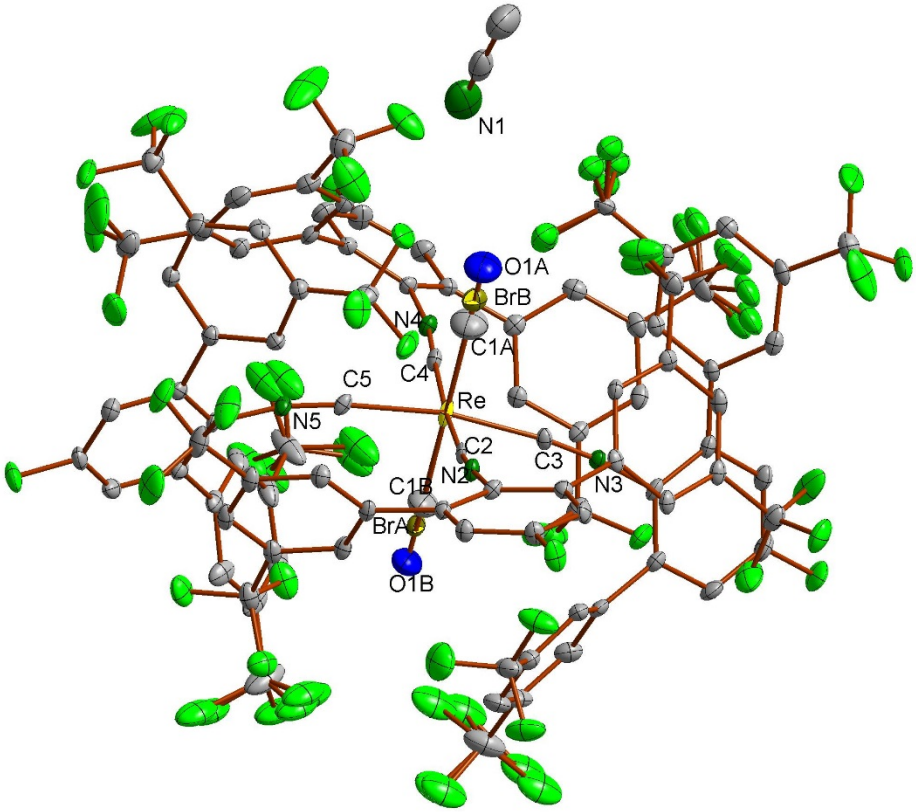

Table S1.2. Selected bond lenghts (Å) and angles (°) for [Re(CO)Br(CNAr^{DArF2})$_4$]·CH$_3$CN.

Re-C1A	1.94(1)	C1B-O1B	1.29(2)
Re-C1B	1.95(1)	C2-N2	1.165(4)
Re-C2	2.031(3)	C3-N3	1.159(4)
Re-C3	2.027(3)	C4-N4	1.161(4)
Re-C4	2.035(3)	C5-N5	1.166(4)
Re-C5	2.021(3)	C1A-Re-C2	86.4(6)
C1A-O1A	1.278(15)	C3-Re-C5	168.6(1)
Re-BrA	2.511(1)	Re-BrB	2.480(1)

Figure S1.2. Ellipsoid representation (50% probability) of $[Na(THF)_6][Re(CO)(CNAr^{DArF2})_4]$/$[Re(CO)(CNAr^{DArF2})_4]$. Hydrogen atoms are omitted for clarity.

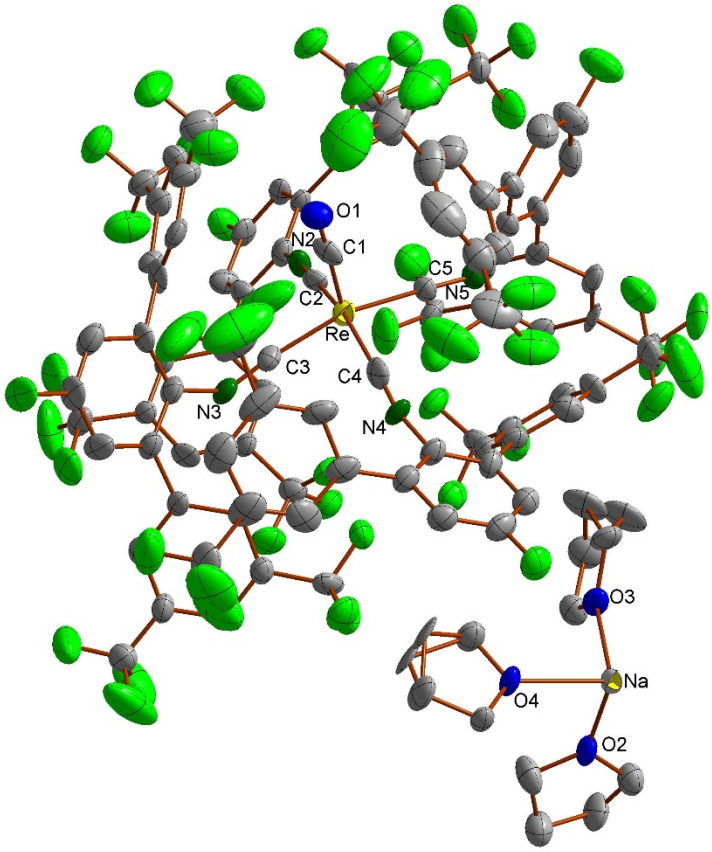

Table S1.3. Selected bond lenghts (Å) and angles (°) for of $[Na(THF)_6][Re(CO)(CNAr^{DArF2})_4]$/$[Re(CO)(CNAr^{DArF2})_4]$.

Re-C1	1.921(13)	C3-N3	1.227(14)
Re-C2	1.976(13)	C4-N4	1.199(14)
Re-C3	1.957(12)	C5-N5	1.206(12)
Re-C4	1.981(14)	C1-Re-C2	105.1(5)
Re-C5	1.980(10)	C2-N2-C28	172.3(11)
C1-O1	1.149(13)	C3-N3-C50	130.8(11)
C2-N2	1.213(14)	C5-N5-C6	134.0(10)

Figure S1.3. Ellipsoid representation (50% probability) of [Re(CO)Cl(CNAr^{DArF2})$_4$]·2(Et$_2$O). Hydrogen atoms are omitted for clarity.

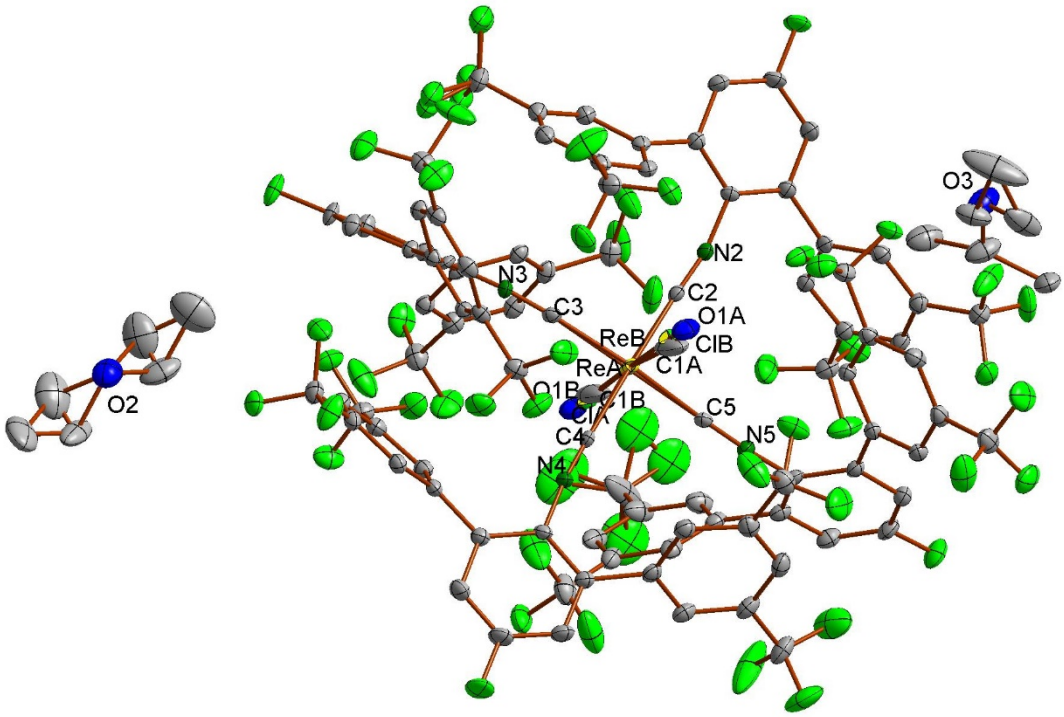

Table S1.4. Selected bond lenghts (Å) and angles (°) for [Re(CO)Cl(CNAr^{DArF2})$_4$]·2(Et$_2$O).

ReA-C1A/ReB-C1B	2.00(2)/1.99(2)	C1B-O1B	1.05(2)
ReA-C2/ReB-C2	2.072(3)/2.028(4)	C2-N2	1.163(4)
ReA-C3/ReB-C3	2.041(3)/2.041(3)	C3-N3	1.156(4)
ReA-C4/ReB-C4	2.012(3)/2.082(4)	C4-N4	1.157(4)
ReA-C5/ReB-C5	2.029(3)/2.003(4)	C5-N5	1.160(4)
C1A-O1A	1.07(2)	C1A-ReA-C2	91.9(5)
ReA-ClA/ReB-ClB	2.471(2)/2.430(3)	C3-ReA-C5	164.9(1)

Figure S1.4. Ellipsoid representation (50% probability) of $[Tc(CO)Cl(CNAr^{DArF2})_4]\cdot C_6H_5CH_3$. Hydrogen atoms are omitted for clarity.

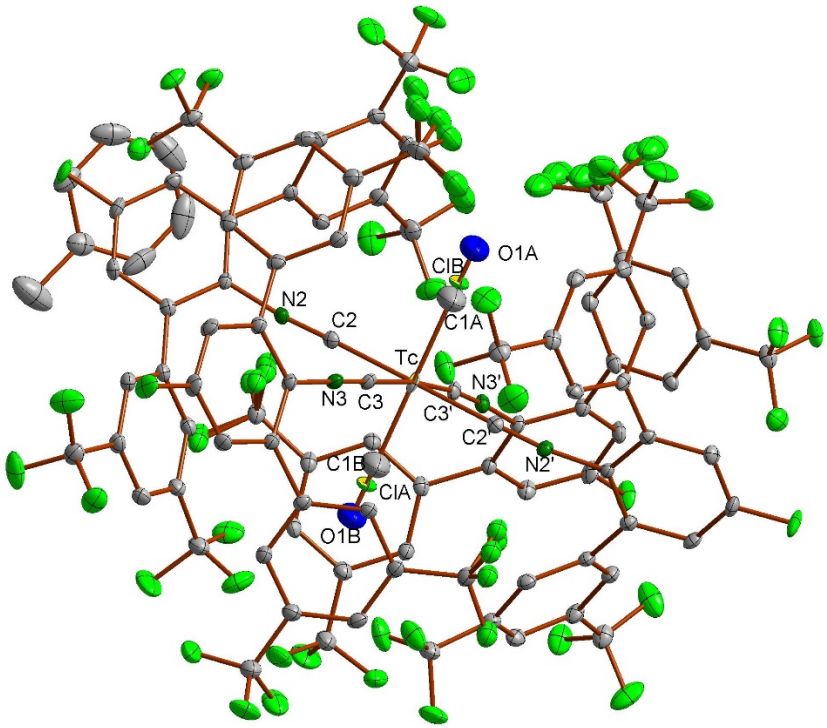

Table S1.5. Selected bond lenghts (Å) and angles (°) for $[Tc(CO)Cl(CNAr^{DArF2})_4]\cdot C_6H_5CH_3$.

Tc-C1A	1.94(1)	N3-C3	1.165(3)
Tc-C1B	1.92(1)	Tc-ClA	1.94(1)
Tc-C2	2.016(2)	Tc-ClB	2.321(3)
C1A-O1A	1.17(1)	C1B-O1B	1.19(1)
Tc-C3	2.029(2)	C2-Tc-C3	82.20(8)
N2-C2	1.164(3)	C1A-Tc-C3	92.87(6)

Figure S1.5. Ellipsoid representation (50% probability) of [Re(CO)Me(CNAr^{DArF2})$_4$]· 0.75(C_6H_6)· 0.5($C_6H_5CH_3$). Hydrogen atoms are omitted for clarity (except at the Re-Me group).

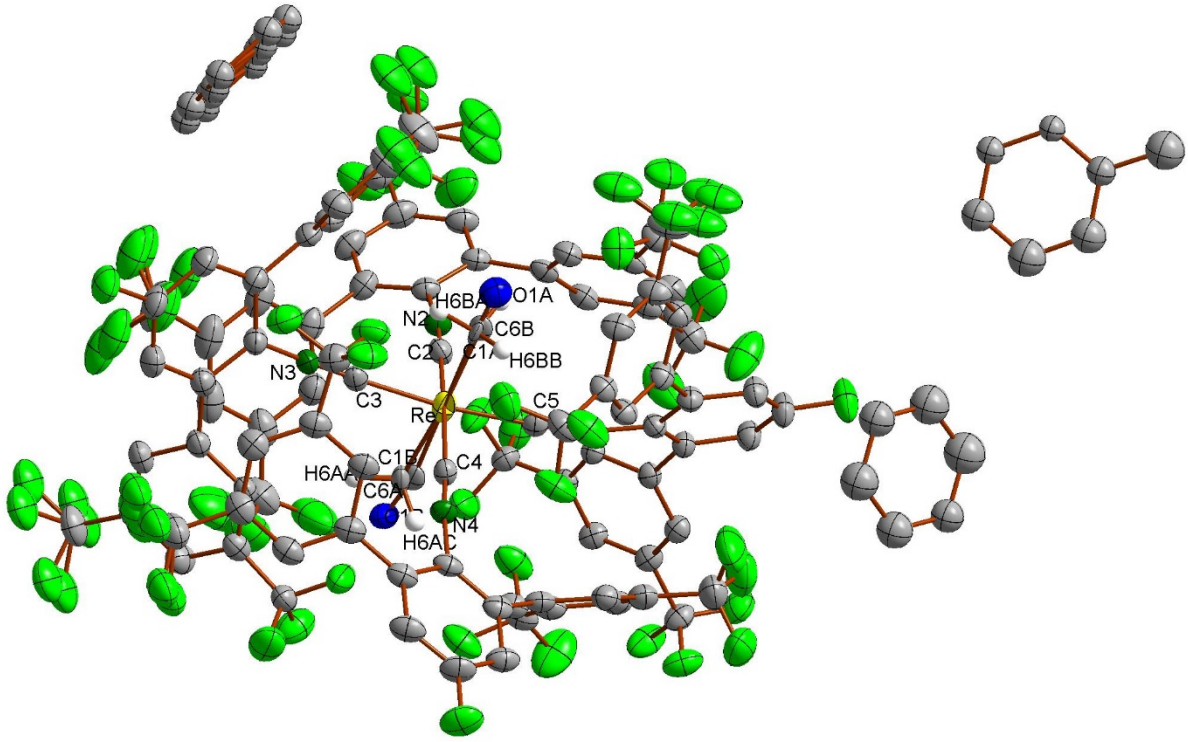

Table S1.6. Selected bond lenghts (Å) and angles (°) for [Re(CO)Me(CNAr^{DArF2})$_4$]· 0.75(C_6H_6)· 0.5($C_6H_5CH_3$).

Re-C1A	2.19(3)	C1A-O1A	1.04(3)
Re-C1B	2.07(3)	C3-N3	1.15(1)
Re-C2	2.047(8)	C4-N4	1.146(9)
Re-C3	2.032(8)	C5-N5	1.171(9)
Re-C4	2.049(7)	Re-C6B	2.15(3)
Re-C5	2.005(7)	C1A-Re-C2	91(1)
Re-C6A	2.15(2)	C3-Re-C4	90.4(3)
C1B-O1B	1.19(3)	C3-Re-C5	172.3(3)

Figure S1.6. Ellipsoid representation (50% probability) of $[Re(CO)_2Br(CNAr^{DArF2})_3]$. Hydrogen atoms are omitted for clarity.

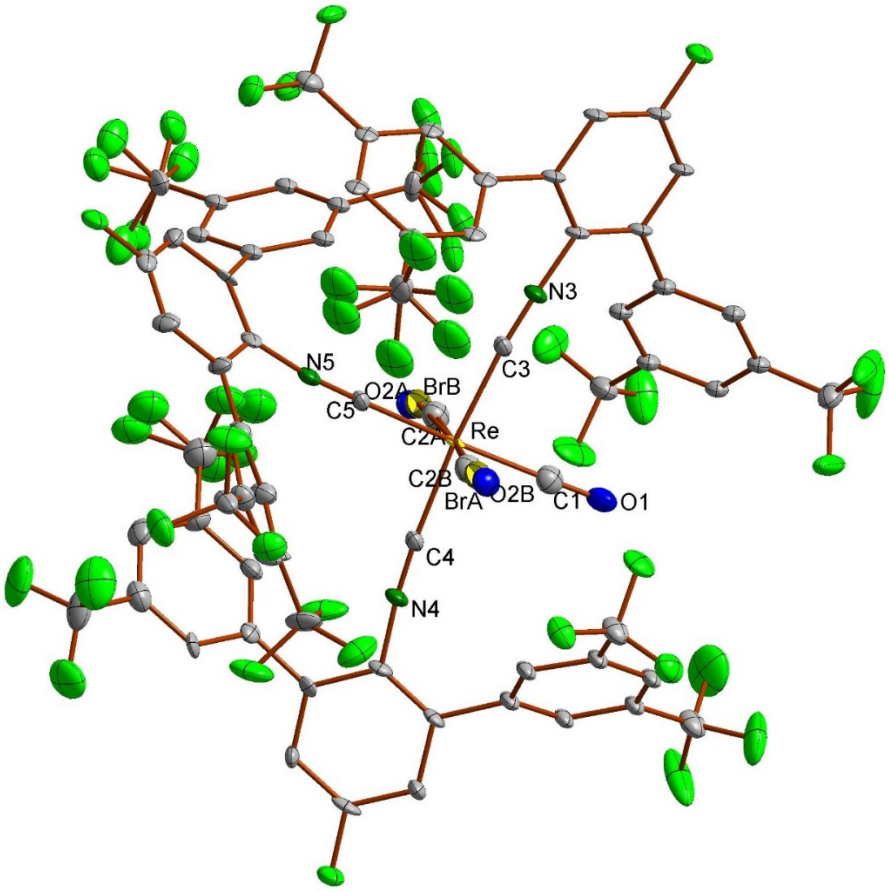

Table S1.7. Selected bond lenghts (Å) and angles (°) for $[Re(CO)_2Br(CNAr^{DArF2})_3]$.

Re-C1	2.01(1)	C3-N3	1.17(1)
Re-C2A	1.91(2)	C4-N4	1.15(1)
Re-C2B	1.71(3)	C5-N5	1.17(1)
Re-C3	2.031(9)	C1-O1	1.09(1)
Re-C5	2.040(9)	C2A-O2A	1.19(3)
Re-C4	2.045(9)	C2B-O2B	1.47(3)
Re-BrB	2.527(3	C1-Re-C3	87.4(4)
Re-BrA	2.543(2)	C1-Re-C5	176.8(4)

Figure S1.7. Ellipsoid representation (50% probability) of [Re(CO)H(CNAr^{DArF2})$_4$]. Hydrogen atoms, except the hydrido one, are omitted for clarity.

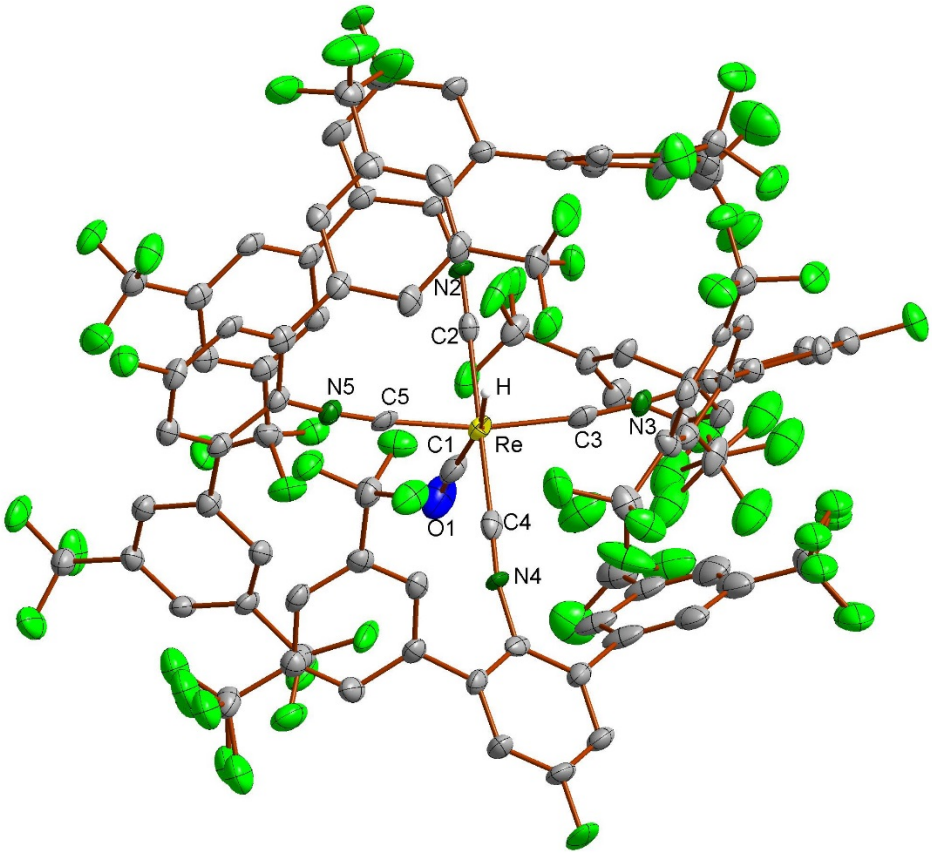

Table S1.8. Selected bond lenghts (Å) and angles (°) for [Re(CO)H(CNAr^{DArF2})$_4$].

Re-C1	2.000(9)	C2-N2	1.18(1)
C1-O1	1.13(1)	C3-N3	1.18(1)
Re-C2	2.024(8)	C4-N4	1.18(1)
Re-C3	2.039(9)	C5-N5	1.19(1)
Re-C4	2.028(9)	C1-Re-C3	94.6(3)
Re-C5	2.009(8)	C2-Re-C3	86.3(3)

S2. Spectroscopic characterization

Figure S2.1. ^{1}H NMR spectrum of $[Re(CO)Br(CNAr^{DArF2})_4]$ in CD_2Cl_2.

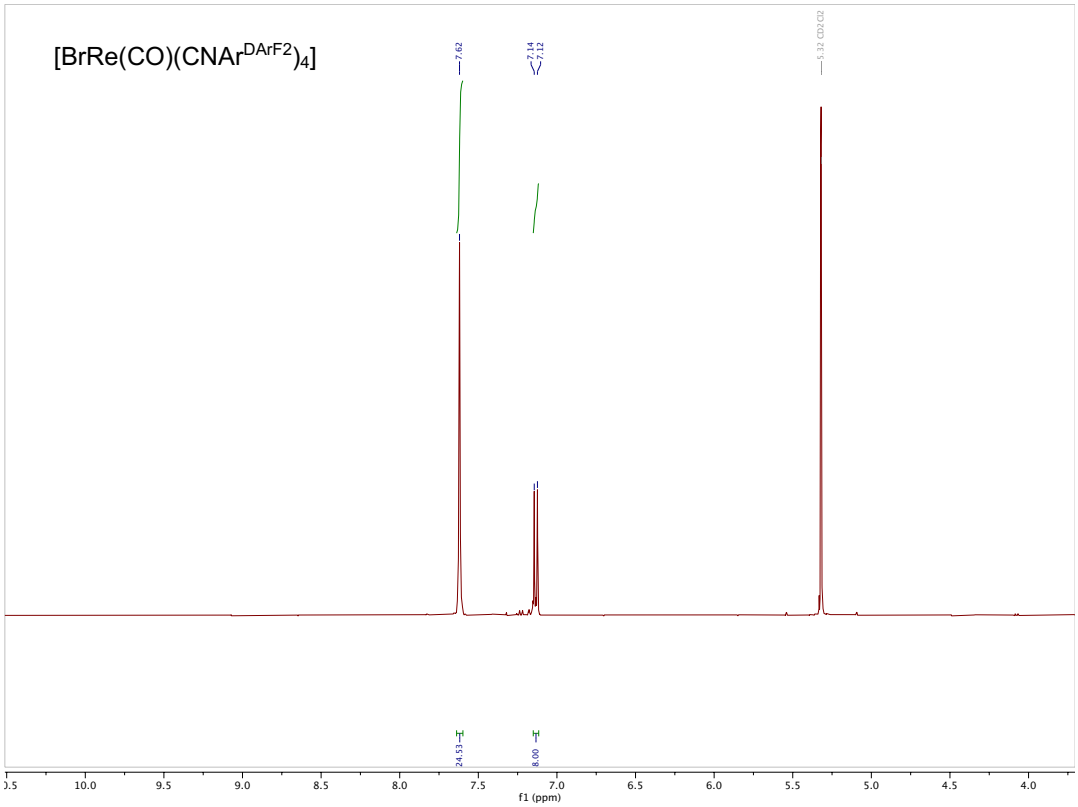

Figure S2.2. ^{19}F NMR spectrum of $[Re(CO)Br(CNAr^{DArF2})_4]$ in CD_2Cl_2.

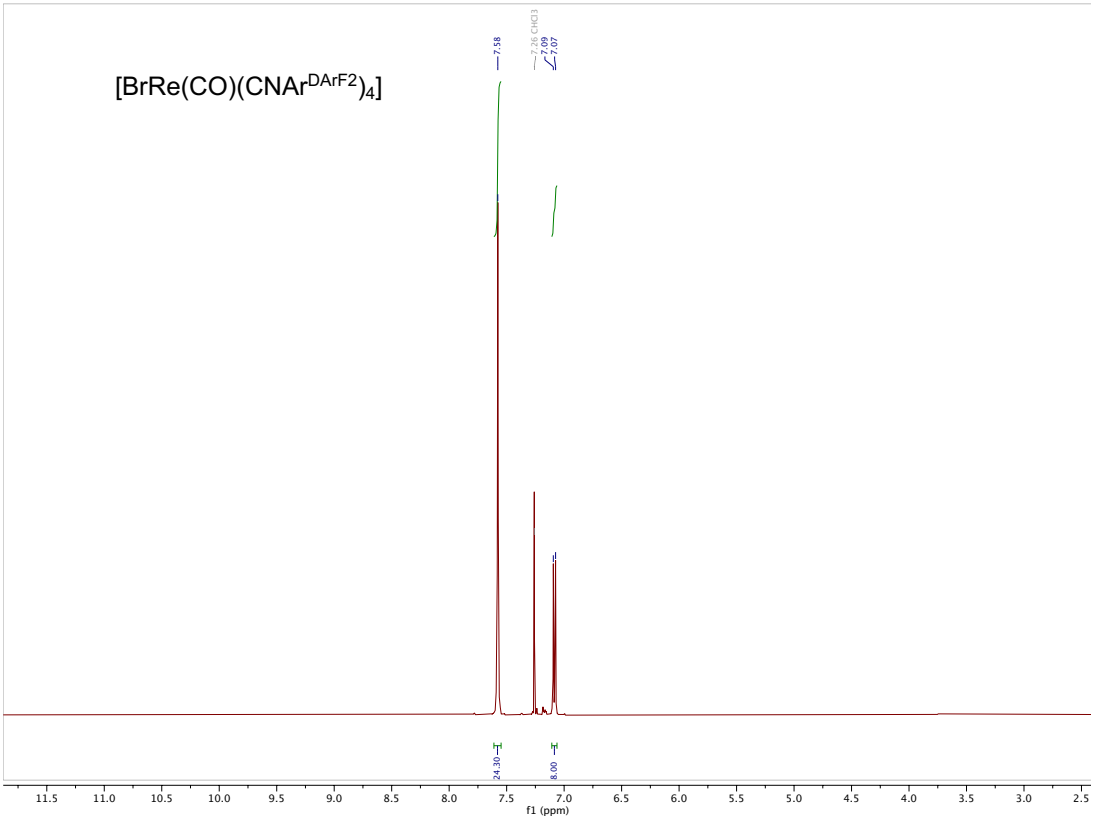

Figure S2.3. ^{19}F NMR spectrum of $[Re(CO)_2Br(CNAr^{DArF2})_3]$ in THF.

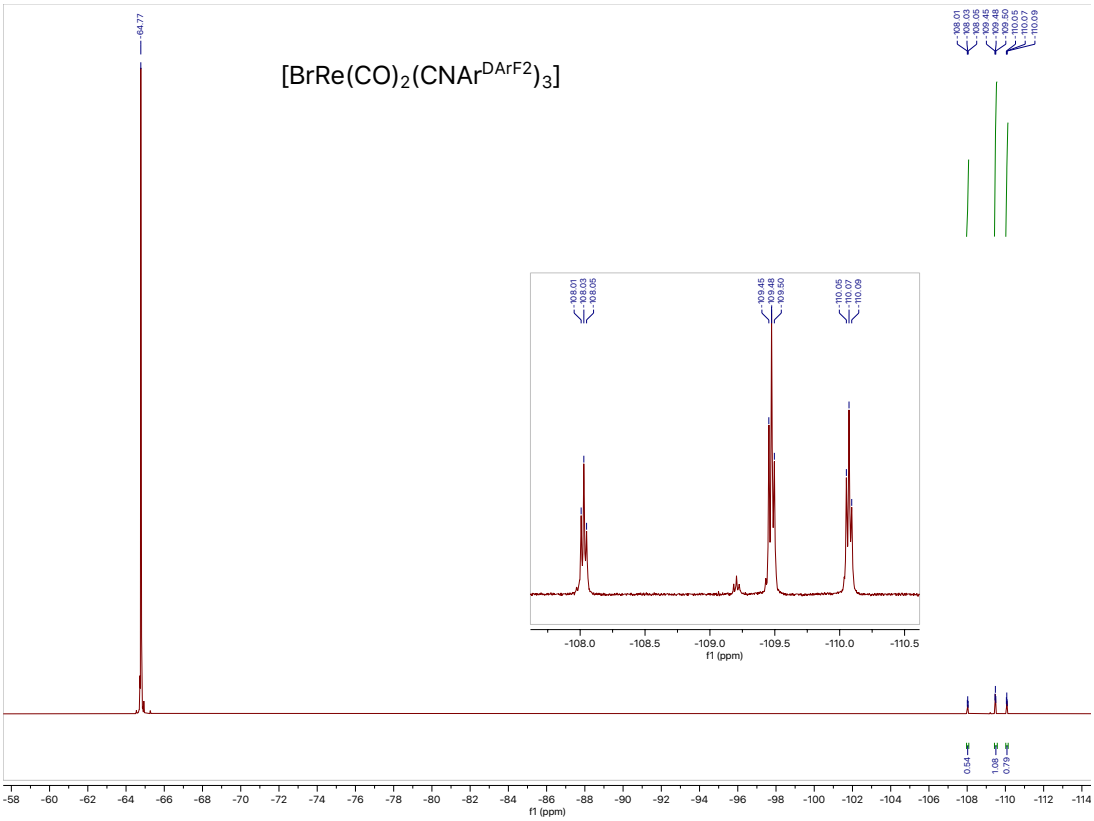

Figure S2.4. ^{1}H NMR spectrum of $[Na(THF)_6][Re(CO)(CNAr^{DArF2})_4]$ in C_6D_6.

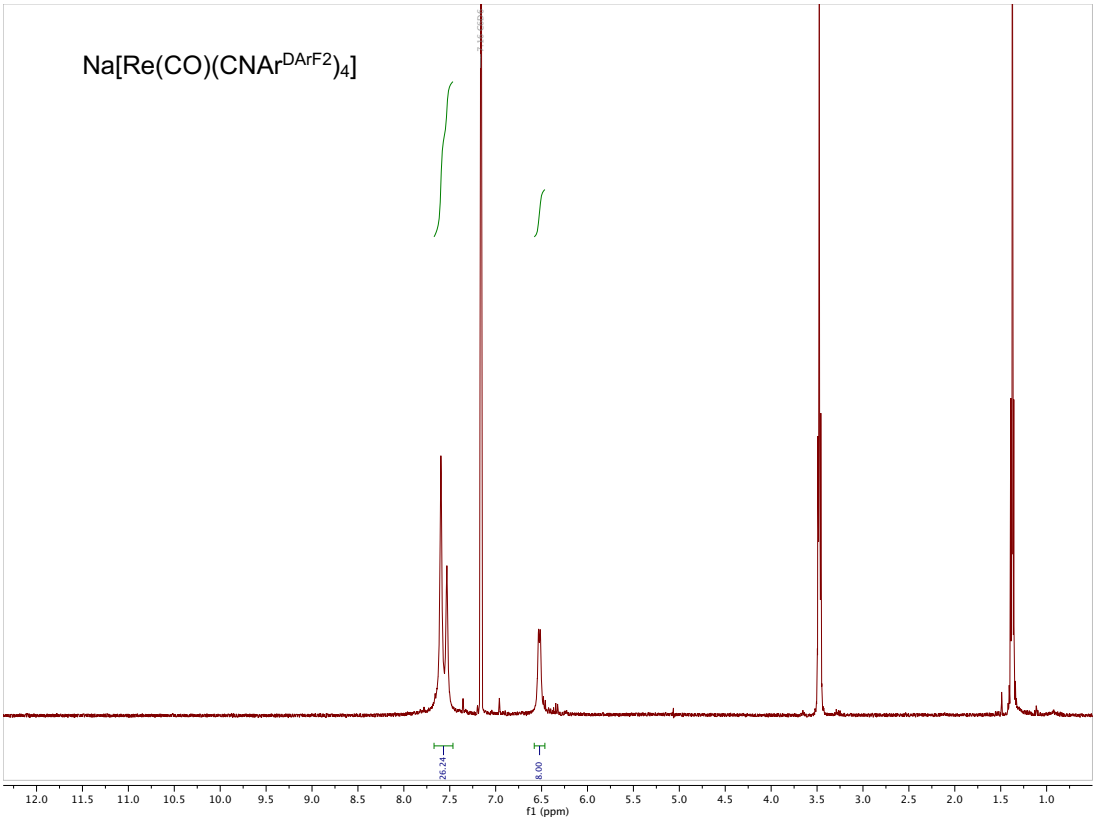

Figure S2.5. ^{19}F NMR spectrum of $[Na(THF)_6][Re(CO)(CNAr^{DArF2})_4]$ in C_6D_6.

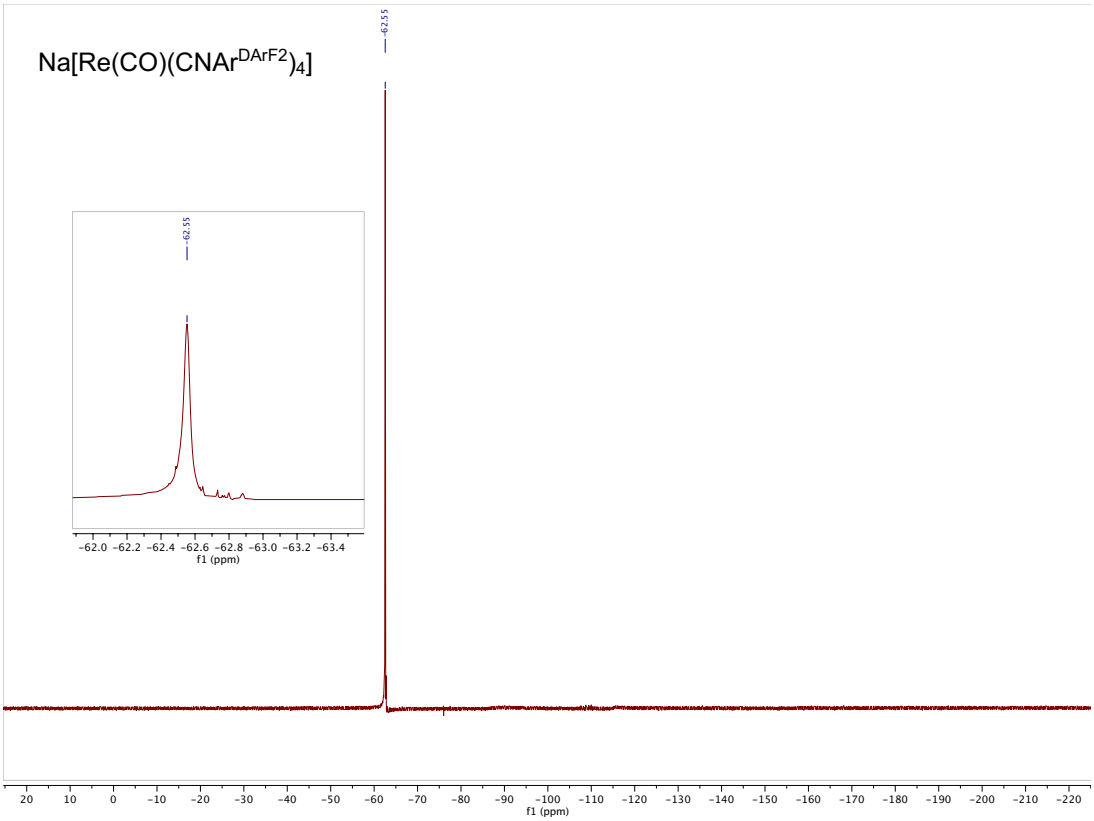

Figure S2.6. ^{1}H NMR spectrum of $[Re(CO)H(CNAr^{DArF2})_4]$ in C_6D_6.

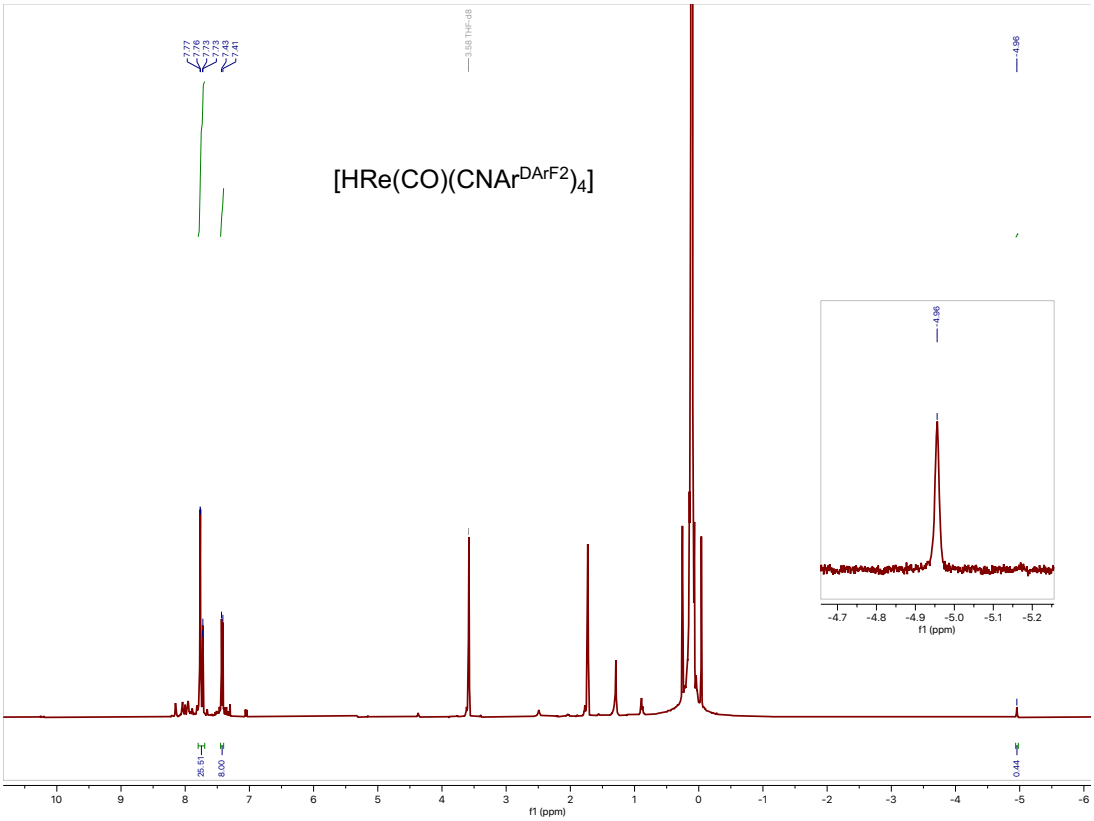

Figure S2.7. ^{19}F NMR spectrum of $[Re(CO)Cl(CNAr^{DArF2})_4]$ in THF.

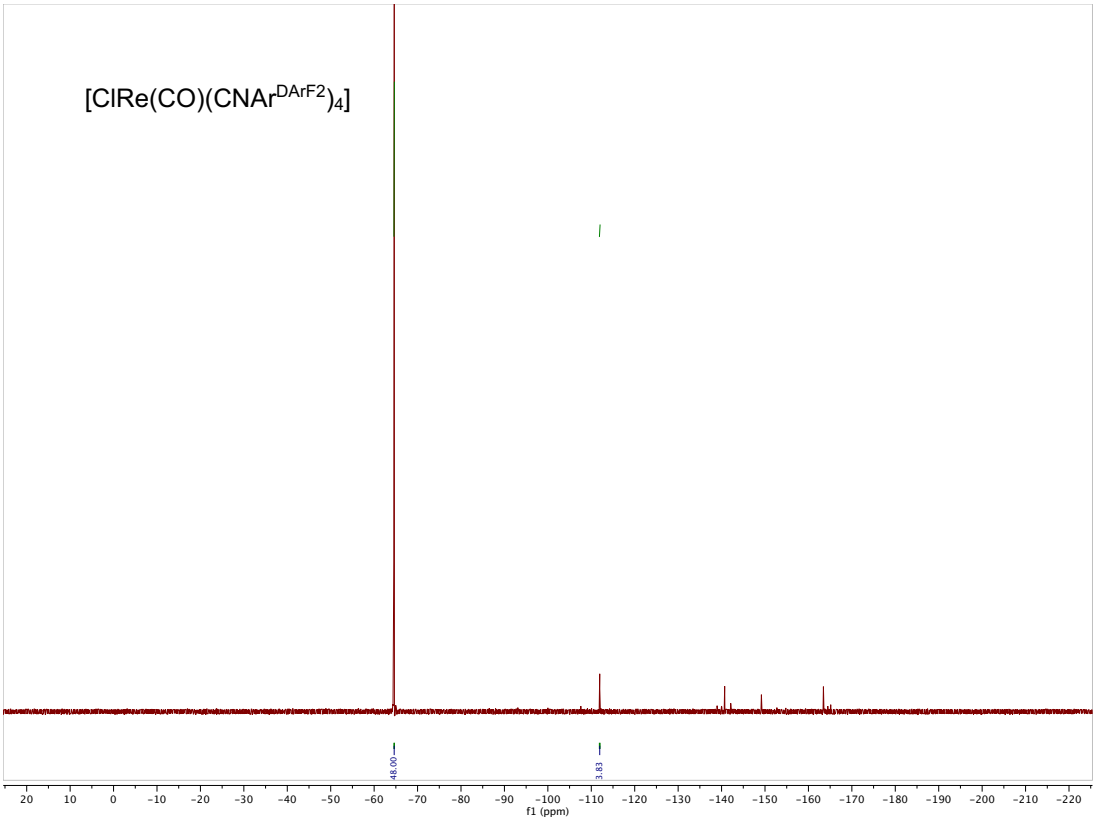

Figure S2.8. ^{1}H NMR spectrum of $[Re(CO)Me(CNAr^{DArF2})_4]$ in THF.

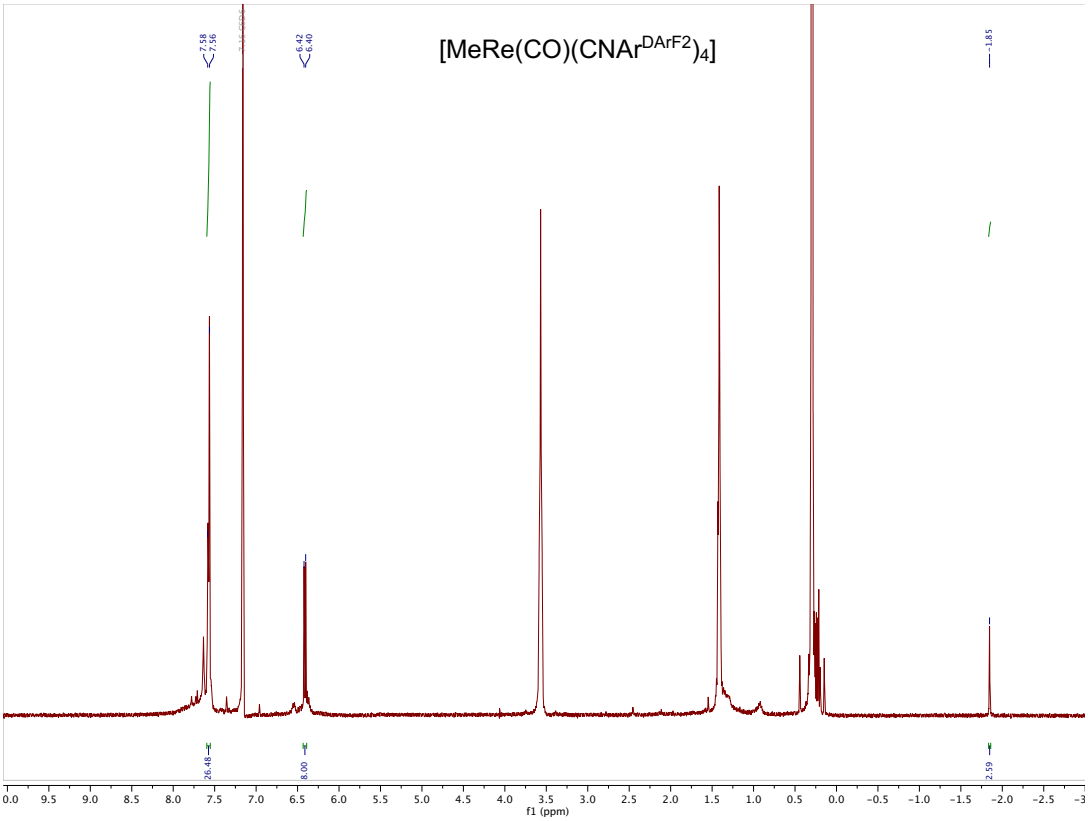

Figure S2.9. ^{19}F NMR spectrum of [Re(CO)Me(CNAr^{DArF2})$_4$] in THF.

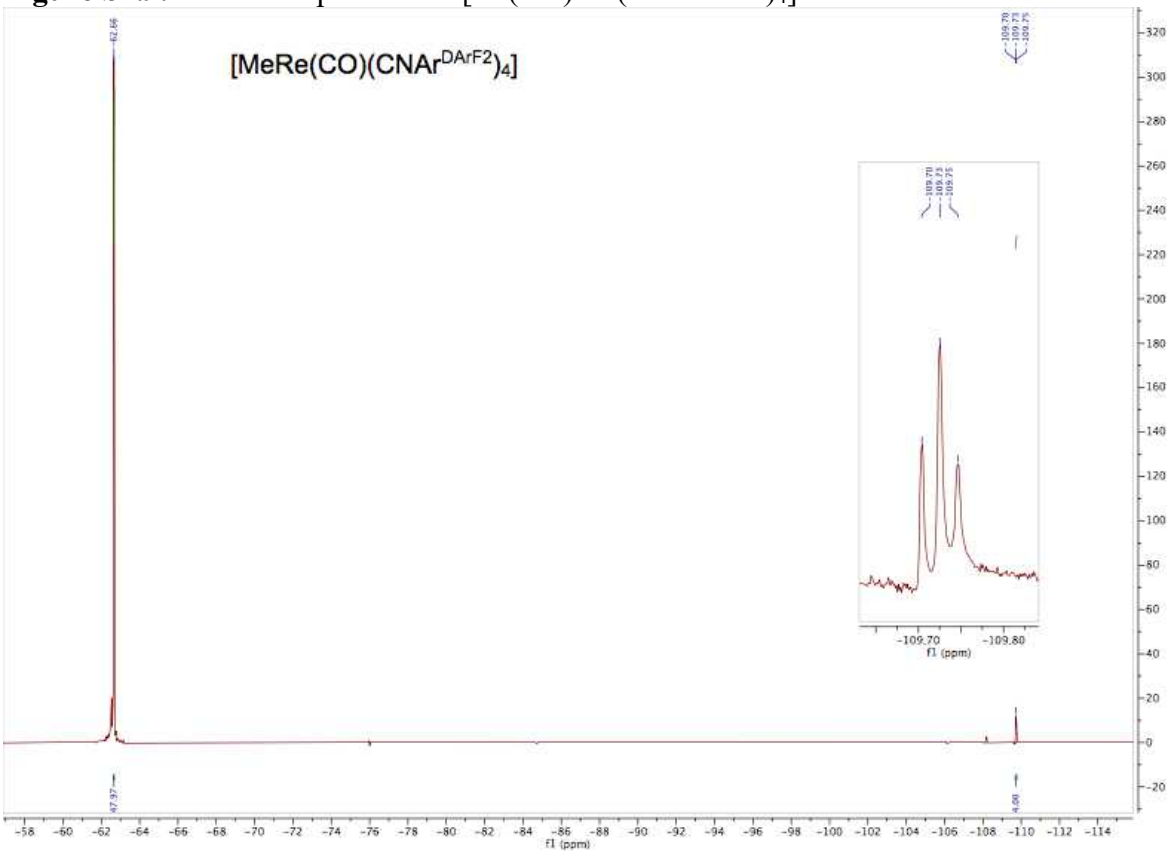

Figure S2.10. ^{1}H NMR spectrum of [Tc(CO)Cl(CNAr^{DArF2})$_4$] in THF.

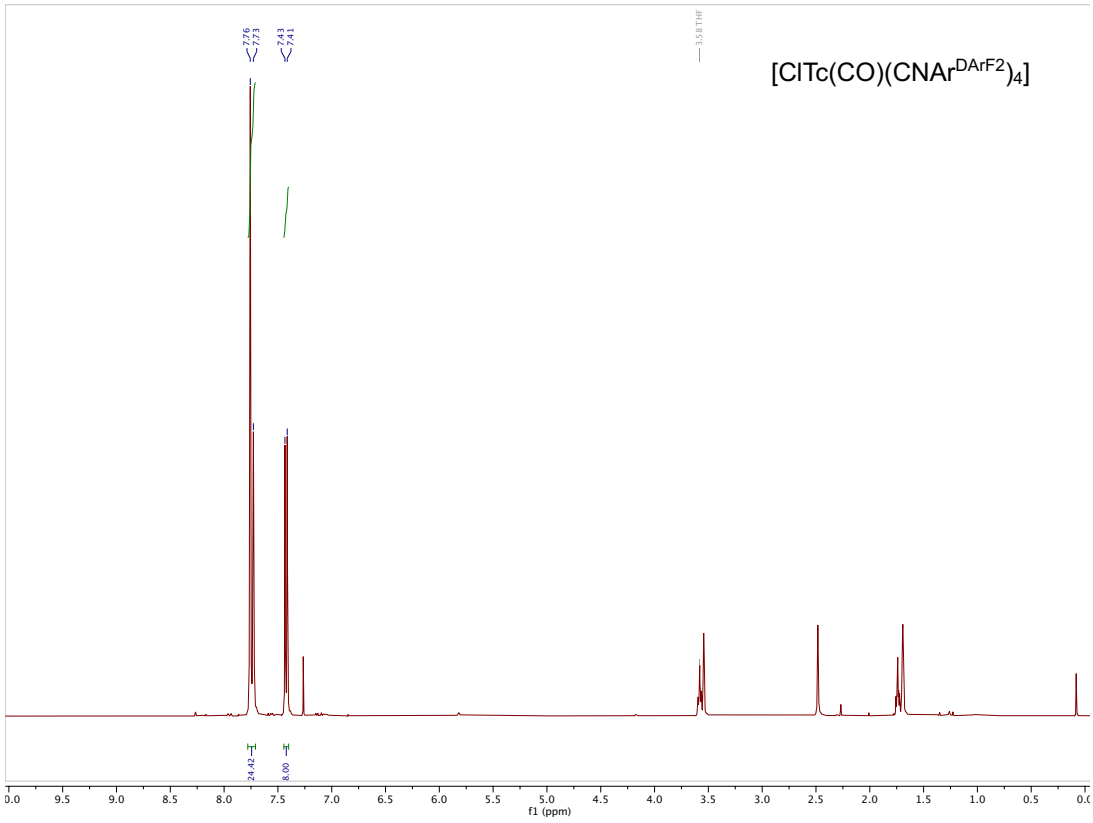

Figure S2.11. ^{19}F NMR spectrum of [Tc(CO)Cl(CNAr^{DArF2})$_4$] in THF.

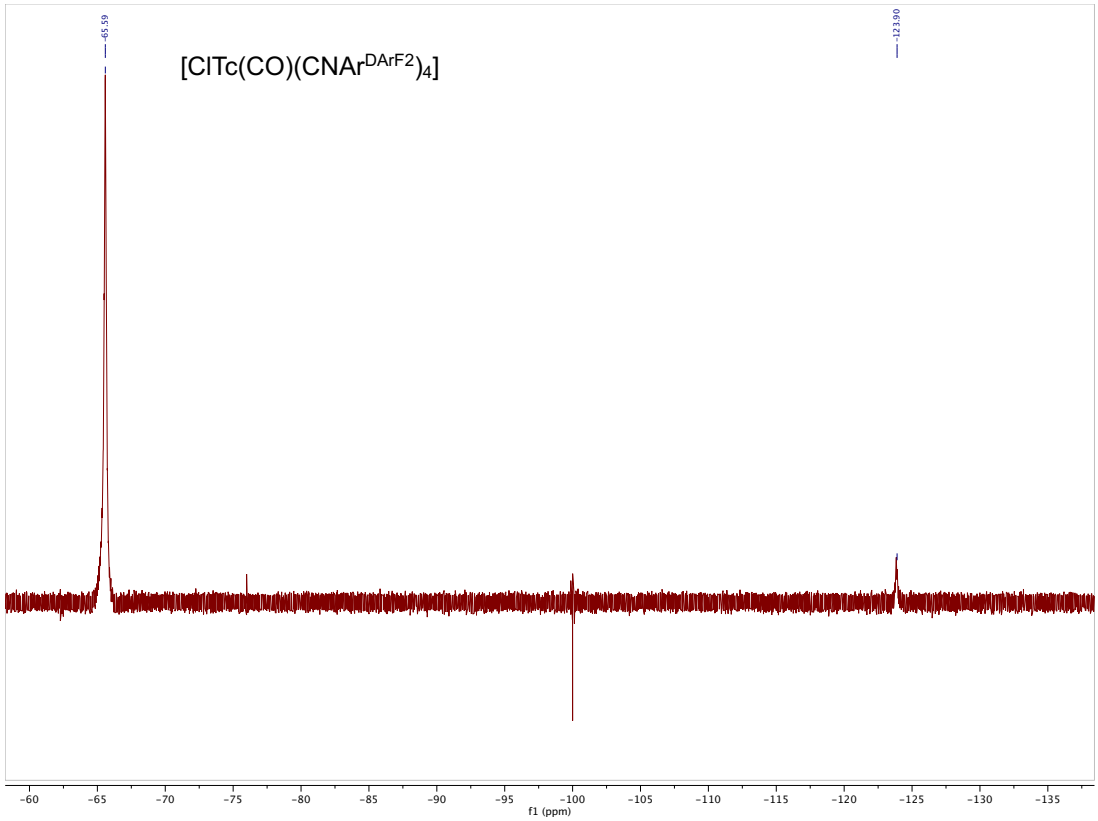

Figure S2.12. ^{99}Tc NMR spectrum of [Tc(CO)Cl(CNAr^{DArF2})$_4$] in THF.

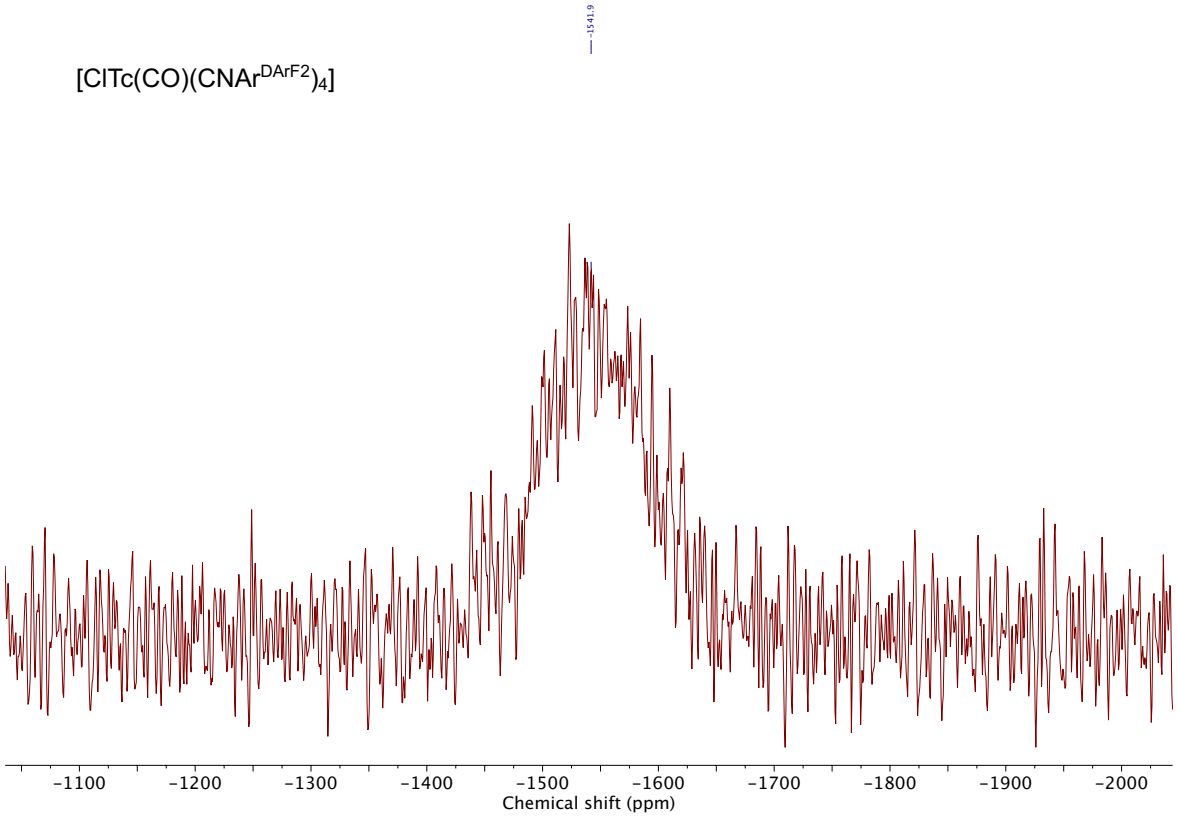

Figure S2.13. ^{19}F NMR spectrum of $Na[Tc(CO)(CNAr^{DArF2})_4]$ in C_6D_6.

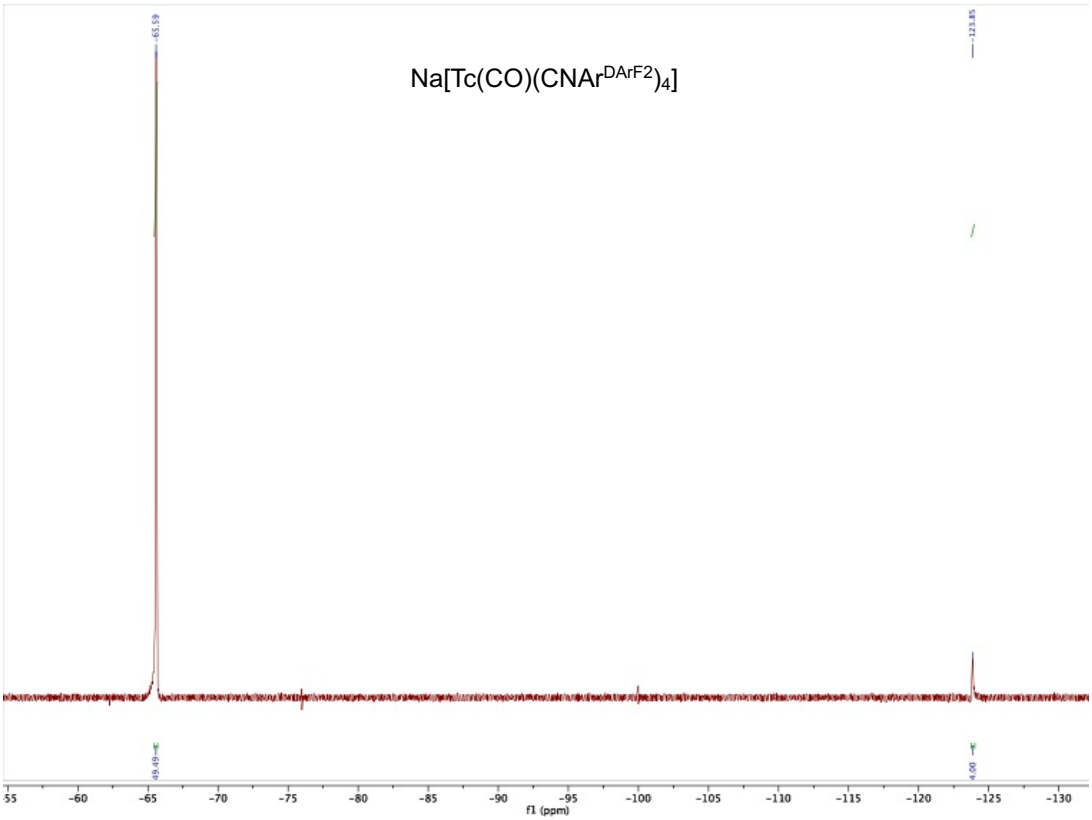

Figure S2.14. ^{99}Tc NMR spectrum of $Na[Tc(CO)(CNAr^{DArF2})_4]$ in C_6D_6.

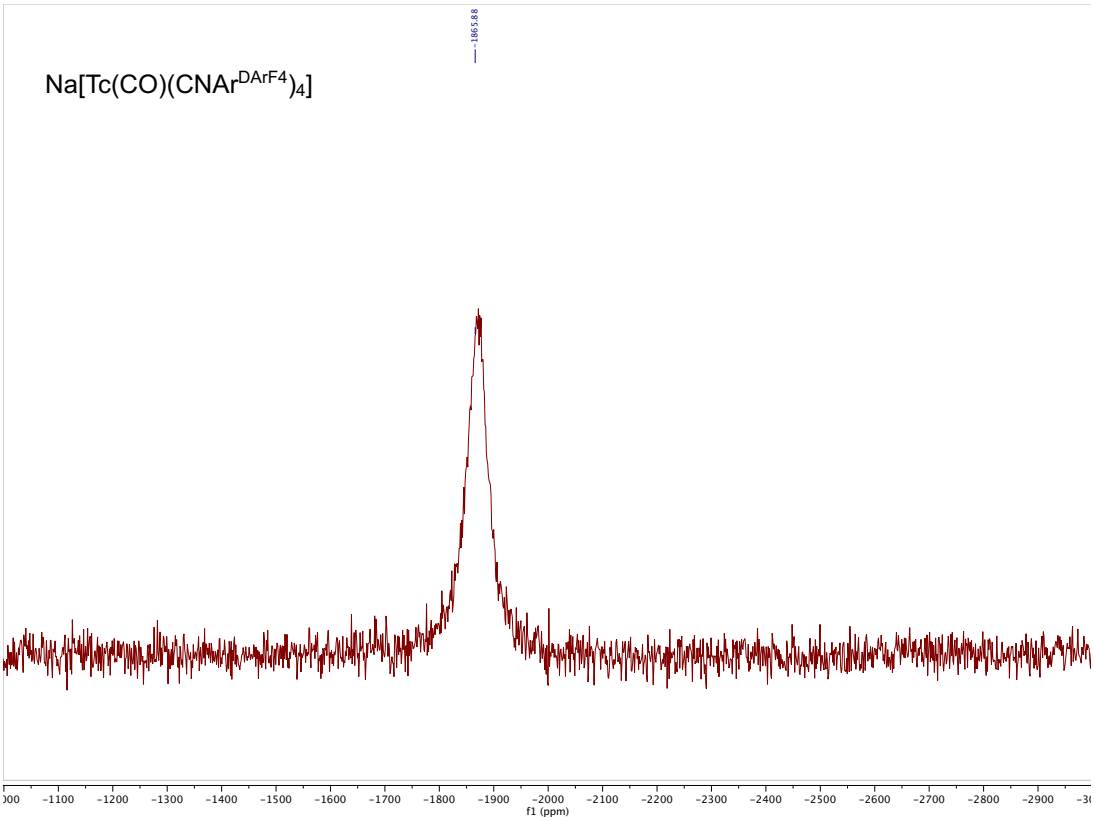

Figure S2.15. ^{1}H NMR spectrum of [Tc(CO)H(CNAr^{DArF2})$_4$] in C_6D_6.

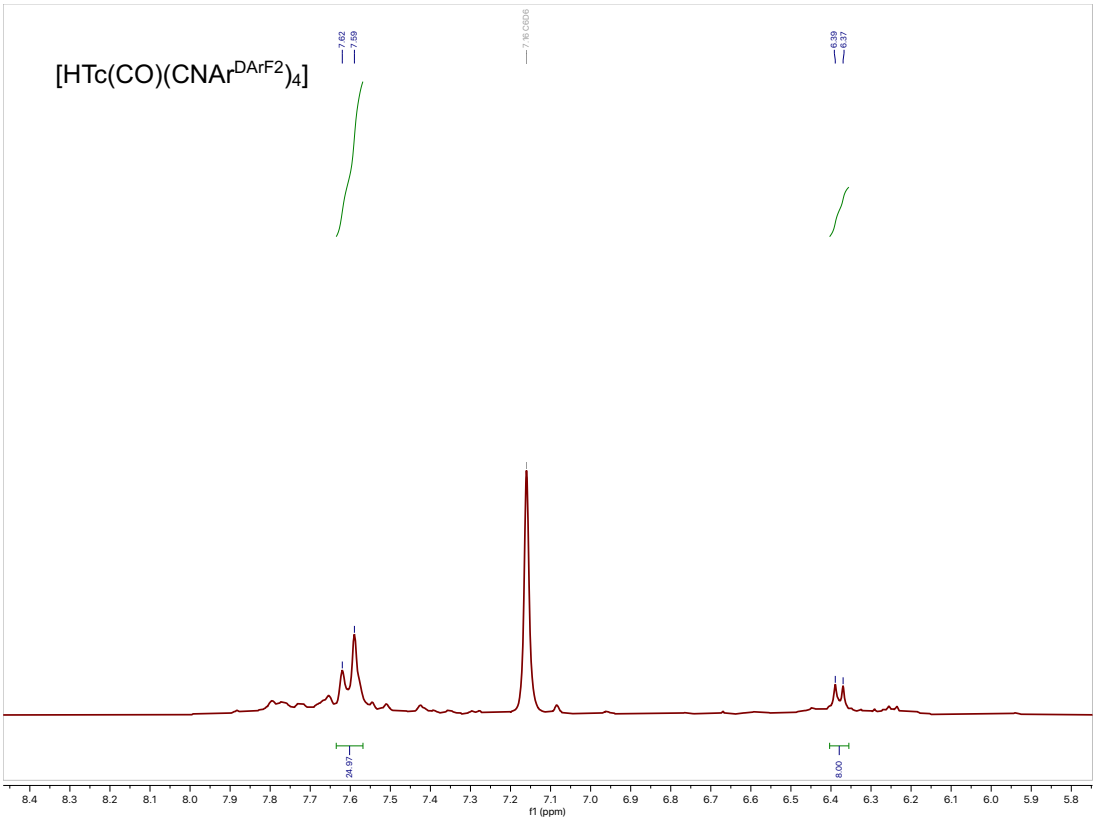

Figure S2.16. ^{19}F NMR spectrum of [Tc(CO)H(CNAr^{DArF2})$_4$] in C_6D_6.

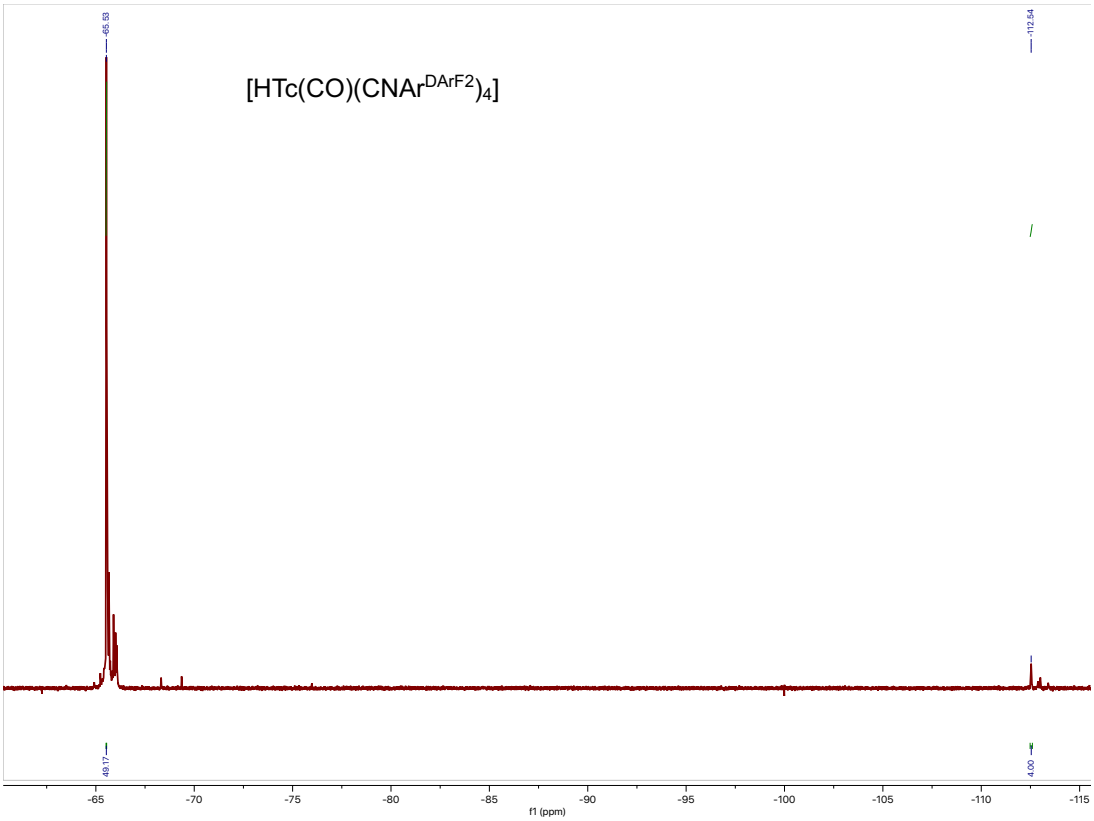

Figure S2.17. ^{99}Tc NMR spectrum of [Tc(CO)H(CNAr^{DArF2})$_4$] in C_6D_6.

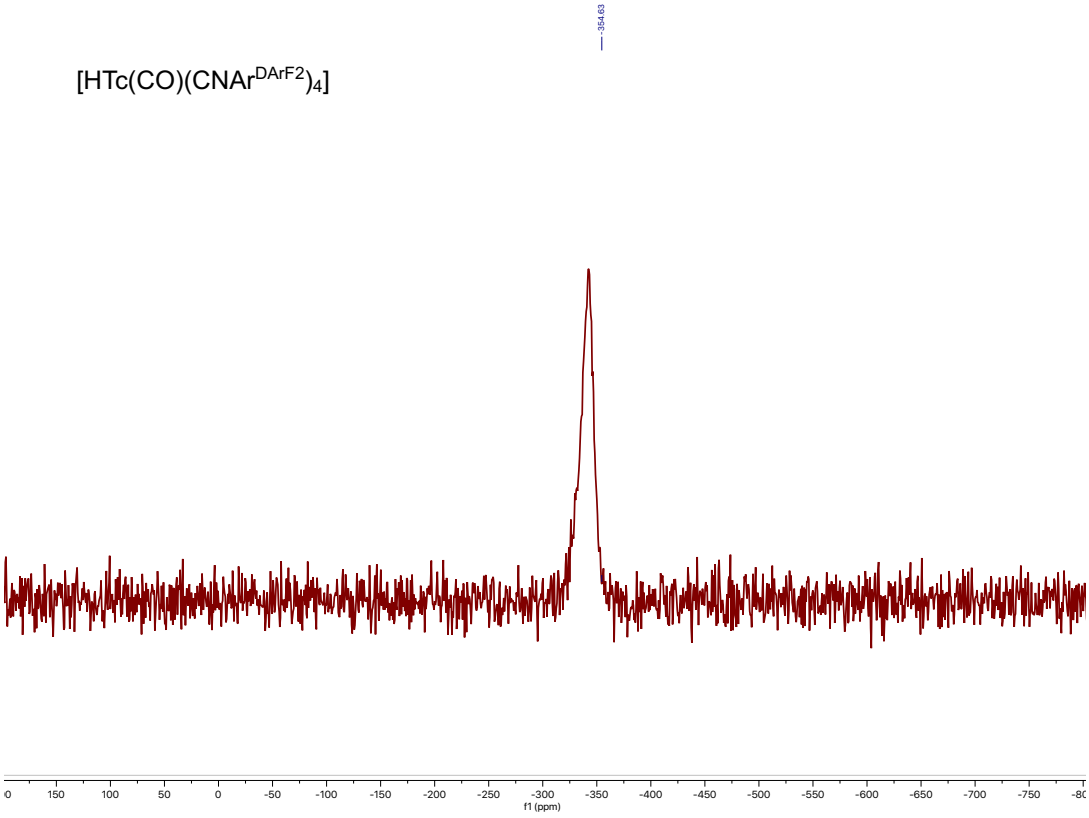

Figure S2.18. IR spectrum of [Re(CO)Br(CNAr^{DArF2})$_4$].

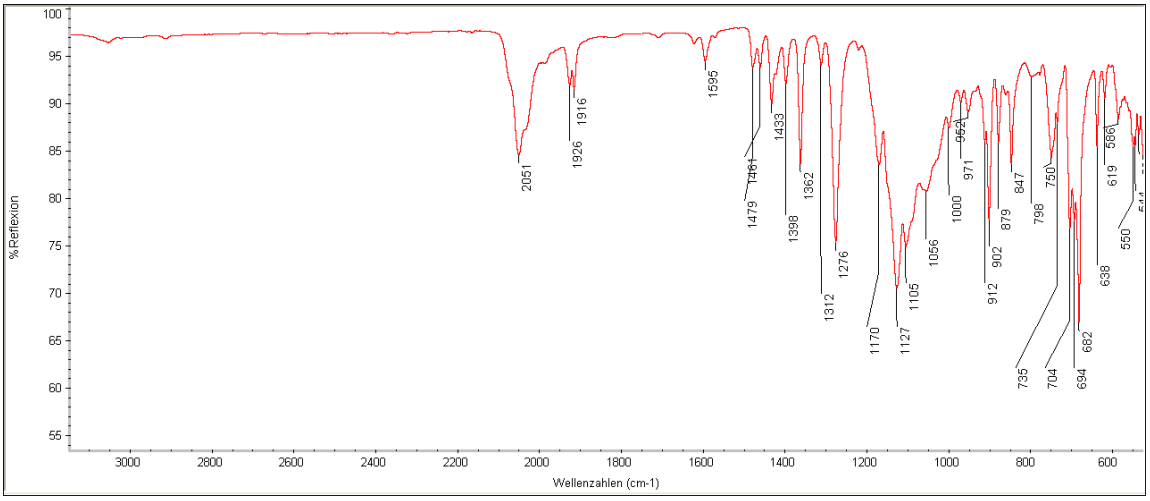

Figure S2.19. IR spectrum of [Re(CO)H(CNAr^{DArF2})$_4$].

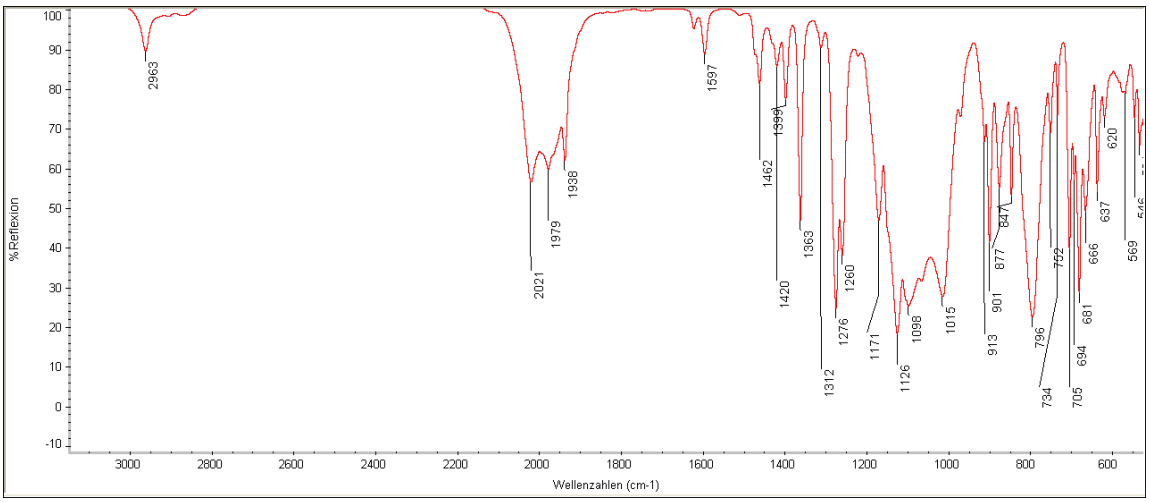

Figure S2.20. IR spectrum of [Re(CO)Cl(CNAr^{DArF2})$_4$].

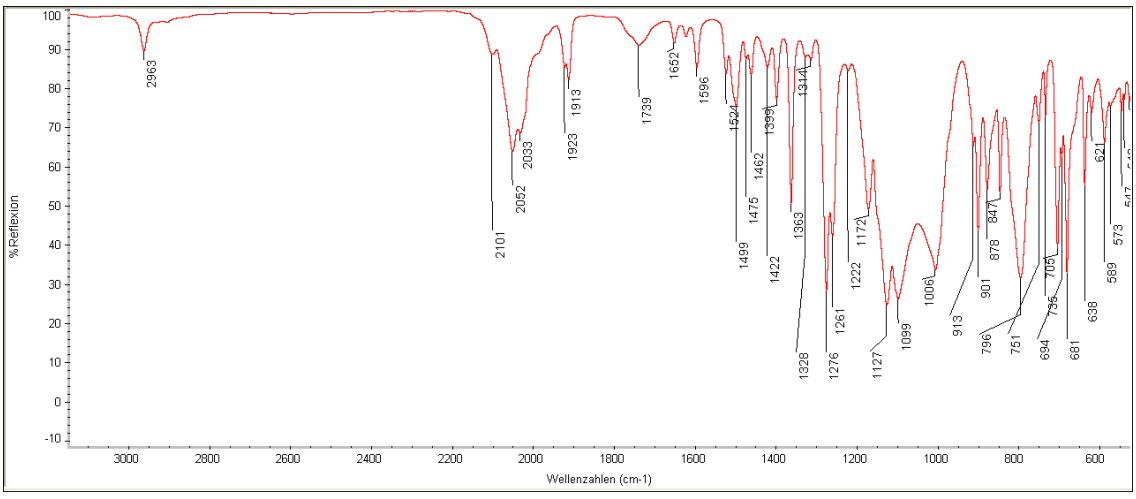

Figure S2.21. IR spectrum of [Re(CO)Me(CNAr^{DArF2})$_4$].

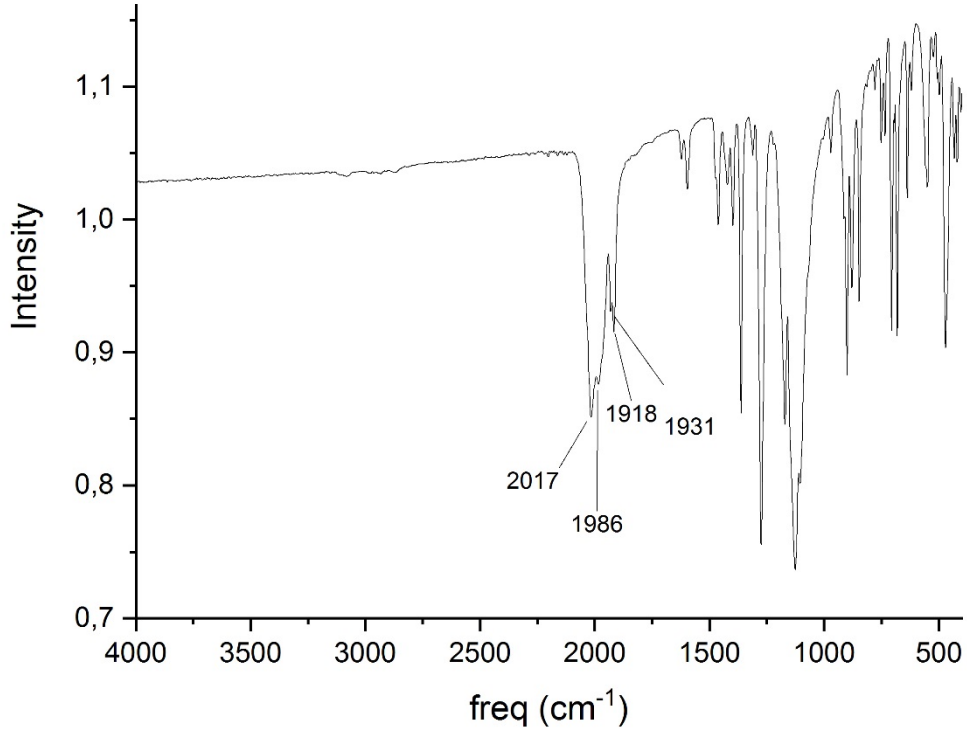

Figure S2.22. IR spectrum of [Na(THF)$_6$][Re(CO)(CNAr^{DArF2})$_4$]/[Re(CO)(CNAr^{DArF2})$_4$].

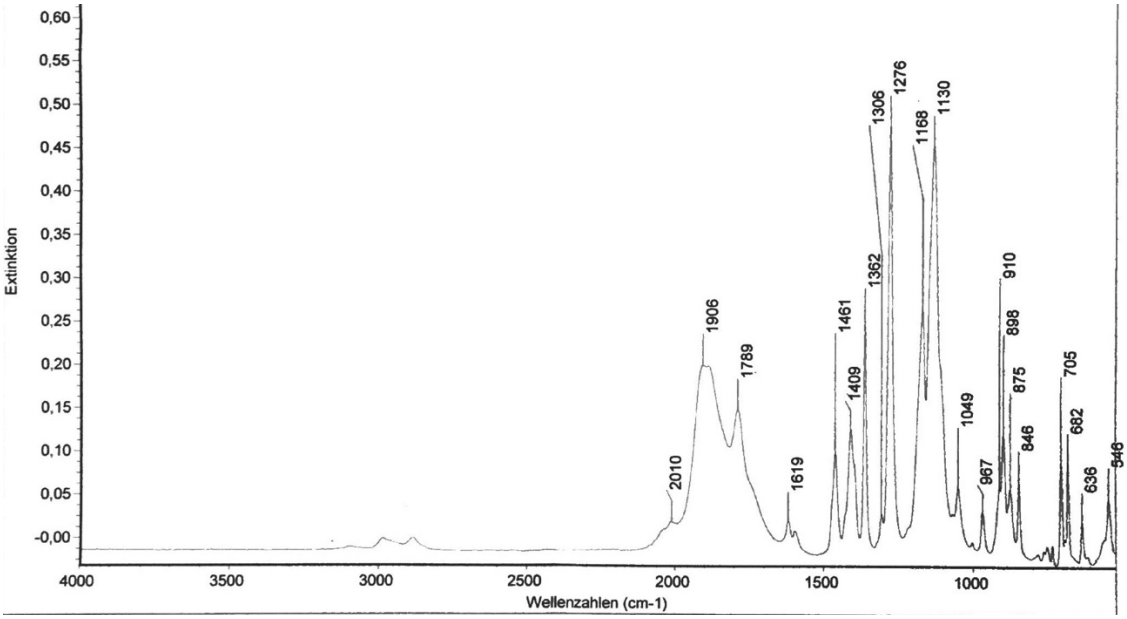

Figure S2.23. IR spectrum of [Tc(CO)Cl(CNAr^{DArF2})$_4$].

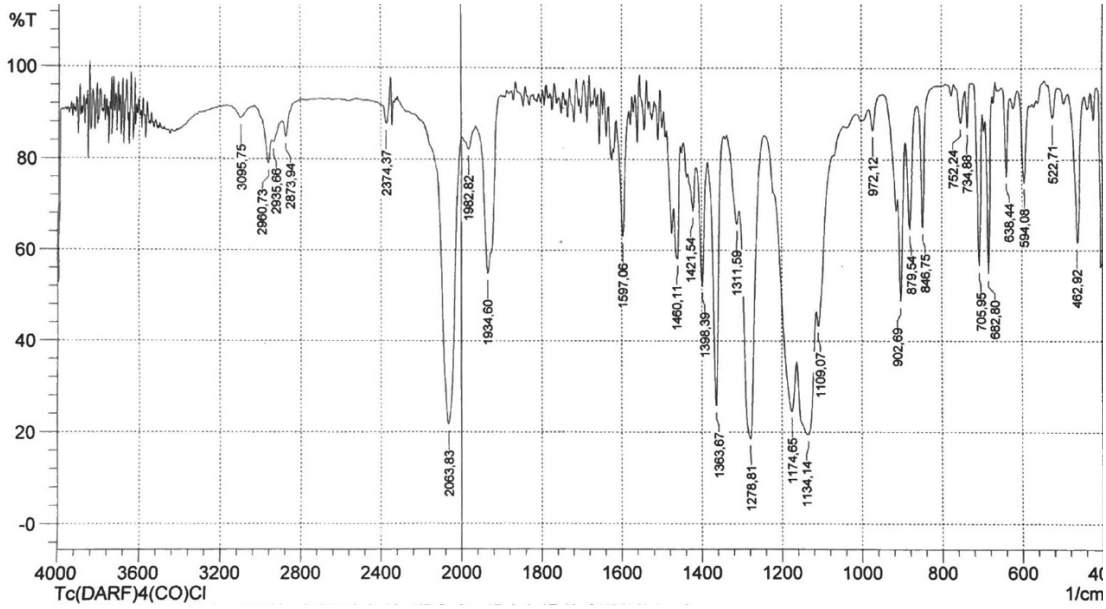

References

(1) G. M. Sheldrick, *Acta Crystallogr. Sect. A*, 2008, **64**, 112-122.

(2) G. M. Sheldrick, *Acta Crystallogr. Sect. C*, 2015, **71**, 3-8.

(3) K. Brandenburg, Diamond- Crystal and Molecular Structure Visualization, Crystal impact GbR, vers. 4.5.1, 2018, Bonn (Germany).

Freie Universität Berlin

Selbstständigkeitserklärung

Name: Salsi	(Nur Block- oder Maschinenschrift verwenden.)
Vorname: Federico	
geb.am:	
Matr.Nr.:	

Ich erkläre gegenüber der Freien Universität Berlin, dass ich die vorliegende Dissertation selbstständig und ohne Benutzung anderer als der angegebenen Quellen und Hilfsmittel angefertigt habe.

Die vorliegende Arbeit ist frei von Plagiaten. Alle Ausführungen, die wörtlich oder inhaltlich aus anderen Schriften entnommen sind, habe ich als solche kenntlich gemacht.

Diese Arbeit wurde in gleicher oder ähnlicher Form noch bei keiner anderen Universität als Prüfungsleistung eingereicht.

Datum: 02.10.2020 Unterschrift: _____